PULSATING CATALYTIC COMBUSTION OF GASEOUS FUELS

A THESIS

Presented to

The Faculty of the Division of Graduate Studies

By

Reuven Gal – Ed

In Partial Fulfillment

of the Requirements for the Degree

Doctor of Philosophy in Aerospace Engineering

Georgia Institute of Technology

July 1988

PULSATING CATALYTIC COMBUSTION OF GASEOUS FUELS

Approved :

Ben T. Zinn, Chairman

Warren C. Strahle

Jechiel I. Jagoda

Date Approved by Chairman : 8/11/88

Dedicated to the memory

my father

Ernst Yitzhak Goldberger

who passed away on July 2nd, 1972.

ACKNOWLEDGEMENTS

I wish to express my appreciation to Professor Ben T. Zinn, my thesis adviser, for his suggestion of the thesis topic, for his guidance and encouragement during this research, and for his thorough examination of the manuscript. I also thank Dr. Jechiel J. Jagoda for his help in acquiring the data logging system that made the measurement of the various parameters in this investigation possible, and for many hours of stimulating discussions concerning this research. In addition, I would like to thank Mr. Brady R. Daniel for his assistance and support while conducting the experiments.

I am grateful for the financial assistance provided by the School of Aerospace Engineering and the Gas Research Institute under the pulsating catalytic combustion research program, and for the leave of absence granted to me by the Armament Development Authority in Israel. Without these two resources, I would not have been able to pursue my studies.

Special thanks to the faculty, the staff and my friends – the graduate students, which created a supportive environment and made the four years I spent at the school meaningful and unique.

Last, but by no means least, I would like to thank my family. My children Ehud, Iddit and Eran have spent a large fraction of their young age in a foreign country and endured many hours without having a father at home. A deep gratitude is expressed to my wife, Lea, who had to cope with the need to provide for the family and manage day to day life mostly by herself. In spite of the difficult times, she was always patient, supportive and encouraging.

TABLE OF CONTENTS

LIST OF TABLES

LIST OF FIGURES

Nomenclature

A : The amplitude of the spatially dependent part of the acoustic pressure as defined in Eqn. (25), $[Pa]$.

$A_{(-)}$: The complex pressure amplitude at $x = 0$ of the acoustic wave propagating in the $+x$ direction, $[Pa]$.

$A_{(+)}$: The complex pressure amplitude at $x = 0$ of the acoustic wave propagating in the $-x$ direction, $[Pa]$.

$\mathcal{A}$: The complex pressure amplitude at $x = 0$ of the acoustic waves propagating in both $+x$ and $-x$ directions, when an acoustic hard wall termination exists at $x = 0$, $[Pa]$.

a : A real function of x defined in Eqn. (25), $[1/m]$.

b : A real function of x defined in Eqn. (25), $[1/m]$.

C_p : The specific heat at constant pressure, $[kCal/kg\ ^\circ K]$.

C_v : The specific heat at constant volume, $[kCal/kg\ ^\circ K]$.

$\bar{c}$: Local speed of sound, $[m/sec]$.

$\dot{m}$: Axial gas mass flux, $[kg/m^2\ sec]$.

P : The real spatially dependent amplitude of acoustic pressure, $[Pa]$.

$\hat{P}$: The complex spatial part of the harmonic representation of the acoustic pressure – defined by Eqn. (23), $[Pa]$.

P_0 : The amplitude of the pressure at $x = 0$, $[Pa]$.

p : Pressure, $[Pa]$.

Q_r : The total heat generated by the combustion per unit cross-section area of the combustor, $[kCal/m^2\ sec]$.

q_r : The rate of heat generation by the combustion per unit volume, $[kCal/m^3\ sec]$.

R : The universal gas constant, $[kCal/kg\ ^oK]$.

$\mathcal{R}e$: The flow Reynolds number, [*dimensionless*].

s : A general dependent variable.

T : Absolute temperature, $[\ ^oK]$.

T_o : Combustor's outer wall temperature, $[\ ^oK]$.

t : Time, [*sec*].

V : The real spatially dependent amplitude of acoustic velocity, [*m/sec*].

v : Axial gas velocity, [*m/sec*].

X_p : Mole fraction of propane in reactants mixture [*dimensionless*].

x : Distance along the axial coordinate, [*m*].

Y_p : Mole fraction of propane in dried products mixture [*dimensionless*].

Y_{CO_2} : Mole fraction of CO_2 in dried products mixture [*dimensionless*].

Y_{O_2} : Mole fraction of O_2 in dried products mixture [*dimensionless*].

γ : Ratio of specific heats, [*dimensionless*].

η_c : Combustion efficiency, [%].

ρ : Density, $[kg/m^3]$.

ρ_0 : Density at $x = 0$, $[kg/m^3]$.

ω : Angular frequency, [*rad./sec*].

Superscripts

$\bar{(\ )}$: Steady-state (time averaged) value of a variable.

$(\ )'$: First-order (deviation from time average) value of a variable.

SUMMARY

The objectives of this research program were to investigate the feasibility of operating catalytic combustors under pulsating conditions and to determine whether acoustic pulsations can improve the performance of such combustors.

An experimental catalytic combustor was developed for this research program. The experimental setup consists of the following subsystems: a heating section for heating the combustion air; a mixing section where the fuel is injected into and mixed with the air stream to obtain a combustible mixture; an igniter for initiating gas phase reactions upstream of the catalytic combustion section; a catalyst section which can have up to four monolith catalyst segments; and an acoustic wave generation system.

A previously developed theoretical model of the axial acoustic motions in a non-isothermal, low Mach number duct flow was utilized to get a description of the spatial distributions of the various dependent variables along the experimental setup. This model consists of a "steady-state" part which yields the time averaged values of the temperature, density and axial velocity distributions along the combustor, and a first-order part which yields an acoustic equation describing the standing wave in the combustor. An approximate solution of the wave equation was found to be in good agreement with the measured pressure data, and was used to calculate the acoustic pressure and velocity amplitudes (the standing wave pattern) along the experimental setup.

Experiments have been conducted to investigate the effect of acoustic pulsations on the heterogeneous combustion of lean fuel/air mixtures on monolith type

platinum catalysts. Commercial methane and propane were used as fuels. Experiments conducted with methane revealed two effects of acoustic pulsations on the catalytic combustion: Onset of acoustic pulsations changed the axial temperature distribution in the experimental setup. This suggests that acoustic oscillations enhance heat transfer between the flowing gas stream and adjacent solid surfaces like the catalyst or the combustor walls. "Unstable" operation of the experimental setup was observed when the catalytic section was placed between an upstream pressure node and a downstream velocity node. When more than one monolith catalyst segment was used, switching between pulsating and non-pulsating conditions caused shifts in the location of the catalytic reaction. Under certain operating conditions the onset of acoustic waves extinguished the reaction or ignited a gas phase flame anchored upstream of the catalytic section.

Investigation of possible improvements in combustion efficiency can be performed when diffusion processes limit the rate of the heterogeneous reaction and prevent its completion. Due to poor catalyst properties, catalytic methane combustion could be stabilized only at high temperatures at which the reaction proceeded to completion. Thus, using methane, incomplete stable catalytic combustion was not reached, and a different, more reactive, fuel was needed to investigate the effect of acoustic pulsations on the combustor performance.

Propane has a much lower activation energy, and stable catalytic combustion of lean propane/air mixtures was easily attained at much lower temperatures than with methane. Stable, incomplete catalytic combustion of propane mixtures was reached with flow rates in the 100 to 160 *lit/min* range and concentrations between 4000 and 9000 *ppm* propane. At these conditions the temperatures measured at the exit of the catalyst were in the 400 to 950 ^{o}C range and the mean axial flow velocity was between 1.4 and 8 *m/sec*. The tests with propane were conducted with a single catalyst segment and "instabilities" (i.e., shifts in location and onset or extinction of gas phase reactions) caused by pulsations were not detected. Changes were

measured in the axial temperature distribution along the combustor upon onset of acoustic waves, and were similar to the changes noted during methane combustion. In addition, when incomplete catalytic combustion was stabilized during non-pulsating operation, excitation of large amplitude pulsations (i.e., more than $140dB$) at different frequencies increased the combustion efficiency by 10 to 50% depending upon the operating conditions. The improvements in the combustion efficiency were achieved when the catalyst was located between an upstream pressure node and a downstream velocity node. This is where the acoustic pressure and the gas particle displacements are in phase. The effect of acoustic pulsations on combustion efficiency when the catalyst was at an "in phase" location was amplitude dependent. The minimum effective sound pressure level which enhanced the combustion and improved its efficiency was about $135dB$, and the combustion efficiency increased with increasing amplitude of pulsations. When the catalyst was at an "out of phase" location (i.e., between an upstream velocity node and a downstream pressure node), the effect of pulsations on combustion efficiency was very small even when high pressure amplitudes were measured in the combustor.

The improvements in the performance of the catalytic combustor when the catalyst was located between an upstream pressure node a downstream velocity node can be explained by the interaction between the acoustic standing wave and the viscous boundary layer near the catalyst surface. This non-linear phenomenon inducing circulatory flows is termed acoustic streaming. The dependence of combustion efficiency and temperature variations on the amplitude of the acoustic pulsations and their insensitivity to the pulsations frequency, as found in the study, are in accordance with the properties of acoustic streaming.

Chapter I
INTRODUCTION

Interest in catalytic combustion has increased in recent years primarily due to the need to control the formation of such pollutants as NO_x and CO, and the interest in burning very lean fuel/air mixtures and low quality fuels. The main disadvantage of using catalytic combustors is the high cost of the catalyst. If a certain conversion rate can be achieved with considerably less catalyst, or the output of a catalytic combustor can be increased, it will make the application of catalytic combustors more attractive. Determining whether the performance of catalytic combustors can be improved by introducing acoustic pulsations is the main objective of this research.

Formation of NO_x from the oxygen and the nitrogen in air happens at elevated temperatures, and can be controlled by limiting the maximum temperature in a combustor, and/or keeping the residence time of the combustion air at high temperature regions in the combustor very short. One way of keeping the temperature down is to burn lean fuel/air mixtures, which yield adiabatic flame temperature of less then 1600 °C – which is approximately the threshold temperature for the formation of NO_x from atmospheric nitrogen. Combustion of ultra-lean mixtures, even at fuel concentrations much lower than the flammability limit, can be accomplished by use of catalytic combustors and yield NO_x free exhaust gases [1,2]. Since most oxidation catalysts lower drastically the activation energy for oxidation of CO to CO_2[3], catalytic combustion can eliminate formation of both CO and NO_x. Catalysts can also improve combustion of low quality fuels due to more

complete combustion of high molecular weight hydrocarbons and other organic compounds. Precious metal catalysts (i.e., *platinum*) lower the activation energy for the combustion of these fuels without considerable poisoning of the catalyst [4], and produce less pollutants than if burned in conventional combustors. In view of these advantages, catalytic combustors are currently being considered for applications in gas turbines [2,5], home appliances [6], exhaust gas cleanup [2], and so on.

Catalytic combustors generally burn mixtures of fuel and air. As the premixed gases enter the catalytic combustion section, the fuel and oxygen molecules diffuse towards the catalyst surfaces where they are adsorbed on its active sites. Heterogeneous combustion reactions take place on the surface causing the adsorbed species to change chemically from reactants to products and generate heat. The products are desorbed from the catalyst surface and diffuse through the boundary layer back to the flowing gas stream. The heat generated at the surface is transferred by convection and radiation to the flowing gases and adjacent solid surfaces.

In some catalytic combustion processes which occur at higher temperatures (i.e., 1300 to 1550 °C), the catalytic combustion is followed by a homogeneous gas phase reactions [2]. Heterogeneous surface reactions start on the upstream catalyst surfaces as in a regular catalytic combustor. The energy generated by the catalytic combustion heats the bulk flow which contains the remaining reactants. At elevated temperatures, the flammability limits broaden and even very lean fuel/air mixtures can undergo gas phase reactions. Thus, if the temperature of the mixture and its concentration can support gas phase reactions, the existance of an ignition source (e.g., an incandescent catalyst surface) will initiate homogeneous gas phase reactions. This type of a catalytic combustion process, which is considered for use in gas turbines [7], combines some of the advantages of catalytic combustors with some of those of conventional combustors. It needs less catalyst surface than

a catalytic combustor where only heterogeneous reactions are taking place, and the temperature can be kept low enough to avoid formation of NO_x (i.e., below 1600 °C). On the other hand, since some or most of the combustion occurs in the gas phase downstream of the catalyst surfaces, the exhaust gases may contain more residual fuel and incomplete products of reaction, such as CO. Improving the performance of the catalytic section of this type of a combustor can change the operation of the entire system (the heat yielding the sufficient temperature for igniting gas phase reactions can be generated using a shorter catalytic section thus saving catalyst) and make implementation of this technology more feasible.

The performance of a catalytic combustor depends on the following three factors:

- The temperature and composition of the combustible mixture.
- The mass and heat transport processes within the catalytic combustion section.
- The properties of the catalyst, which includes the type of the active catalytic material, the number of active catalytic sites, the shape and the porosity of the solid catalyst microstructure, the shape and dimensions of the catalyst macrostructure, and so on.

Although at low catalyst surface temperatures the overall reaction rate is kinetically controlled, for most practical cases the surface temperature is high enough to exceed this operating region. At higher catalyst temperatures the reaction rate is controlled by the rates of diffusion of reactants and products to and from the catalyst surfaces, respectively. Thus, increasing the rate of mass transfer between the gas stream flowing at the centers of the channels existing in the catalyst and its surfaces can either increase the catalytic combustor output or enable the combustor to have the same output with less catalyst. Research conducted in related areas [8,9,10,11,12,13,14,15] has shown that the presence of pulsations (i.e., acous-

tic waves) in either a liquid or a gaseous medium enhances the rates of both mass and heat transfer between the pulsating flow and adjacent surfaces. Arkhangel'skii and Statnikov[8] analyzed theoretically the effect of pulsations on convective diffusion at a liquid-solid interface and found that the diffusion rate of reactants toward the solid surface is increased. The analysis predicted the enhancment of the diffusion to be the greatest near velocity nodes. Experiments of developing photographic emulsion plates were conducted under non-pulsating conditions and compared to the development of identical plates in standing wave ultrasonic fields having frequencies of $800kHz$ and $3MHz$. The optical density of the films, which was used as a measure of the chemical reaction taking place on the liquid-solid interface, was found to be 50% higher near the velocity nodes than for films developed in a non-pulsating liquid developer. In spite of the large difference between the two frequencies used, the results in both cases were very similar.

Borisov et al [9,10] investigated experimentally the effect of acoustic pulsations on drying wet particles in air. The first study [9] is concerned with drying filter papers placed at a velocity node in an acoustic dryer oscillating at $1080Hz$ with sound pressure levels ranging between 150 and 163 dB. The time needed to dry the paper from 40% to 20% moisture was 150, 80,28 and 20 sec. at acoustic fields of 150,156,160 and 163 dB, respectively. When the specimen were placed at a pressure node the drying was found to be enhanced even more, and the drying time for oscillations of 143 dB was 25 $sec.$ – shorter than the time that was needed when operating at 160 dB when the specimen were located at the velocity node. The second study [10], compares acoustic drying to both contact heating by electrical heaters, and infrared radiation. Drying quartz sand from 21% to 4% moisture took 60 minutes for contact drying at 70 °C compared to 28 minutes in a 7000 Hz acoustic field having sound pressure level of 168 dB at room temperature. When in addition to the acoustic field heaters were turned on and the air was kept at 40 °C, the same amount of moisture was removed in 11 minutes. Drying

of asbestos boards by an acoustic field was compared to drying by infrared radiation and a two- or threefold acceleration of moisture elimination was achieved acoustically with the specimen at considerably lower temperatures than under infrared radiation. Burdukov and Nakoryakov [11] also investigated the effect of acoustic pulsations on evaporation and diffusion. Camphor balls were evaporated into air oscillating at 11.5 and 18 kHz with sound pressure levels between 150 and 163 dB. Mass transfer coefficients increased with increased pressure amplitude, and were inversely proportional to the square root of the frequency. Similar investigation was performed by Hodgins et al [14] using naphtalene coated beads. Frequencies up to $12kHz$ and acoustic sound levels up to $160dB$ were used. Mass transfer rates increased exponentially with the increase in the pressure dB level. The largest effects were observed in the frequency range of 100 to $700Hz$, and the lower threshold pressure amplitude at which the effects of pulsations on the evaporation rate were first detected was $120dB$. The evaporation rate under pulsating operation increased up to 220% for a single ball, and up to 120% for a bed of naphtalene coated balls, compared to the evaporation rate under non-pulsating conditions.

Research done by Zinn and co-workers[12,13,15] with a Rijke type pulsating combustor showed that both the heat and mass transfer rates, and the combustion efficiencies measured under pulsating conditions were higher than the values reported in the literature for non-pulsating combustors.

The above mentioned and related investigations [16,17,18,19], show that heat and mass transfer rates are enhanced by acoustic fields covering a wide frequency range. Furthermore, the improvements were observed at different locations along the standing wave pattern. There seems to be an agreement among researchers that these improvements are larger as the amplitudes of the acoustic field are increased. There are conflicting results regarding the effects of frequency and the importance of the location relative to the standing wave pattern. These findings

suggested that operating catalytic combustors under pulsating should improve their performance while preserving their other advantages. The increase in the rate of mass transfer of reactants and products to and from the catalyst surfaces is expected to increase the overall reaction rate. Consequently, the amount of heat generated by the surface reactions should increase. Despite the higher energy production rate, the catalyst surface temperature is not expected to change considerably, since the rate of heat transfer from the catalyst surfaces to the main stream of flowing gases is also expected to increase.

Additional benefits might also result from the introduction of pulsations in catalytic combustors. One of the difficulties encountered in the application of these combustors in gas turbines is the spatial nonuniformity of fuel/air concentrations [5] which introduces temperature gradients downsteam of the catalyst and creates "hot spots" on the turbine blades. Since pulsations tend to enhance both heat and mass transport, their introduction could improve the mixing of the species, and reduce the temperature nonuniformities at the exit of the catalyst section. As a result of the pulsations, temperature gradients should decrease even further as the gases flow downstream of the catalyst due to improved mixing, and the "hot spots" on the turbine blades could be possibly eliminated.

The acoustic enhancement of both mass and heat transfer, and the possible improvement of heterogeneous reactions due to these effects, initiated several investigations regarding the effect of pulsations on heterogeneous reactions. Most of these investigations are theoretical and try to explain the mechanisms that can cause pulsations to enhance surface reactions. Several second order acoustic phenomena can contribute to the enhancement of the heat and the mass transfer. Chendke and Fogler [20] suggest that acoustically induced cavitations is the most important mechanism in liquid systems, and acoustic streaming has a dominant effect in gaseous catalytic reaction systems. Other investigators [21,22,23] developed mathematical models to show that the reaction rate should increase due to

the effect of acoustic oscillations on either the diffusion or the adsorption steps of the heterogeneous reaction. Experimental investigations of the effect of pulsations on the reaction rate of the gas-phase catalytic decomposition of cumene to benzene and propylene were conducted by Zhorov and by Lintner [24,25]. In his studies Lintner found that the rate of this catalytic reacion can be increased up to 160% by introduction of ultrasonic vibrations.

No experimental investigation regarding the effect of pulsations on the catalytic combustion of gaseous fuels with air has been uncovered in the literature in spite of existing evidence that considerable improvement in the performance of catalytic combustors can be achieved by operating such combustors in a pulsating mode. This research program has been undertaken to investigate the feasibility of operating catalytic combustors under pulsating conditions and to get quantitative data which will determine the range of pulsating flow conditions that could optimize the performance of catalytic combustors.

Chapter II
DESCRIPTION OF THE EXPERIMENTAL SETUP

Design Considerations

The objectives of the experimental setup developed under this program were to provide capabilities for burning different fuels in a catalytic combustor under different pulsating and non-pulsating conditions. Based upon information derived from the literature [1,4], and the objectives of this research program, it was decided that the experimental setup should include an air heating section, a fuel/air mixing section, and a catalytic combustion section. The "acoustical part" of the setup should include a sound generation system, a "known" acoustic termination upstream of the catalytic combustion section that would help to "identify" the excited standing wave pattern, and an ability to move the catalyst section along the combustor to provide a capability for positioning the catalyst at any desired location on the standing wave pattern. In order to avoid the need to use special materials, the system was designed of a carbon steel tube with no optical windows and without insulation. This made the combustor simple to build and inexpensive, but ruled out any possibility of measuring radiation along the combustor, and introduced large heat losses through the walls which produced large radial temperature gradients.

The parameters for investigation were the fuel/air ratio, flow velocity, inlet temperature to the catalyst section, location of catalyst on the standing acoustic wave and the amplitude and frequency of the driving pulsations. Starting a test

was done by first letting air flow through the heating system and then heat the upstream part of the combustor, including the catalyst segments. Upon reaching a desired temperature in the catalytic section, the fuel supply line was opened. Proper setting of fuel and air flow rates and the energy output by the heaters determine the total flow rate, the fuel/air ratio and the mixture temperature at the inlet to the catalyst. The mixture should "light-off" upon contact with the hot catalyst, but an ignition system can start a gas phase flame if the catalyst temperature is not sufficiently hot. The relative location of the catalyst on the standing wave pattern is determined mainly by its axial distance fron the acoustic termination which is set prior to starting the test, the frequency of the pulsations and the temperature distribution between the acoustic termination and the catalyst. Changing the frequency and power of the electrical signal to the drivers determines the frequency and amplitude of the pulsations in the combustor.

Description of the Experimental Setup

The developed experimental setup is shown in Fig. 1. It consists of a vertical pipe which connects to a horizontal pipe. Air is supplied at the top of the vertical section and it passes through four electrical heaters which are located along the vertical pipe. The heated air enters the mixing section in the horizontal part of the combustor through a porous plate. Fuel is injected into the air stream just downstream of the porous plate. An ignition system located upstream of the catalytic combustor section is capable of igniting combustible mixtures and anchoring the flame on a flame holder. The hot gases are used to preheat the catalyst surfaces to a desired temperature. The catalyst section is located downstream of the ignition system. When there is no flame upstream of the catalytic combustion section, and the catalyst surfaces are sufficiently hot, the combustible mixture reacts upon contact with the catalyst surfaces. In addition to the heterogeneous surface

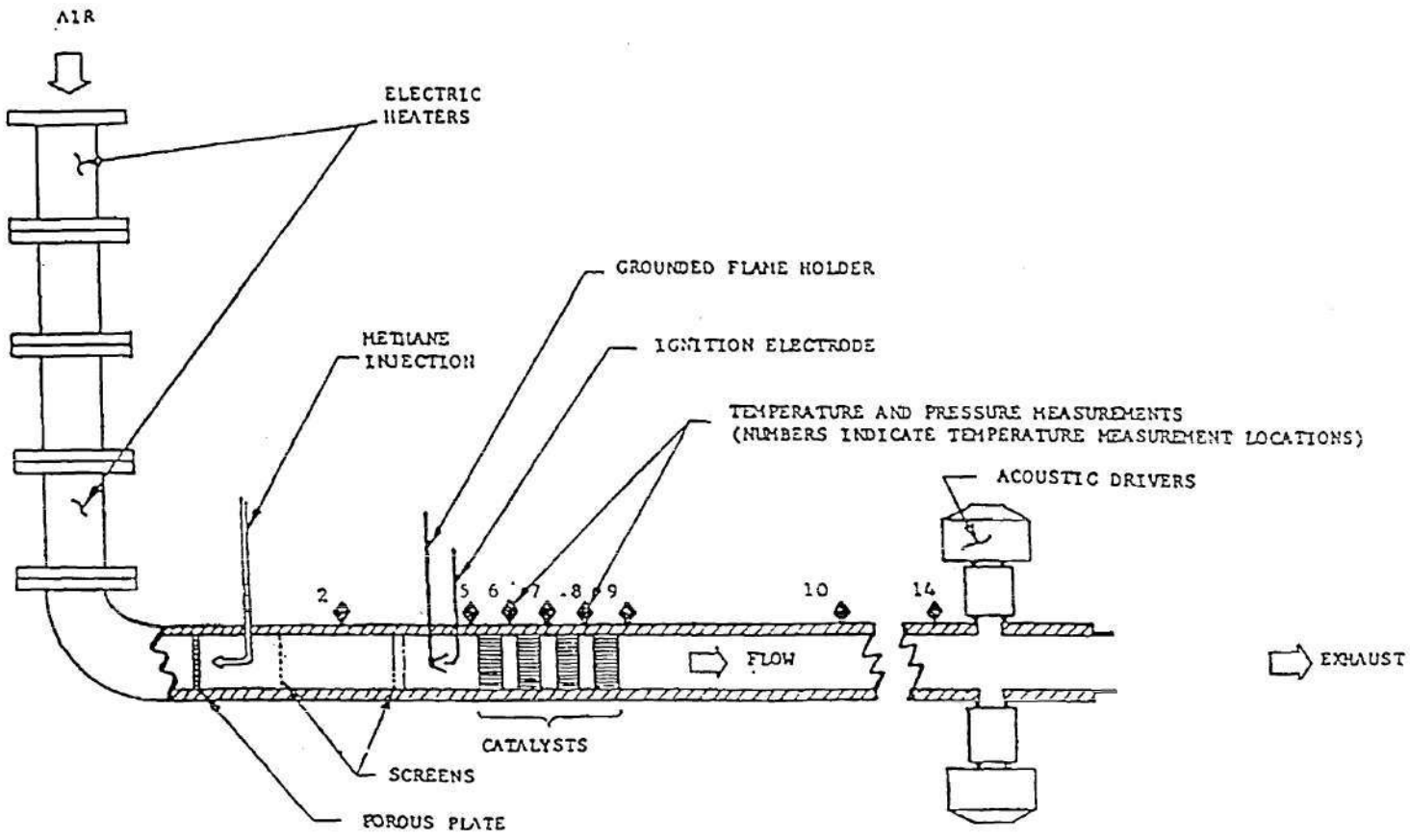

Figure 1: A Schematic of the Developed Pulsed Catalytic Combustor

reactions, gas phase reactions can also be initiated and take place in the catalyst section. The combustion products leave the catalytic combustion section and move along the horizontal pipe towards its open end where they are exhausted. The sound generation system is attached to the horizontal pipe just upstream of the exit plane. The horizontal part of the combustor which consists of the mixing section, the ignition system, the catalytic combustion section and several hollow pipe sections, is made of interchangeable pipe segments. This design provides a capability for moving the catalytic combustor section to various locations along the combustor.

An inner diameter of 2.5 inches was chosen for the catalytic combustor. This diameter represents a compromise between the need to minimize wall heat losses and total fuel flow. The latter also reduces operating costs and safety hazards. This decision was also influenced by experience at the *Alzeta Corp.* [26] where accurate and repetitive temperature and velocity measurements in catalytic combustors were achieved only when combustors having diameters of 2″ or larger were used.

Monolith type platinum catalyst segments, which have been widely used in recent investigations [1,2] as well as in automotive catalytic converters have been chosen for this research project. A monolith type catalyst consists of a ceramic honeycomb substrate coated with a thin layer of porous "washcoat". The "washcoat" has a very large specific surface area on which the active catalytic material is deposited. The stucture of typical monolith catalyst segments is shown in Fig. 2. The open channels in the honeycomb structure minimize the pressure drop in the gas flowing through the catalyst, and the "washcoat" provides a large surface area over a relatively short catalyst segment. An additional reason for using monolith type catalyst segments was the belief that due to the presence of straight and relatively large channels, the acoustic attenuation provided by these catalysts will be small compared to that exerted by other types of available catalysts. Up to

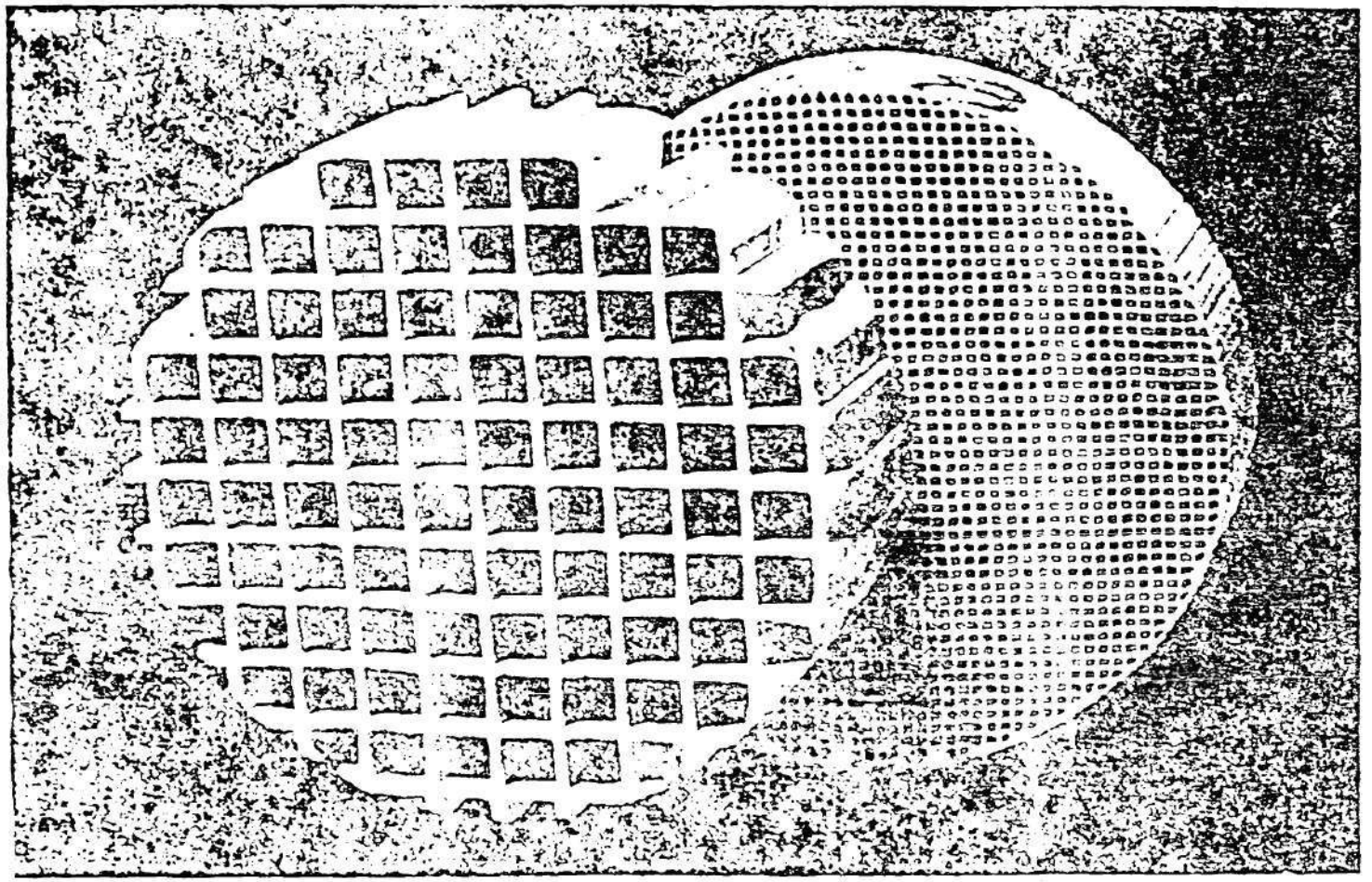

Figure 2: Typical Monolith Type Catalyst Segments.

four monolith units, each of them 1" long, could be used simultaneously in the developed experimental setup. There was no intention in this research to investigate which type of catalyst is optimal for use in pulsating catalytic combustors. Catalyst segments similar to those used at other facilities researching catalytic combustion were chosen for this study.

The combustion air is supplied from a compressed air line. Prior to entering the experimental setup, the air passes through a filter system which removes any particulates, moisture and oil mist from the flow. The air pressure is controlled by a pressure regulator and its flow rate is measured by a rotameter system. The flow rate is determined by the pressure and the line resistance which is changed by a needle valve downstream of the rotameter on the air line connected to the experimental setup.

The air enters the combustor at the top of the vertical pipe section where it is preheated. Four electric heaters with total output of up to $12kW$ were selected for the heating of the combustion air. To attain air temperature control, some of the heaters were powered by on-off toggle switches while others were connected to a variable voltage regulator. The maximum mixture temperature needed for "light-off" of methane/air catalytic reaction at the entrance to the catalyst section was assumed to be 500 ^oC.

The fuel (commercial methane or propane) is supplied from a high pressure bottle equipped with a pressure regulator that lowers the pressure to approximately 120 psi. The fuel then flows through a 1/4" stainless steel tube to the fuel flow rate measuring system, which is similar to that of the air, consisting of a second pressure regulator, a rotameter and a needle valve. The fuel flows from the valve to the injector at the inlet of the mixing chamber through a solenoid valve and a flame arrestor. The solenoid acts as a shut-off valve and it can stop the flow of fuel to the combustor instantaneously. The flame arrestor is a safety device which prevents the upstream propagation of the flame into the fuel line.

The combustion products are exhausted through an 8″ circular duct with its inlet 2 feet from the combustor exit plane. The duct connects to a high output exhaust fan which pumps additional air from the area adjacent to the combustors exit to cool down the combustion products.

The Acoustic System

A catalytic combustor is known to operate at very low noise levels in comparison with gas-phase combustors, and spontaneous self-driven pulsations were not expected. Thus, in order to excite the desired pulsations, an acoustic driving system had to be incorporated into the system.

A voltage signal changing sinusoidally with time at any desired frequency is created by a function generator and serves as the input of the acoustic driving system. The signal is amplified by a $100 watt$ acoustic amplifier and its high-level voltage output is fed into two *University Sound* electric acoustic drivers operated in tandem. The two acoustic drivers are set to generate its pulsations in phase so that their outputs are additive.

Upstream of the mixing section, a stainless steel porous plate is installed to restrict the air flow and create a pressure drop between the heating and fuel mixing sections. In addition to eliminating the posibility of flow of a combustible mixture upstream into the heating section, the porous plate reflects the acoustic waves and acts, acoustically, as a hard wall termination. The downstream end of the experimental setup is an open tube. Both the "open" tube and hard wall terminations are supposed, theoretically, to reflect the entire acoustic energy back into the tube. The hard and smooth inner combustor surface is known to produce negligible amount of acoustic energy dissipation. Thus, theoretically, a standing wave pattern should be created by any acoustic instability with resonance frequencies at values corresponding to odd number of quarter wavelengths. In reality, acoustic

energy losses exist, mainly due to viscous and radiative effects, and they increase as the temperature increases. The *Sound Pressure Level* excited by the system in the experimental setup depends upon the acoustic energy input by the driving system and the acoustic losses which are a function of the driving frequency and the characteristics of the experimental setup.

During the initial phase of this research it became clear that the location of the catalytic combustion section with respect to the acoustic standing wave might be one of the important parameters. Hence, provisions have been made to allow positioning the catalytic combustion section at several different locations along the horizontal part of the experimental setup. The interchangeable segments of the horizontal part of the experimental setup can be moved around or taken out. This provides the capabilities for positioning the catalytic combustion section at different locations with respect to the standing wave pattern, and for changing the acoustic characteristic of the system.

Measurements

The flow rate of both the air and the fuel are measured by rotameter systems consisting of a pressure regulator and a needle valve located upstream and downstream of the rotameter, respectively. The needle valve and the regulator together control the pressure in the rotameter, which is measured by a *Bourdon* type pressure gauge. The rotameters were calibrated at room temperature and atmospheric pressure for air, and their readings are corrected for pressure, temperature and composition of the gas flowing through it. Since the rotameters are accurate only within a limited range of flow rates, several rotameters for each gas were used for measuring the entire range of flow rates investigated in this research program.

Temperatures are measured at different locations along the center line of the expermental setup. K–type (Chromel — Alumel) thermocouples with no zero (ice

point) compensation are used. The thermocouple voltage is amplified by a *NEFF* amplifier, usually by a factor of 90, so that the maximum measurable temperature (approx. 1400 °C) would not exceed 5 *Volts,* which is the maximum voltage that the A/D converter can digitize.

Acoustic pressures are measured by *Kistler piezotron* miniature pressure transducers. These transducers are acceleration-compensated and produce a low impedance voltage signal which is proportional to the dynamic pressure input. The output from the pressure transducer is fed into a *Kistler* amplifier which generates a high-level signal that can be measured accurately by the data acquisition system.

A previously developed gas composition analysis system capable of measuring the concentrations of CO, CO_2, NO_x, O_2, SO_2, and *hydrocarbons* is utilized to measure these species' concentrations in the exhaust products.

A 220 *Volt* 60 *Amp.* line, controlled by a switching system and a variable voltage regulator, supplies the 12 *kw* electrical power for the air heating system. A 115 *Volt* line supplies the power needed for the operation of the acoustic driving system, the fuel solenoid shut-off valve and the instrumentation used in the experiment.

The Data Acquisition System

A 32 channel model 8013A *LeCroy* data logger equipped with a 12 bit A/D converter and an independent storage memory of 256 kilowords of 12 bit each is used in this research. The data logger can operate only one A/D converter and is thus limited to one sampling frequency at a time. It can acquire data from 32, 16, 8 or 4 channels simultaneously with a maximum sampling rate of 5, 10, 20, and 40*kHz*, respectively. The minimum sampling rate is not limited since the logger can be triggered by an external clock at any desired sampling frequency below the maximum sampling rate. The internal clock can be set for sampling frequen-

cies of 0.2, 1, 2, 5, 10, 20 and $40kHz$, but cannot exceed the maximum allowed rate. The data logger can store the data in its memory unit without moving the data to another storage location, and act as an accurate digital scope. In this configuration the data is erased every time a new set of measurements is started. This mode of operation is used when the time dependent data is not needed for future analysis, as in a calibration process. Alternatively, the data can be demultiplexed and transferred to the computer storage disk automatically after each set of measurements, to be analyzed later.

The data logger is controlled by an *IBM* Personal Computer AT with $640kbytes$ of RAM, a $30Mbyte$ hard drive, one double-sided double-density ($360kbyte$) and one double-sided high-density ($1.2Mbyte$) flexible disk drives. The data logger transfers the demultiplexed data from its independent storage unit to the hard drive. Each $12bit$ word is stored on two single-*byte* memory units of $8bit$ each on the hard drive. The computer is equipped with a *SYSGEN QIC-FILE* fast tape backup system which enables to transfer the data periodically for storage on backup tapes and free the hard drive for storage of new data.

Chapter III
THE DATA ANALYSIS

Time Dependent Data

The *CATALYST* software controlling the data logger stores the data of each set of measurements on the computer's hard drive as a *FORTRAN* unformatted sequential file. The *CATALYST* file starts with a header that contains the information needed for the interpretation of the data. This information includes the number of the starting channel, the number of channels, the sampling time interval, the *offset* and *amplitude* of the digitized voltage signal, the units in which the data is recorded, the size of a data block, the number of data blocks and the type of data recorded. After the header there is a space for a comment or message of up to 161 characters. The comment area and file name are used to identify the data set. Beyond the comment area the data is stored in blocks having the number and size defined by the file header. Each data point is stored as a two byte integer having a value between 0 and 4095. The *offset* value states which integer value corresponds to zero input voltage to the digitizer. Thus, all values smaller than this integer indicate negative input voltages and larger integers correspond to positive voltages. The *amplitude* specifies the value in *Volts* of one digit difference in the integer data. The data logger is generally used at its highest *amplitude*, which is 2.4414 *milliVolts,* and the *offset* is set to 2047, which corresponds to the range from -5 *Volts* to $+5$ *Volts*. It should be noted that the *CATALYST* software limits the highest sampling rate specified for an external clock to a time interval

of 9999 *microseconds* which corresponds to a sampling frequency of $100Hz$. If the sampling frequency is lower than $100Hz$, the header information must be corrected.

An *ILS* (Interactive Laboratory System — by *Signal Technology, Inc.*) software package is utilized for analyzing the data. This software requires information to be stored as *FORTRAN* unformatted sequential files, one file for each channel. *ILS* handles two types of files. Sampled data is stored as two byte integers. The *ILS sampled data* file is very similar to a *CATALYST* file except that it contains the data of only a single channel. *ILS* manipulates data using files where the data are stored as single precision floating point numbers, calling this type of files *records*. *ILS* provides programs which can change *sampled data* to *records*, and vice versa, when needed. The *CATALYST* software contains a program which transfers a *CATALYST* data file with n channels to n *ILS sampled data* files with consecutive numbers. A programming error which can cause an incorrect sampling frequency to be written in a *ILS sampled data* file was detected, and a correction of the sampling rate of the *ILS* files, is occasionally needed.

Due to simpler and quicker data manipulation when using *sampled data* files, all time dependent information is handled by this type of files. A program was developed that takes the original *CATALYST* data file, writes the *ILS sampled data* files, allows correction of the sampling rate and converts the data to its appropriate units. More information about the translation of the measured voltages to actual temperatures, pressures and species concentrations is given in the following paragraphs.

Calibration of the channels of temperature measurement are done by adjusting the zero output of the *NEFF* amplifier and setting an appropriate amplification gain. The maximum temperature a K – type thermocouple can measure is approximately 1400 °C, yielding a voltage difference of $55 milli Volts$. An amplification gain of 90 covers the entire measurable temperature range with a resolution of $27 micro Volts$ which corresponds to 0.6 – 0.8 °C. Since the thermocouple readings have

a large time constant, temperature data files are recorded at sampling frequencies of 5 to 10Hz. If higher sampling rates are used, the sampling frequency is reduced to save storage space. The program divides the measured voltage by the amplification gain to calculate the thermocouple output voltage and uses the 9th order *NBS* [27] polynomial to calculate the corresponding temperature. Since the individual channels do not have an ice point compensation unit, the calculated temperature is the difference between the actual temperature and the temperatue of the input board at the instrumentation panel. This temperature is, approximately, the ambient temperature. The (uncorrected) calculated temperature values in °C are written to the hard drive in an *ILS sampled data* format.

Calibration of the channels measuring dynamic pressure is done utilizing a *Photocon Systems* acoustic calibrator which inputs a 1000Hz signal whose amplitude can be set to any desired level between 95 and 160dB. The *Kistler* amplifier output signal is measured by an AC voltmeter. The program asks for the the amplitude of the pressure signal and the AC calibration voltage. It assumes the calibration signal to be sinusoidal and the voltage to be a true RMS value to establish the ratio between the pressure acting on the transducer and the input to the data logger. Since the pressure transducers' response is linear, only the header information in the *ILS* file is altered, changing the units to *psi* and setting the correct *amplitude.*

The chemical analysis system consists of six individual analyzers for CO, CO_2, SO_2, O_2, NO or NO_x and *hydrocarbons.* Detailed information about the principles of their operation, calibration and use, is presented in the systems' operation manual [28]. The calibration of each analyzer is done with a *zero concentration gas,* which is used to adjust the zero reading, and a *calibration gas* which has a specified concentration of the gas the analyzer is supposed to detect. Each analyzer output can be set to a desired amplification by changing the *range* and *gain* settings, and reading the DC output voltage. The time constants of the

analyzers are larger than those of the thermocouples, and the sampling rate is decided by the temperature data.

The first three analyzers (CO, CO_2, and SO_2) have nonlinear response, and the output voltage per unit of species concentration decreases as the concentration increases. Originally, the analyzers were calibrated for each region of concentration and supplied with factory calibration charts. However, in order to computerize the data analysis, the calibration charts were used to calculate a response curve for each analyzer. The response curves state what is the ratio of voltage output at any concentration to the output at the maximum concentration specified for the analyzer. By letting a specific voltage output correspond to the calibration gas concentration, the response curve can be interpreted in terms of voltage response to the concentration input. Polynomial correlations for the voltage output as a function of the concentration (i.e., forward polynomial) and the concentration as a function of the measured voltage (i.e., backward polynomial) were developed. The forward polynomial is used to convert the response curve units to voltage by utilizing the calibration data and the backward polynomial is used to calculate the concentration data from the measured voltage. The calculated concentration is stored as integer data in *ILS sampled data* format.

The O_2, NO/NO_x, and *hydrocarbon* analyzers have linear responses which means that the measured voltage is proportional to the species concentration. The calibration gas concentration and the DC calibration voltage of the analyzer specify the proportionality constant, and as in the case with the dynamic pressure channels, only the header information in the *ILS* file is altered; that is, changing the units to proper species concentration and setting the correct *amplitude*.

The data measured by the hydrocarbon, O_2 and CO_2 analyzers was used to calculate combustion efficiencies. Explanation about the determination of the combustion efficiency is given in Appendix A.

Spectral Analysis

The *ILS* software package enables calculation of various spectral relationships, but with limited spectral resolution of these functions (i.e., the *FFT* program limits the analysis to 1024 data points and cross-spectra are limited to 256 points). It also has no provisions for calculation of ensemble averages and *SPL* values. In view of these limitations, only the basic *ILS FFT* program was used with additional analysis software which was developed on an as needed basis. The *CATALYST* data acquisition system cannot transfer partial data to the computer memory, and the transfer of data to the computer takes several minutes. Thus, data collected during a single run must be utilized for ensemble averaging. Spectral analysis of the pressure data at the maximum possible sampling frequency (i.e., $10kHz$ for 16 channels) at the entire range of frequencies explored (i.e., 200 to $2000Hz$) showed that the spectrum was dominated by the driving frequency set by the function generator with peaks of several higher harmonics being more than an order of magnitude (i.e., $20dB$) weaker. The peaks had narrow bandwidth, and it was assumed that a Nyquist frequency 25% higher than the driving frequency would be sufficient for the spectral analysis. Using a low Nyquist frequency provides a better spectral resolution of the *FFT* information.

The spectral analysis program takes one block of 1024 consecutive points from the measured time series and calculates the *FFT* transform in polar form at the original sampling rate, which is usually $5kHz$. The program than finds where the peak of the spectral signal is located, and decides by which factor (power of 2) to downsample the data to get the best Nyquist frequency for that data set. The program then rearranges all the data in the time series file into blocks of 1024 points with time intervals corresponding to the assigned Nyquist frequency, and performs *FFT* transformation on all blocks. Since the phase information in the *FFT* data is arbitrary, and is the outcome of DC noise, the program shifts the phases of all blocks except the first, so that the phase at the spectral peak is

identical to the phase of the first block. This procedure corresponds to triggering a data logger to start acquiring data for every block at the same location on the sinusoidal pressure signal of the driving frequency. The program then averages the real and imaginary parts of the *FFT* data and stores the averaged *FFT* data in an *ILS record.* When more than 16 channels were monitored, only 8 blocks of 1024 data points each were measured for each pressure channel. Averaging these eight ensembles for each channel resulted in considerably lower noise level.

The averaged *FFT* data are used to calculate the autospectrum. Usually, this information is given in logarithmic scale compared to the threshold of hearing, in *dB* units. The spectral analysis program calculates the *SPL* level in *dB* for each point in the frequency domain. To get the total power of the signal, integration of the pressure is performed over the entire frequency range. Ninety nine percent of the contribution to the total power is from about 10 points, 5 on each side of the main spectral peak. The spectral analysis program writes an *ASCII* file which includes a header, the spectral data and the total calculated acoustic power. The file header gives information about the nature of the data. The spectral data includes the *FFT* information for each frequeny in both polar and rectangular forms, and the frequency resolved *SPL* in *dB*.

The cross-spectrum is used to find phase differences between channels. The cross-spectrum is calculated using the averaged *FFT* data. The phase difference is meaningful only at the driving frequency, and should converge to a constant value as the driving frequency is approached from either direction. Away from the driving frequency, the calculated phase is due to noise, and has arbitrary values.

The values of the pressure amplitudes along the combustor, and its phase difference were used to correlate the experimental data with data calculated using a developed theoretical model, which is presented in Chapter IV.

Chapter IV

THEORETHICAL REPRESENTATIVE MODEL

Overview

In this chapter equations which describe the behavior of acoustic waves in a duct with a low velocity gas flow and a steady temperature gradient are developed. The steady-state equations and the measured temperature data are used to derive continuous, approximate functions describing the axial dependence of the gas mixture temperature, density and mean flow velocity in the developed experimental setup. The first order equations are manipulated to derive a wave equation for a tube with temperature gradients and a low Mach number flow, which represent the conditions inside the developed catalytic combustor setup. The wave equation is solved by an approximate analytical approach which uses the steady-state density and temperature profiles and a single measurement of acoustic pressure to calculate the distribution of the acoustic pressure and velocity amplitudes and phases along the combustor. Since we are not measuring the acoustic velocities in our experimental setup, and dynamic pressures are only measured at several discrete locations along the combustor, the calculated dynamic pressure and velocity distributions yield important information regarding the location of pressure and velocity nodes and antinodes and the location of the catalytic combustion section with respect to the excited acoustic wave.

In this analysis we assume that a one-dimensional representation of the flow in the tube is adequate, and that the gaseous medium is inviscid and thermally

perfect. Since our experimental setup is not insulated and considerable heat losses to the combustor walls are present, such heat losses are taken into account in the energy balance. Large radial temperature gradients exist in the experimental combustor, and the mixture temperatures used in the analysis were those measured along the centerline of the combustor. A good agreement was found between the calculated and measured acoustic pressures, as will be presented in Chapter V.

The Steady-State Solution

The flow of the gaseous medium through a tube of a fixed diameter is governed by the following one-dimentional conservation equations:

- Continuity:

$$\frac{\partial \rho}{\partial t} + \frac{\partial}{\partial x}(\rho v) = 0 \tag{1}$$

- Momentum:

$$\rho \frac{Dv}{Dt} = -\frac{\partial p}{\partial x} \tag{2}$$

- Energy:

$$\rho C_p \frac{DT}{Dt} = \frac{Dp}{Dt} + q_r - U(T - T_o) \tag{3}$$

- State:

$$p = \rho RT \tag{4}$$

Where ρ, v, p, T, U, C_p, q_r, R, x, and t are the gas density, the gas velocity, the pressure, the absolute temperature, the heat transfer coefficient per unit length of the tube, the specific heat of the gas mixture at constant pressure, the rate of heat generation by the reaction per unit length of the tube, the universal gas constant, the axial coordinate, and the time, respectively. T_o is the tube's outer wall temperature, and the term $U(T - T_o)$ represents heat losses through the tube's walls. $\frac{D}{Dt}$ is the substantial derivative.

Assuming that any variable s can be expressed as a sum of the time averaged value $\bar{s}$ and higher order perturbations denoted by s', etc., the expressions for the density, temperature, pressure, velocity and the heat generated become:

$$\begin{aligned}
\rho(x,t) &= \bar{\rho}(x) + \rho'(x,t) + \cdots \\
T(x,t) &= \bar{T}(x) + T'(x,t) + \cdots \\
p(x,t) &= \bar{p}(x) + p'(x,t) + \cdots \\
v(x,t) &= \bar{v}(x) + v'(x,t) + \cdots \\
q_r(x,t) &= \bar{q}_r(x) + q_r'(x,t) + \cdots
\end{aligned} \tag{5}$$

The equations involving only the time averaged values for each variable – the *zero order* equations, yield the time averaged "steady-state" representation of the physical behavior of the gases flowing through the tube. The steady-state conservation equations are derived from Eqs. 1 through 4 by replacing each dependent variable $s(x,t)$ by its time averaged value $\bar{s}(x)$. In addition, the assumption that momentum convection can be neglected is made based on having a low mean flow velocity and inviscid fluid, yielding –

- Continuity:

$$\bar{\rho}\,\bar{v} = \dot{m} = Constant \tag{6}$$

where $\dot{m}$ is the mass flux.

- Momentum:

$$\frac{d\bar{p}}{dx} = 0 \qquad \text{or} \qquad \bar{p} = Constant \tag{7}$$

- Energy:

$$\bar{\rho}\bar{v}C_p\frac{d\bar{T}}{dx} = \bar{q}_r - U(\bar{T} - \bar{T}_o) \tag{8}$$

- State:

$$\bar{p} = \bar{\rho}R\bar{T} \tag{9}$$

The axial dependence of the time averaged temperature, density and velocity is calculated utilizing Eqs. (6) to (9) and measured temperature, concentration and flow data. The mass flux $\dot{m} = \bar{\rho}\bar{v}$ is calculated by dividing the sum of the measured flow rates of the air and the fuel by the tube's cross-section area. In Eq. (9) we have two unknown parameters – the heat transfer coefficient – U, and the heat generated by the chemical reaction per unit length – $\bar{q}_r$. The specific heat of the gas mixture as function of temperature can be found in thermodynamical data. The average mass flow rate $\dot{m}$ and the reactants concentrations at the inlet and exhaust of the combustor specify the total energy input by the chemical reaction per unit time – $\bar{Q}_r = \int \bar{q}_r \, dx$. Since the reaction is spatially limited to the catalyst section region, and most of the reaction occurs on a short axial distance on the surface of one active catalyst segment, a *flame sheet approximation* was used. This approximation assumes a plane of discontinuity at the center of the active catalyst segment, where the entire heat of reaction is added to the system. Discontinuity in the average temperature, density and velocity exist at this axial location. The energy equation on both sides of the *"flame sheet"* becomes:

$$\bar{\rho}\bar{v}C_p\frac{d\bar{T}}{dx} = -U(\bar{T} - \bar{T}_o) \tag{10}$$

The heat transfer coefficient – U can be estimated by matching the measured temperature drops both upstream and downstream of the catalyst under non-pulsating conditions, with the results obtained by integrating numerically Eq. (10) assuming $\bar{T}_o$ to be equal to the ambient temperature, and using different values for U. The best fit yields an axial average temperature profile $\bar{T}(x)$ for the combustor. If Eq. (9) is used assuming the average pressure to be equal to the barometric pressure, the calculated temperature profile can be used to yield the average axial density profile. Dividing the mass flux $\dot{m}$ by the local average density yields the axial dependence of the mean flow velocity, thus completing the determination of the steady-state distributions of the dependent variables within the developed combustor.

The First Order Equations

First order conservation equations are used to derive the wave equations for the developed catalytic combustor which consists of a constant diameter tube with heat losses at the walls and containing a low Mach number flow. To get the conservation equation for the first order perturbations, the expressions in Eq. (5) are substituted into Eqs. (1) through (4), and all terms of order higher than second are neglected. In addition, the steady-state conservation equations are substracted, and the convective terms involving $\bar{v}$ are neglected because of the low Mach number assumption. This yields:

- Continuity:

$$\frac{\partial \rho'}{\partial t} + \frac{\partial}{\partial x}(\bar{\rho} v') = 0 \tag{11}$$

- Momentum:

$$\bar{\rho} \frac{\partial v'}{\partial t} = -\frac{\partial p'}{\partial x} \tag{12}$$

- Energy:

$$\bar{\rho} C_p \frac{\partial T'}{\partial t} + \bar{\rho} v' C_p \frac{d\bar{T}}{dx} = \frac{\partial p'}{\partial t} + q_r' - U(T' - T_o') \tag{13}$$

  Further simplification of the energy equation is done by neglecting the last two terms on the right handside of Eq. (13). These two terms represent the fluctuating heat addition and removal to and from the system. This investigation shows that the acoustic waves can have considerable effect on both heat generation by the reaction (i.e., the improvement in combustion efficiency) and heat losses through the wall of the tube (due to the changes in temperature distribution). These improvements prove that the pulsations affect the time averaged heat addition and removal from the combustor, but it was not possible to measure the effect on their perturbations. Periodic heat inflows and outflows, when located at certain positions on the acoustic standing wave pattern with proper phase relative to the local pressure oscillations, induce self-driven pulsations. Since in catalytic combustion with

heterogeneous reactions, spotaneous acoustic pulsations are not detected, it is reasonable to assume that these terms are negligible. Thus the final simplified energy equation is:

$$\bar{\rho}C_p \frac{\partial T'}{\partial t} + \bar{\rho}C_p v' \frac{\partial \bar{T}}{\partial x} = \frac{\partial p'}{\partial t} \tag{14}$$

- State:

$$p' = \bar{\rho}RT' + \rho' R\bar{T} \tag{15}$$

The four equations describing the first order deviation from the time averaged values of the flow variables in the catalytic combustor (11, 12, 14 and 15) can be used to derive a wave equation valid in a one-dimentional, non-isothermal low Mach number flow. First, the state equations are used to express the temperatures in terms of the pressures and densities, yielding:

$$\frac{1}{\bar{T}}\frac{d\bar{T}}{dx} = -\frac{1}{\bar{\rho}}\frac{d\bar{\rho}}{dx} \tag{16}$$

and:

$$\bar{\rho}\frac{\partial T'}{\partial t} = \frac{1}{R}\frac{\partial p'}{\partial t} - \bar{T}\frac{\partial \rho'}{\partial t} \tag{17}$$

Equations (16) and (17) are now substituted into the energy equation (14), and using the thermodynamic identity $C_p - C_v = R$ gives:

$$\frac{C_v}{R}\frac{\partial p'}{\partial t} - C_P \bar{T}\left(\frac{\partial \rho'}{\partial t} + v'\frac{\partial \bar{\rho}}{\partial x}\right) = 0 \tag{18}$$

Substituting the expression for $\frac{\partial \rho'}{\partial t} + v'\frac{\partial \bar{\rho}}{\partial x}$ from the first order continuity equation (11) and defining a local speed of sound $\bar{c}^2(x) = \gamma R\bar{T} = \frac{C_p}{C_v}R\bar{T}$, Eq. (18) can be written as:

$$\frac{1}{\bar{c}^2}\frac{\partial p'}{\partial t} + \bar{\rho}\frac{\partial v'}{\partial x} = 0 \tag{19}$$

Differentiating Eq. (19) with respect to time gives:

$$\frac{1}{\bar{c}^2}\frac{\partial^2 p'}{\partial t^2} + \bar{\rho}\frac{\partial^2 v'}{\partial x \partial t} = 0 \tag{20}$$

Differentiating the first order momentum equation (12) with respect to the axial coordinate x yields:

$$\bar{\rho}\frac{\partial^2 v'}{\partial x \partial t} = -\frac{\partial^2 p'}{\partial x^2} + \frac{1}{\bar{\rho}}\frac{d\bar{\rho}}{dx}\frac{\partial p'}{\partial x} \tag{21}$$

Finally, the wave equation for a one-dimensional, non-isothermal low Mach number flow is derived by substituting Eq. (21) into Eq. (20):

$$\frac{1}{\bar{c}^2}\frac{\partial^2 p'}{\partial t^2} - \frac{\partial^2 p'}{\partial x^2} + \frac{1}{\bar{\rho}}\frac{d\bar{\rho}}{dx}\frac{\partial p'}{\partial x} = 0 \tag{22}$$

This equation was suggested by Cummings [29] for analysis of acoustic pulsations in non-isothermal low Mach number flow. The last term in equation (22) represents the deviation from the classical one-dimensional wave equation in homogeneous medium due to temperature gradients along the axial coordinate. When isothermal conditions exist in the tube, $\frac{d\bar{\rho}}{dx}$ is zero and the conventional one-dimensional wave equation for isothermal, low Mach number flow, is obtained.

Approximate Solution of the Helmholtz Equation

Assuming that

$$p'(x,t) = \hat{P}(x)\, e^{i\omega t} \tag{23}$$

where $\hat{P}(x)$ is a spatially dependent complex variable, and substituting Eq. (23) into the wave equation (22) yields the corresponding *Helmholtz* Equation:

$$\left(\frac{\omega}{\bar{c}}\right)^2 \hat{P} + \frac{d^2\hat{P}}{dx^2} - \frac{1}{\bar{\rho}}\frac{d\bar{\rho}}{dx}\frac{d\hat{P}}{dx} = 0 \tag{24}$$

Cummings suggested two ways to solve this ordinary, second-order, differential equation with variable coefficients; a numerical solution [29], and an approximate analytical approach [30] which was adopted in this study.

In order to solve the Helmholtz equation analytically, it is assumed that the complex amplitude function $\hat{P}(x)$ can be represented by:

$$\hat{P}(x) = A\, e^{\int [a(x)+ib(x)]dx} \tag{25}$$

where a and b are real functions of x. a represents the change in the amplitude due to the temperature gradient and b the phase velocity of the axial traveling wave. Substituting Eq. (25) and its spatial derivatives into the *Helmholtz* equation (24) yields:

$$\left[\frac{\omega}{\bar{c}(x)}\right]^2 + (a+ib)^2 + \left(\frac{da}{dx} + i\frac{db}{dx}\right) = (a+ib)\frac{1}{\bar{\rho}}\frac{d\bar{\rho}}{dx} \tag{26}$$

Separating Eq. (26) into its real and imaginary parts yields:

$$\left[\frac{\omega}{\bar{c}(x)}\right]^2 + [a(x)]^2 - [b(x)]^2 + \frac{da(x)}{dx} = a(x)\frac{1}{\bar{\rho}}\frac{d\bar{\rho}}{dx} \tag{27}$$

and

$$2a(x)\,b(x) + \frac{db(x)}{dx} = b(x)\frac{1}{\bar{\rho}}\frac{d\bar{\rho}}{dx} \tag{28}$$

Rearranging Eqs. (27) and (28) gives:

$$[b(x)]^2 = \left[\frac{\omega}{\bar{c}(x)}\right]^2 + [a(x)]^2 + \frac{d\,a(x)}{dx} - a(x)\frac{1}{\bar{\rho}}\frac{d\bar{\rho}}{dx} \tag{29}$$

and

$$a(x) = \frac{1}{2\bar{\rho}}\frac{d\bar{\rho}}{dx} - \frac{1}{2b(x)}\frac{d\,b(x)}{dx} \tag{30}$$

a and b can be determined by an iterative solution technique. First, the assumption is made that a and its first spatial derivative are small enough to be neglected in comparison to the wave number in Eq. (29), and the following approximate value of b is obtained:

$$[b(x)]^2 = \left[\frac{\omega}{\bar{c}_{(x)}}\right]^2 \qquad or \qquad b(x) = \pm\left[\frac{\omega}{\bar{c}(x)}\right] \tag{31}$$

The first spatial derivative of b, assuming γ to be constant is:

$$\frac{db(x)}{dx} = \pm\frac{d}{dx}\left(\frac{\omega}{\bar{c}}\right) = \pm\omega\frac{d}{dx}\left(\frac{1}{\sqrt{\gamma R\bar{T}}}\right) = \pm\frac{\omega}{\sqrt{\gamma R}}\frac{d}{dx}(\bar{T}^{-0.5}) =$$

$$= \mp\frac{\omega}{2\sqrt{\gamma R}}\bar{T}^{(-1.5)}\frac{d\bar{T}}{dx} = \mp\frac{\omega}{2\sqrt{\gamma R\bar{T}}}\frac{1}{\bar{T}}\frac{d\bar{T}}{dx} \tag{32}$$

Using Eq. (16), Eq. (32) becomes:

$$\frac{d\,b(x)}{dx} = \pm\frac{\omega}{2\sqrt{\gamma R\bar{T}}}\frac{1}{\bar{\rho}}\frac{d\bar{\rho}}{dx} = \pm\frac{\omega}{2\,\bar{c}(x)}\frac{1}{\bar{\rho}}\frac{d\bar{\rho}}{dx} \tag{33}$$

Substituting the expression for $b(x)$, Eq. (31), and its derivative Eq. (33) into the expression for $a(x)$, Eq. (30), gives:

$$a(x) = \frac{1}{2\bar{\rho}}\frac{d\bar{\rho}}{dx} - \frac{1}{4\bar{\rho}}\frac{d\bar{\rho}}{dx} = \frac{1}{4\bar{\rho}}\frac{d\bar{\rho}}{dx} \tag{34}$$

Eqs. (31) and (34) are the first iterative approximations for $b(x)$ and $a(x)$, respectively. The expression for a in Eq. (34) can now be utilized to get a better approximation for b, and so forth. It should be noted that the first approximation should be applicable when the temperature (and density) gradient is relatively small. Cummings [30] found that when using the above relations, the calculated and the experimental data fit very well even when the temperature gradient was large. In view of Cummings' results, the first order approximations were used in this investigation to calculate the acoustic pressure and velocity, both upstream and downstream of the catalytic combustor section.

Using the approximate relation for $a(x)$, one gets:

$$\int_0^x a(x)\,dx = \frac{1}{4}\int_0^x \frac{1}{\bar{\rho}}d\bar{\rho} = \frac{1}{4}\int_0^x d\ln\bar{\rho} = \ln\left[\frac{\bar{\rho}(x)}{\bar{\rho}_0}\right]^{\frac{1}{4}} \tag{35}$$

Next, substituting Eqs. (31) and (35) into Eq. (25) yields the following solution for the acoustic pressure in the non-isothermal case:

$$\hat{P} = A\,e^{\ln\left[\frac{\bar{\rho}(x)}{\bar{\rho}_0}\right]^{\frac{1}{4}}} e^{\,i\int_0^x b(x)\,dx} = \tag{36}$$

$$= \left[\frac{\bar{\rho}(x)}{\bar{\rho}_0}\right]^{\frac{1}{4}}\left\{A_{(-)}\,e^{\,-i\int_0^x \frac{\omega}{\bar{c}(x)}dx} + A_{(+)}\,e^{\,+i\int_0^x \frac{\omega}{\bar{c}(x)}dx}\right\}$$

Equation (36) includes two complex constants $A_{(-)}$ and $A_{(+)}$ which are the complex amplitudes at $x = 0$ of the waves propagating in the $+x$ and $-x$ directions, respectively. These two constants must be known in order to calculate the acoustic

pressure along the combustor. In general, if the acoustic pressure and velocity (or the acoustic pressure and impedance) are known at a certain location, these two constants can be calculated. In the present study, the origin of the axial coordinate was chosen to be the porous plate at the entrance to the mixing section, where the acoustic conditions approximate a hard wall termination. Thus, at $x = 0$ the acoustic wave is totally reflected (i.e., $A_{(-)} = A_{(+)} = \mathcal{A}$), and the acoustic velocity is zero. Since the phase at one point can be set arbitrarily, the phase at $x = 0$ is taken to be zero. The amplitude at $x = 0$ thus becomes $P_0 = \Re\{\hat{P}_{(x=0)}\} = 2\mathcal{A}$, and the expression for the pressure amplitude in the experimental setup is:

$$P(x) = \Re\left\{\hat{P}(x)\right\} = \mathcal{A}\left[\frac{\bar{\rho}_{(x)}}{\bar{\rho}_0}\right]^{\frac{1}{4}} \left\{e^{-i\int_0^x \frac{\omega}{\bar{c}(x)}dx} + e^{+i\int_0^x \frac{\omega}{\bar{c}(x)}dx}\right\} \tag{37}$$

As in the isothermal case, $\hat{P} \equiv P$, and is always real. The pressure oscillations are in phase (or 180 degrees out of phase) everywhere in the combustor. The expression for acoustic pressure becomes simpler and more meaningful when expressed as a trigonometric function, and when $2\mathcal{A}$ is replaced by the pressure amplitude P_o at $x = 0$; that is:

$$P(x) = P_0\left[\frac{\bar{\rho}_{(x)}}{\bar{\rho}_0}\right]^{\frac{1}{4}} \cos\left\{\int_0^x \frac{\omega}{\bar{c}_{(x)}}dx\right\} \tag{38}$$

And the expression for the acoustic pressure p' is:

$$p'(x,t) = P_0\left[\frac{\bar{\rho}_{(x)}}{\bar{\rho}_0}\right]^{\frac{1}{4}} \cos\left\{\int_0^x \frac{\omega}{\bar{c}_{(x)}}dx\right\} \cos\omega t \tag{39}$$

The acoustic velocity v' is calculated from the acoustic pressure using the first order momentum equation (12):

$$i\omega V(x)e^{i\omega t} = \frac{\partial v'(x,t)}{\partial x} = -\frac{1}{\bar{\rho}}\frac{\partial p'}{\partial x} = -\frac{1}{\bar{\rho}}\frac{dP(x)}{dx}e^{i\omega t} \tag{40}$$

The acoustic velocity leads (or lags) the pressure by 90 degrees and its amplitude can be calculated from the acoustic pressure amplitude using the following relationship:

$$V(x) = \frac{1}{\bar{\rho}\omega}\frac{dP(x)}{dx} \tag{41}$$

It should be noted that $P(x)$ and $V(x)$ in this derivation, have both positive and negative values. This is different from the usual definition of amplitude whose magnitude is always positive. $P(x)$ is the instantaneous acoustic pressure at the time when the pressure at the "acoustic hard wall termination" reaches a maximum value. $V(x)$ is the instantaneous acoustic velocity half a cycle later, when the velocities near even and odd pressure nodes reach maximum and minimum values, respectively. This description of the acoustic amplitudes was chosen because when the data is presented the locations of the nodes and the relative phase differences are shown clearly in a single figure, as in Fig. 3. The negative values of either pressure or velocity indicate a 180 degree phase change with respect to the positive values. When both the pressure and the velocity have the same sign (i.e., for $0 < x < .5$ and $1 < x < 1.5$ in Fig. 3), the acoustic velocity leads the pressure by 90 degrees and the acoustic pressure and gas particle displacements are in phase (i.e., as the pressure increases the gas particles move in the downstream direction, and vice versa). When the signs are opposite (i.e., for $.5 < x < 1$ and $1.5 < x < 2$ in Fig. 3), the velocity lags the pressure by 90 degrees. In this case the acoustic pressure and velocity are out of phase and the gas particle displacements are in the upstream direction when pressure increases, and in the downstream direction when the pressure decreases.

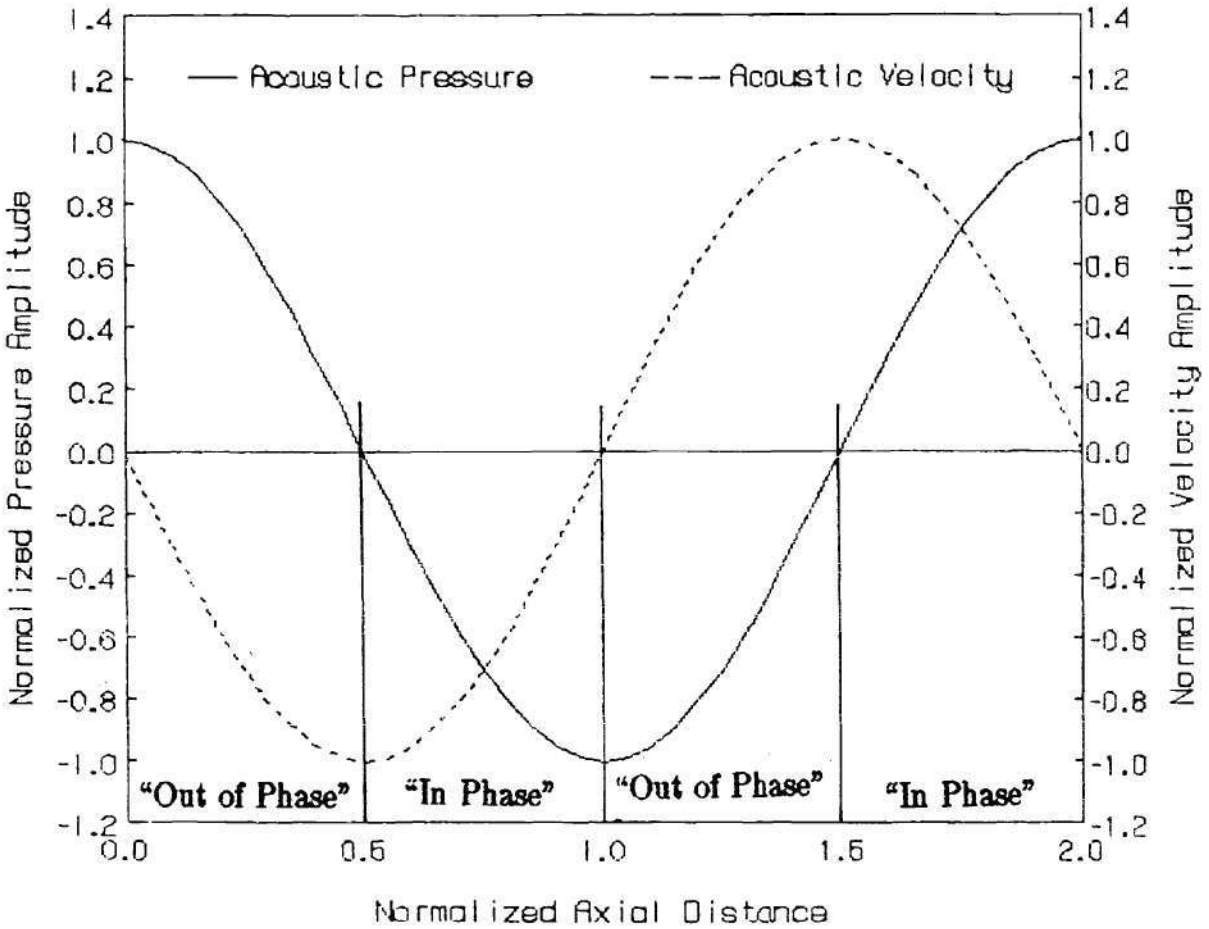

Figure 3: Normalized Pressure and Velocity Amplitudes for a Single Wavelength along the Axial Coordinate.

Chapter V
RESULTS AND DISCUSSION

Introduction

The objectives of this research were to investigate the feasibility of operating a catalytic combustor under pulsating conditions and to determine whether acoustic pulsations would improve the combustor's performance. In order to attain these objectives, the experimental system should be capable of maintaining incomplete but stable catalytic combustion with no gas phase reactions under non-pulsating operation, and react stably upon the introduction of acoustic oscillations. Since commercial methane is the most widely used gaseous fuel and the sponsor of the research program was interested in the investigation of its combustion, methane was chosen as the fuel in the first stage of this investigation.

Methane was used to check the proper operation of the experimental setup and to develop an appropriate test procedure. These initial tests revealed that the available catalyst was not as active as it should have been according to the literature. Spontaneous ignition of surface reactions did not occur at catalyst temperatures below 500 °C, although the literature [3,4,31] reported that ignition should occur at temperatures below 400 °C. Consequently, a new ignition method had to be developed. Additional tests with methane revealed that the measurements of temperatures and acoustic pressures along the combustor in different tests conducted under identical conditions were not repetitive and that stable incomplete catalytic combustion of methane could not be reached due to the poor

performance of the catalyst. Since operating conditions of the developed experimental setup for which the combustion of methane was incomplete could not be found, another fuel which is more reactive and could ignite spontaneously on the catalyst at low temperatures had to be found in order to meet the objectives of this study. Propane was found to satisfy these requirements. In what follows, the results of the tests with methane are presented in the first part of this chapter, and those obtained with propane are presented in the second part.

Catalyst Light-Off

According to the literature [3,4,31] ignition of methane on a catalytic surface occurs in the 250 – 400 °C temperature range for a wide range of methane/air ratios. Since our heating system was capable of delivering mixture temperatures of up to, approximately, 500 °C, it was assumed that spontaneous catalytic combustion can be started by flowing a hot methane/air mixture over the catalyst. Initial attempts to ignite the catalytic combustor with methane concentrations both above and below the lower flammability limits (i.e., methane concentrations in the range of 2 to 6 percent by volume) failed in spite of the fact that the catalyst was preheated with hot air to 525 °C and a mixture temperature of approximately 500 °C was used. Contacts with investigators at the *Alzeta Corp.* (the supplier of the catalyst segments) revealed that the catalyst surfaces needed to be heated to a very high temperature (i.e., approximately 1300 °C) in order to start catalytic reactions. Consequently, it was decided to preheat the catalyst surfaces with a flame produced at the beginning of every test by igniting a flammable methane/air mixture upstream of the catalytic combustion section. The resulting flame heated the catalytic surfaces to the desired high temperature in a very short time. Subsequently, the methane flow rate was cut off for a period of 2 to 3 seconds to extinguish the gas phase flame. The methane valve was then opened

again to establish a flow rate needed for catalytic heterogeneous reaction. This was generally below the lower flammability limit for ambient temperatures; that is, between 1 and 4 percent methane by volume. Following this procedure heterogeneous catalytic reaction could be attained repeatedly. Catalytic surface reaction under non-pulsating conditions could not be stabilized at extremely low flow rates or when very lean methane/air mixtures were used.

When flow rates below 50 *Std. lit/sec* were used with methane concentrations higher than approximately 2.3 percent methane by volume the reaction shifted upstream and a gas phase flame anchored itself on the flame holder of the ignition system. This happened because heat generated by the reaction on the catalyst surfaces was conducted upstream and heated the incoming mixture. At the elevated mixture temperatures the lower flammability limit decreased and methane concentrations in excess of 2.3 percent could support gas phase reactions. Since at the low flow rates mixture flow velocities were lower than 2 *m/sec*, the flame velocity was higher than the flow velocity and the flame shifted upstream. When flow rates below 50 *lit/min* and methane concentrations between 1.5 and 2.3 percent were used, the reaction stopped after a short period of time, usually after a gas phase flame was detected. It is believed that the same phenomenon occurred in these cases, but the lower methane concentrations generated less heat due to the combustion. The heat generation rate was lower than the rate of heat losses through the walls and caused the temperatures along the combustor to decrease. Due to less heat conduction from the combustion zone in the upstream direction, the incoming methane/air mixture temperature decreased until the gas phase reaction was extinguished. The catalytic surfaces were too cold and could not reignite the surface reactions. When the mixture concentration and flow rate were too low (e.g., 1.5 percent methane at a flow rate of 50 *lit/min* or 1 percent at a flow rate of 90 *lit/min*, or less) the reaction stopped. It is believed that in these cases the heat supply by the reaction was lower than the heat losses through the

walls, resulting in cooling of the catalyst surfaces. Catalytic reaction was stable only when a temperature of 800 °C or higher was measured downstream of the active catalyst segment. When the mixture flow rate and methane concentration were decreased to below the above mentioned values, the temperature decreased gradually until the reaction stopped.

The temperature downstream of the catalytic section increased sharply with increasing flow rate and methane concentration. This happened because the heat input was larger than the heat losses through the walls. Operation of the experimental setup at catalyst temperatures in excess of approximately 1100 °C was not desirable. At about this temperature, onset of gas phase reactions occurred and damage to the catalyst starts. Consequently, stable catalytic combustion of methane with no gas phase reactions was possible only for a limited range of flow rates and methane concentrations. At flow rates of about 100 *lit/min* stable catalytic combustion was achieved with methane concentrations between 1.3 and 5 percent. At flow rates of about 600 *lit/min* the operation of the experimental setup was possible with methane concentrations between 1.5 and 2.1 percent, and for flow rates of 1000 *lit/min* or higher the temperatures were always in excess of 1100 °C, and operation of the combustor without gas phase reaction and damage to the catalyst was not possible.

Repetition/Hysteresis of Experimental Results

In the initial phase of this study the repeatability of the measured data was investigated. It was found that tests conducted at the same flow rates, methane concentrations, mixture inlet temperatures and catalyst configurations did not yield the same (or close) quantitative data. Temperature variations of 50 to 100 °C, and acoustic pressure variations of approximately 100% (i.e., 4 to 6 *dB*) were measured when tests were repeated.

There are several possible explanations for the observed variations in the measured parameters. The accuracy of the rotameters used to measure the flow rates of both the air and the fuel is $\pm 2\%$ of full scale, which can produce errors of 5% or more in the methane concentration. Such unnoticed variations can cause even larger differences in the heat generated by the reaction and, consequently, in the temperature of the catalyst surfaces. The preheating of the catalyst by the methane/air flame can cause large differences in catalyst surface temperatures due to the changes in fuel concentration, in the heating time and in the length of time the methane flow is cut off to extinguish the gas phase flame before catalytic surface combustion is ignited. The different catalysts' surface temperatures can affect the spatial location where the reaction takes place on the catalysts. Different heat inputs and different temperatures of the catalyst surfaces are created by the inaccuracies in flow measurements. These differences cause changes in the temperature of the gases flowing through the channels of the catalysts and to the temperatures of adjacent solid surfaces. In addition the room temperature increased considerably (about 10 °C) during normal operation of the combustor due to the heat released to the surroundings.

The variations in heat generation and heat losses and the different catalyst sufaces' temperature stabilized in the combustor can cause changes in both the axial and the radial temperature distributions in the experimental setup, as was detected. The variations in the temperature distribution in the combustor change its acoustic characteristic and can cause different rates of acoustic energy dissipation and greatly affect the acoustic energy content stabilized in the combustor. This can explain the variations in pressure amplitudes measured during identical operating conditions. In addition, results of tests run under the "same" conditions but with different time histories (e.g., two periods of non-pulsating operation before and after a period when pulsations were turned on), were usually less consistent than when effort was made to conduct (i.e., repeat) identical sequences of tests

from the ignition stage. This suggests that hysteresis effects might also exist and affect the operation of the catalytic combustor.

Although the tests were not repetitive from a quantitative point of view, the observed phenomena were repeated qualitatively even when test conditions were not exactly the same.

The Effect of Acoustic Oscillations on Methane Combustion

During the first phase of this study, four catalyst segments were used in the catalytic section. Tests with this configuration revealed that the catalytic surface reaction took place mainly on one of the catalyst segments at all of the investigated flow rates. This was indicated by the temperatures measured upstream and downstream of the four catalysts. Test No. 16 was a typical test of catalytic combustion of methane in which such temperature distributions in the catalytic combustion section were measured, as shown in Fig. 4. Temperature distributions in the catalytic combustion section at three different instances are presented in Fig. 4. These temperature data show that at the indicated instances catalytic surface reaction stabilized on the third, the second and the first catalyst segments, respectively. In all three cases sharp temperature increases were measured by the thermocouples upstream and downstream of the "active" catalyst segment, with temperature decreases measured further dowmstream. This suggests that most of the combustion took place on a single catalyst segment. Figure 4 also shows calculated temperature distributions which were obtained by assuming that an infinitely thin flame was positioned at the center of the "active" catalyst segment. The reasonable fit between the measured and calculated temperatures along the combustor justified the use of the calculated axial temperature distribution for evaluation of the standing wave pattern in the combustor, as explained in the previous chapter.

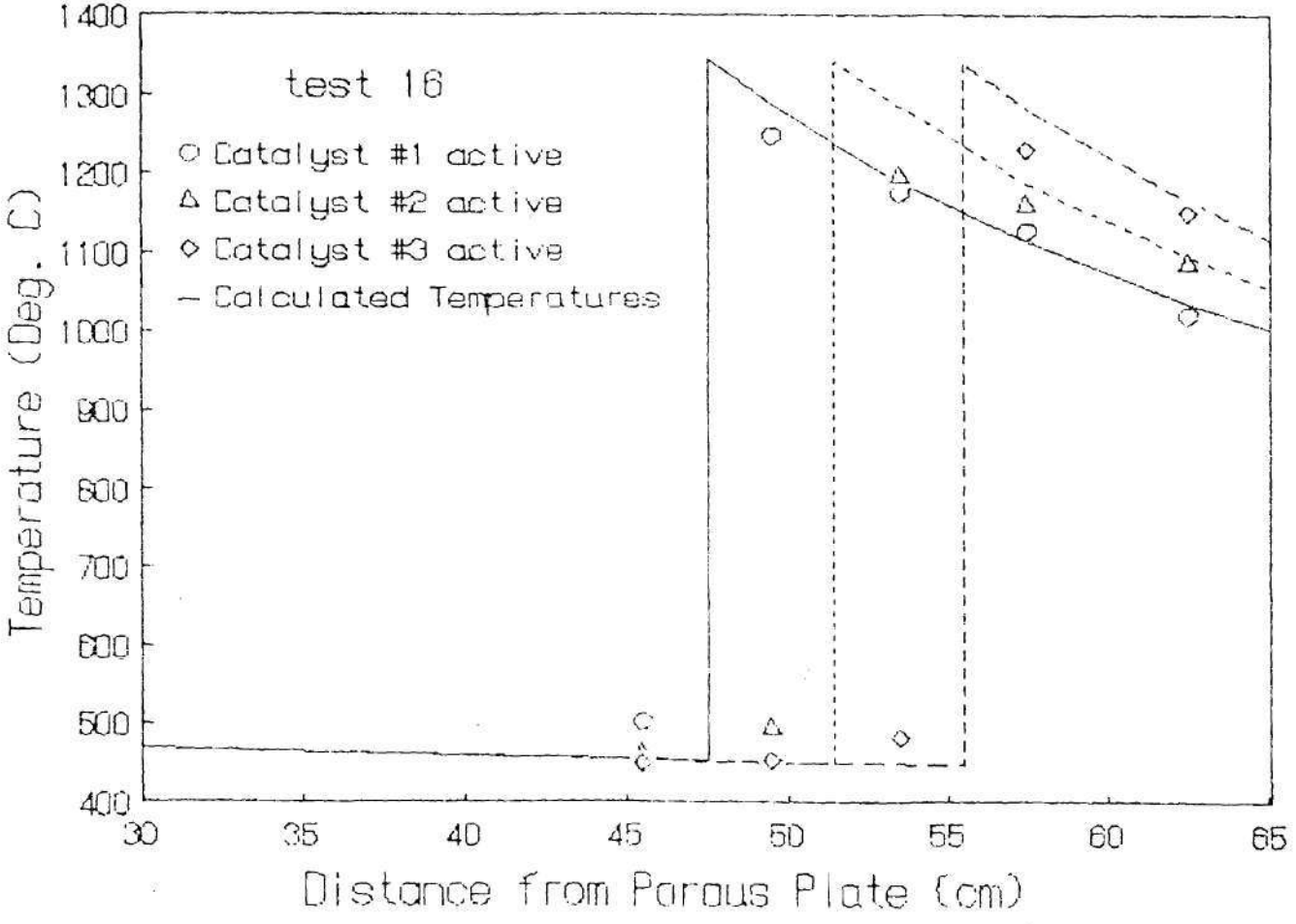

Figure 4: The Temperature Distribution in the Catalytic Combustion Section – Test No. 16

The part of Test No. 16 for which the data appears in Fig. 4 was conducted as follows. After "igniting" the catalytic surface reaction, the combustion stabilized on the third catalyst segment. Introduction of pulsations of 144 dB at a frequency of 800Hz shifted the reaction to the second catalyst segment. When the acoustic drivers were turned off, the combustion remained anchored on the second catalyst segment. The second set of data shown in Fig. 4 was measured during this period of non-pulsating operation. Turning the acoustic drivers on once again at the same frequency and amplitude forced the reaction to move further upstream and stabilize on the first catalyst segment. Again, the stoppage of pulsations did not cause the active catalytic site to change. The temperature data for the first catalyst being chemically active was taken again during the non-pulsating operation.

After extinguishing the reaction by shutting off the fuel supply and letting the catalyst cool for several seconds, the catalytic reaction was reignited and stabilized on the fourth catalyst segment. When acoustic pulsations at the same frequency of 800Hz but with an amplitude of 149 dB were introduced, the surface reaction moved from the fourth catalyst to the flame holder of the ignition system, changing to a gas phase reaction. This change in location was detected both by temperature readings and by the shift upstream of the red glowing circumference indicating the hottest region in the combustor. The existence of gas phase reactions was immediately noticed by the occurrence of combustion noise characterized by a broadband frequency spectrum with amplitudes in the 125 to 130dB range. Such spontaneously excited pulsations were never present when only a surface reaction was present. It seems that the shifting of the combustion location is amplitude dependent, and that at the higher dB levels we detect the same effect as with the lower amplitudes, but with stronger shifts.

The response of the experimental setup to the onset of acoustic oscillations varied with frequency and amplitude of the acoustic waves. Acoustic pulsations at low amplitudes (i.e., *Sound Pressure Levels* below 135 dB) did not shift the location of

the reaction. The response varied when high amplitude acoustic oscillations were excited in the experimental setup. In some cases the reaction continued stably on the same catalyst segment where it stabilized before the onset of the pulsations. In other cases the reaction was shifted either upstream or downstream, was extinguished or transformed into a gas phase reaction. In order to find the causes for this behavior, the characteristics of the acoustic standing wave in the setup was studied. Figure 5 shows the wave pattern for a frequency of $800Hz$ calculated using the temperture data of Test No. 16. According to Fig. 5, the catalytic section is located between an upstream pressure node and the downstream pressure antinode. Figure 6 shows the structure of the acoustic pattern for a frequency of $285Hz$. The introduction of pulsations at this frequency also shifted upstream the location of the combustion, although the amplitude was only $139dB$. In this case the catalytic section was also located between an upstream pressure node and a downstream velocity node. When a small shift in frequency from $285Hz$ to $300Hz$ was made, pulsations at an amplitude of $140dB$ caused an opposite effect; that is, the combustion shifted downstream from the third to the fourth catalyst segment. Figure 7 shows the acoustic standing wave pattern for this frequency, which is only slightly different from the one for the $285Hz$ frequency. When $300Hz$ pulsations at an amplitude of $145dB$ were driven, the reaction was extinguished.

Driving acoustic pulsations at a frequency of $200Hz$ with varying amplitudes (from $138dB$ to $158dB$) did not cause any shift in the active catalyst site and did not cause extinction of the reaction. It should be noted that at this frequency the location of the catalytic section on the standing acoustic wave pattern is upstream of the first pressure node. In this region the acoustic pressure leads the acoustic velocity by 90 degrees, which means that during an increase in the acoustic pressure, the acoustic velocity causes gas particles in this region to move in the upstream direction. The acoustic pressure and the gas particle displacements are "out of phase". There were many tests in which onset of pulsations at different

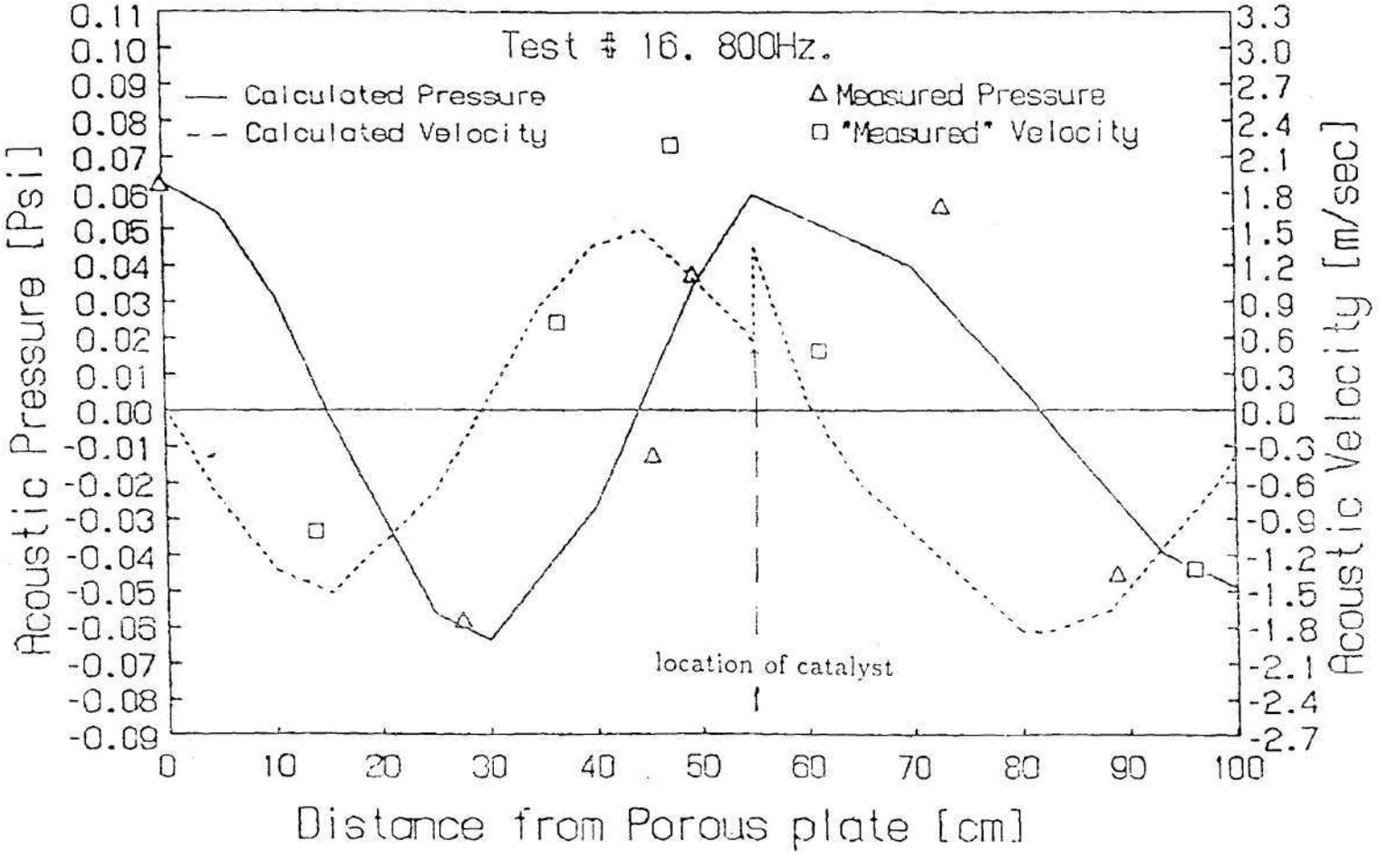

Figure 5: Comparison of Measured and Calculated Acoustic Pressure and Velocity for a Frequency of 800Hz in Test No. 16

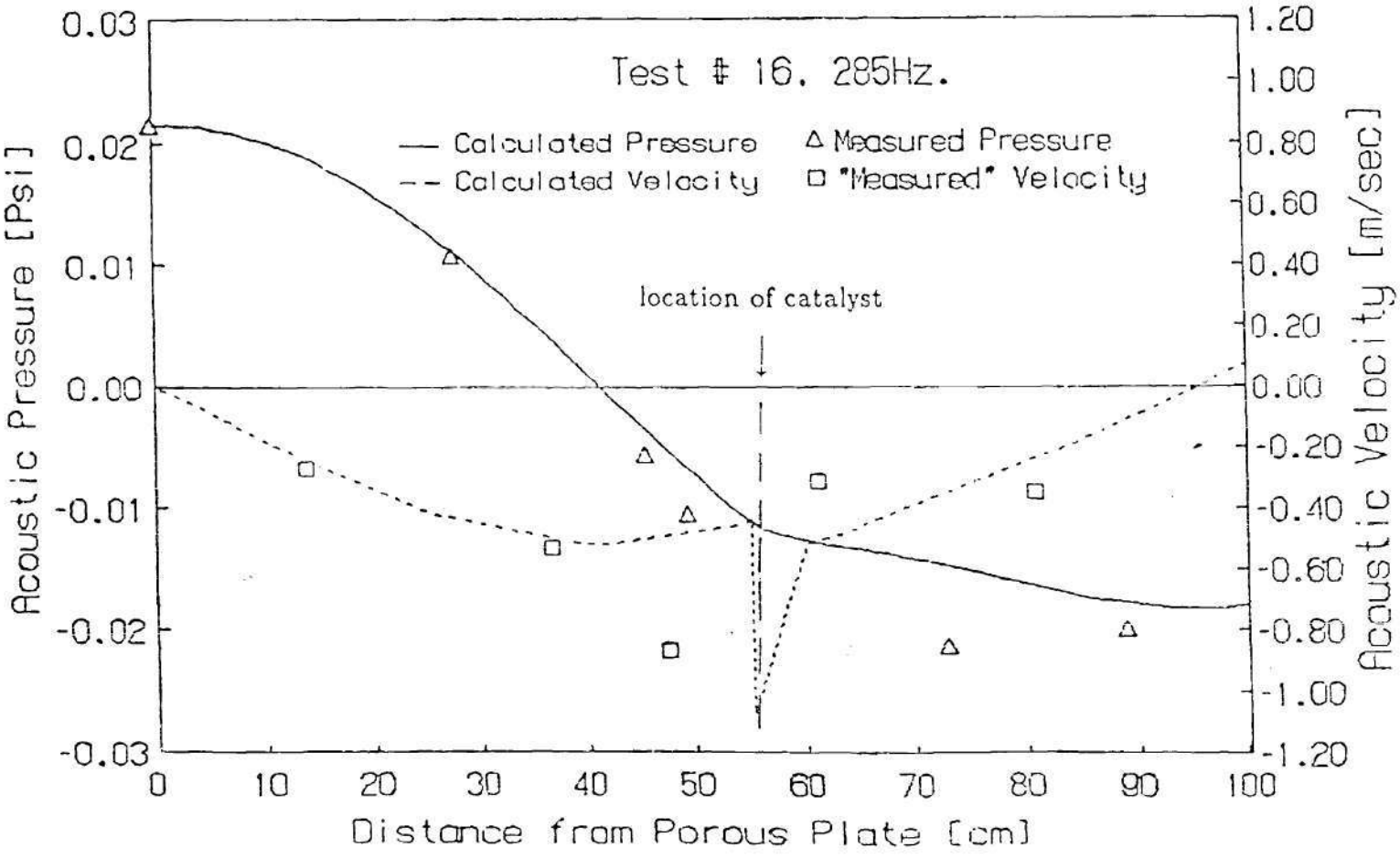

Figure 6: Comparison of Measured and Calculated Acoustic Pressure and Velocity for a Frequency of 285Hz in Test No. 16

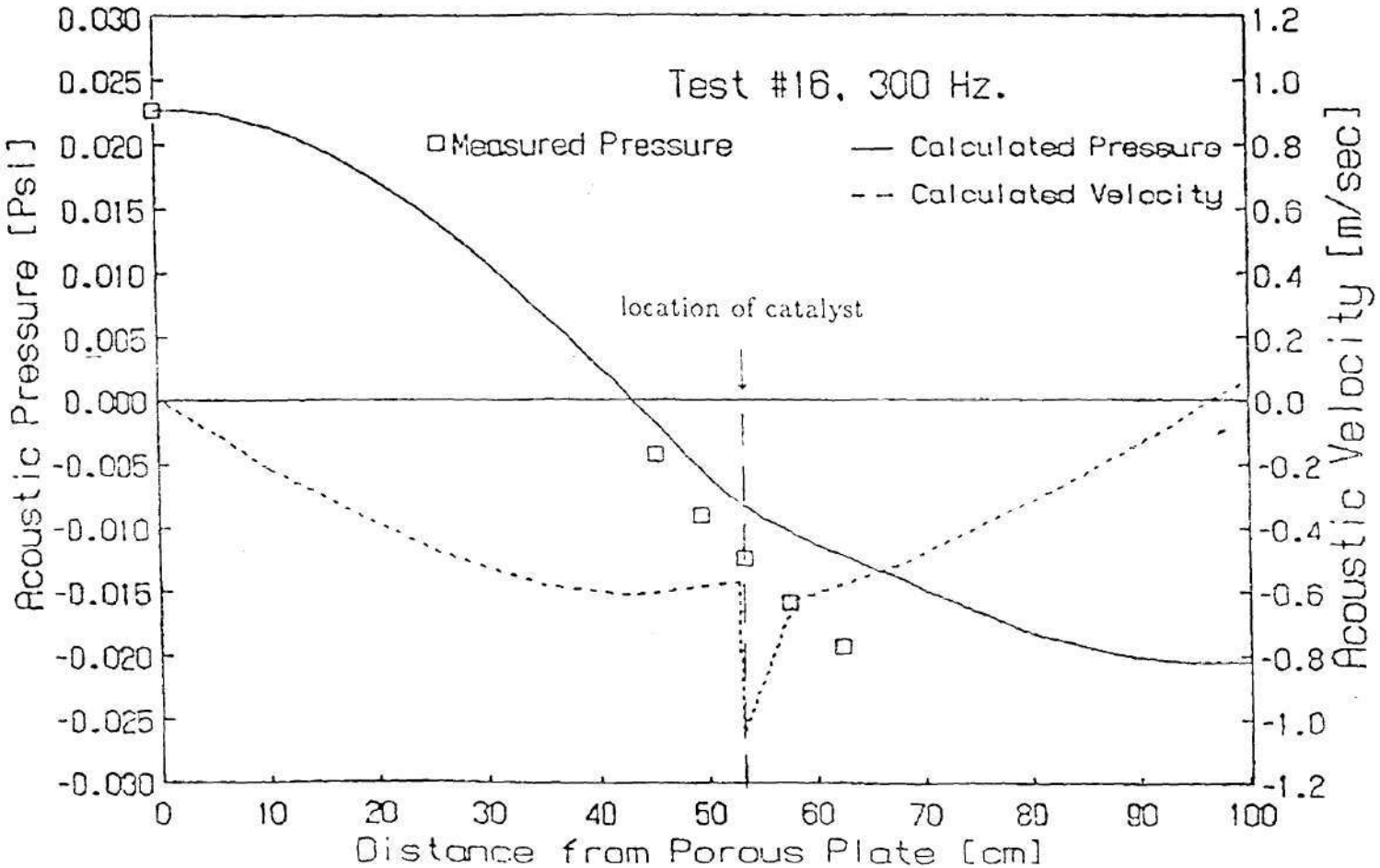

Figure 7: Comparison of Measured and Calculated Acoustic Pressure and Velocity for a Frequency of $300Hz$ in Test No. 16

frequencies did not cause a shift in the location of the catalytic reaction when several catalyst segments were used. This behavior occurred either when the catalyst was in an "out of phase" condition, or when the amplitudes were lower than $138dB$. Figure 8 shows such an acoustic pattern for pulsations at $500Hz$ for which no shift in the reaction site was detected.

Shifts in the location of the combustion were detected in many tests with the catalytic combustion section consisting of either four or two catalyst segments. These shifts occurred only when the acoustic pressures and velocities were "in phase"; that is, when during a pressure increase, the gas particle displacements due to the acoustic oscillations were in the downstream direction, and when the amplitude was at least $137dB$. No differences in the operating conditions were found that could explain why in some cases the shift was in the upstream direction, while in others it was in the downstream direction. When the amplitudes of the acoustic pulsations were high and the combustible mixture not very lean (i.e., methane concentrations above 2.4%), there were cases when the excitation of acoustic waves produced a gas phase reaction which stabilized on the flame holder. In other cases, and when the fuel concentration was below 2.4%, high amplitude pulsations extinguished the reaction. The dB level of the acoustic pulsations causing extinction of the reaction or onset of gas phase flames was not repetitive. In some instances combustion was extinguished by $142dB$ pulsations, whereas in other cases even pulsations of $158dB$ did not extinguish the reaction although the acoustic pressure and the particle displacement were "in phase". Similar observations were made when shifts to gas phase reactions occurred. When only a single catalyst segment was used, a shift in the location of reaction was not detected, but in many cases excitation of acoustic pulsations at a frequency that positioned the catalyst between an upstream pressure node and a downsteam pressure antinode extinguished the catalytic reaction or "ignited" a gas phase reaction.

In most of the cases when the reaction shifted its location upon the excitation

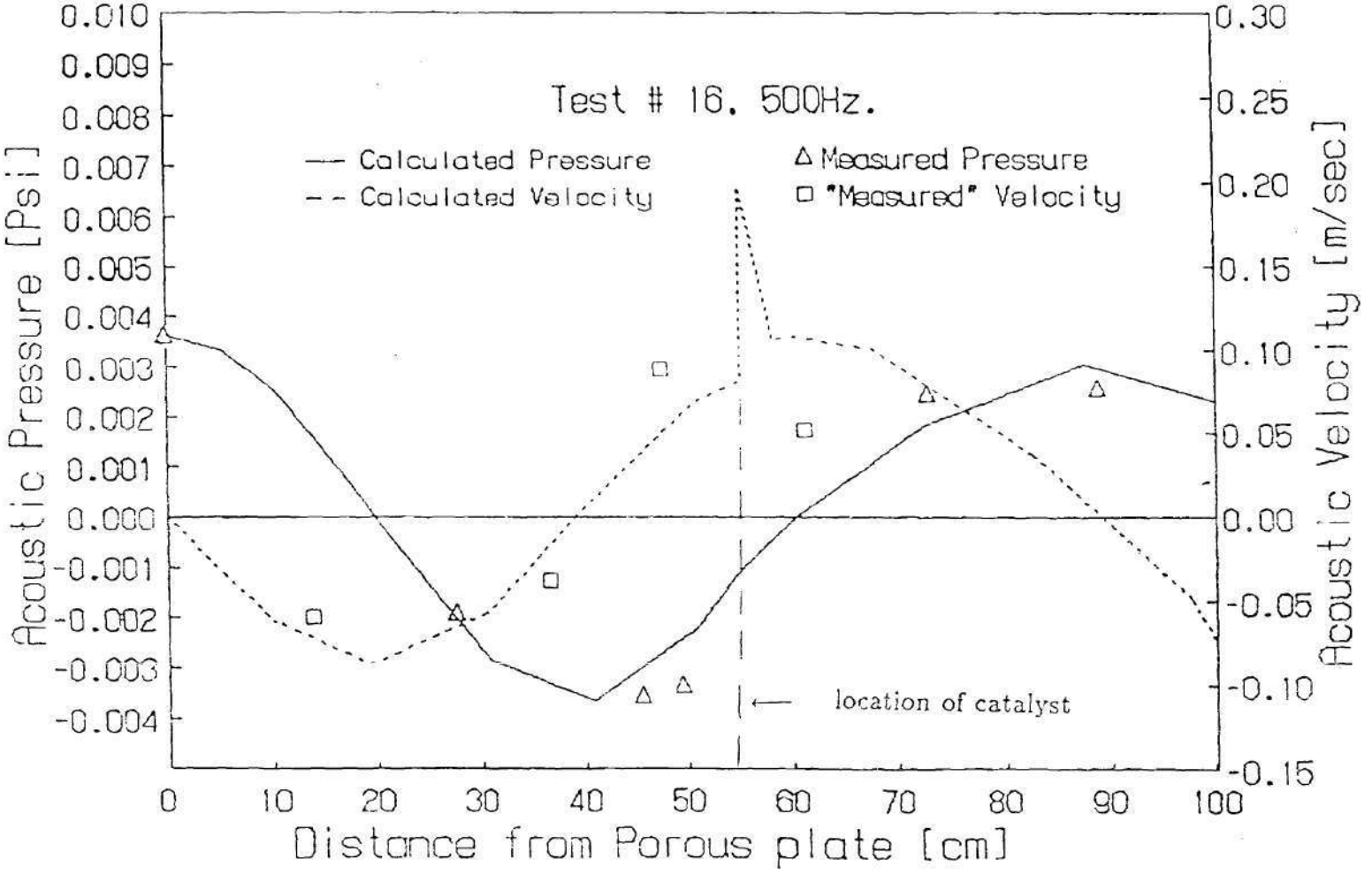

Figure 8: Comparison of Measured and Calculated Acoustic Pressure and Velocity for a Frequency of $500Hz$ in Test No. 16

of acoustic waves, the stoppage of the oscillations did not change the location of the reaction. In other instances, the stoppage of the pulsations caused the reaction to shift back to the original location. No differences in operation which could explain these different responses were detected.

The shift in the reaction zone, the extinction of the reaction and the onset of gas phase reactions can be viewed as different responses to instabilities in the catalytic combustor. Such instabilities occurred when the catalytic combustion section was located between an upstream pressure node and a downstream velocity node (i.e., in an "in phase" condition). These instabilities were amplitude dependent, but the specific threshold amplitudes causing the instabilities differed from test to test.

A second phenomenon caused by the excitation of acoustic pulsations was a sudden change in temperatures at some locations along the experimental setup. Figure 9 shows the temperature histories in the catalytic combustion section during Test No. 17, in which this phenomenon was investigated. During a period of about 34 minutes catalytic surface reaction occurred on the third catalyst. Three thermocouple measurements in the catalytic combustion section are shown; that is, upstream of the first catalyst segment (TC 5), between the first and the second segments (TC 6), and between the third and the fourth segments (TC 8). Acoustic pulsations at relatively low amplitudes and six different frequencies were excited during this period. The frequencies were 200, 150, 400, 500, 600, and $800 Hz$. The electrical power input into the acoustic drivers was $80 watt$ which according to previous experience did not cause the location of the reaction to move. The system responded differently to different frequencies, and the *Sound Pressure Level* reached in the experimental setup varied from frequency to frequency. The pressure amplitudes ranged from $122 dB$ for pulsations of $600 Hz$ to $138 dB$ for pulsations of $800 Hz$. The amplitudes of the pulsations are plotted at the bottom of Fig. 9, with the vertical scale proportional to the acoustic pressure. It can be seen that the mixture temperature upstream of the first catalyst segment there was not

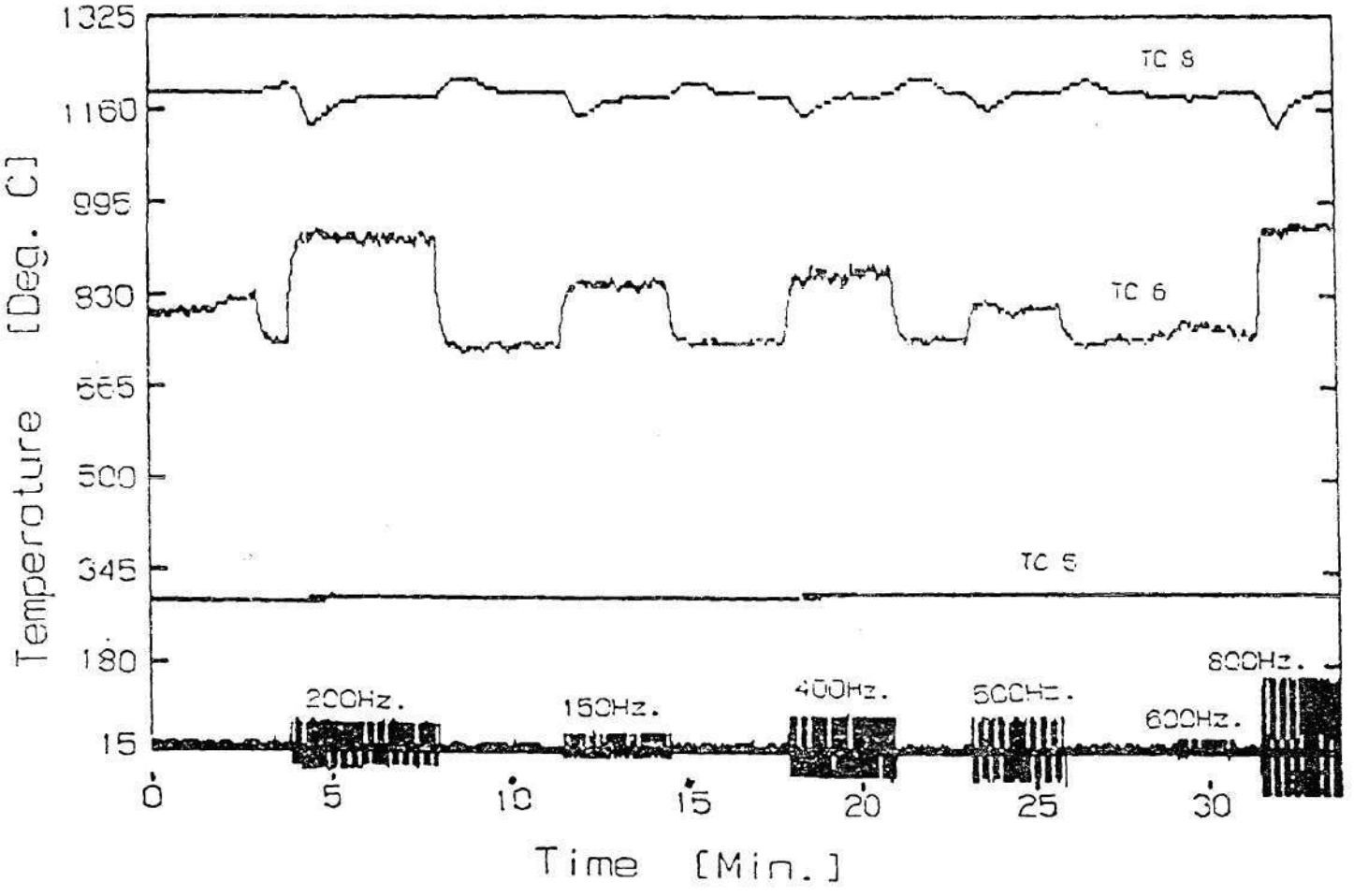

Figure 9: Temperature Histories in the Catalytic Section in Test No. 17

affected by the acoustic pulsations. Similarly, no effect of pulsations upon temperature was observed at the igniter and in the mixing section which were also located upstream of the first catalyst segment. Downstream of the first catalyst segment, large temperature variations occurred. The temperature increased within a short period of time upon the excitation of acoustics, and decreased rapidly after the pulsations were stopped. The changes were frequency dependent. The change caused by the $200Hz$ pulsations was slightly larger than the change caused by the $800Hz$ pulsations, although the latter had more than double the amplitude. The same can be concluded from comparing the effects of 150 and $500Hz$ pulsations. Downstream of the third (and the "active") catalyst segment the effects of acoustic pulsations were much smaller. They caused a temperature change for only a limited time period both when the drivers were switched on and when they were switched off.

Figure 10 describes the temperature histories in Test No. 17 downstream of the catalytic combustion section for the same period of time as in Fig. 9. Temperature histories measured 50, 100, 200, 300, and 400 *cm.* downstream of the center of the catalytic section are presented (i.e., thermocouples TC 10 to TC 14). The effect of the acoustic pulsations on the temperatures at 50 and 100 *cm.* downstream from the catalytic combustion section are almost negligible. The temperature measured by the third thermocouple (TC 12) deceased when acoustic pulsations were excited. This temperature shifted back to the original temperature when the pulsation stopped. A comparison of the changes due to 200 and $500Hz$ waves with those produced by 150 and $800Hz$ waves show that the frequency dependence is different at this location from that observed in the catalytic combustion section. The effect of pulsations on the temperature readings of thermocouple TC 13 were similar to those of TC 12, but with considerably smaller temperature changes. The effect of acoustic pulsations on the temperatures measured by thermocouple TC 14 were negligible. The temperature changes due to the onset of acoustic oscil-

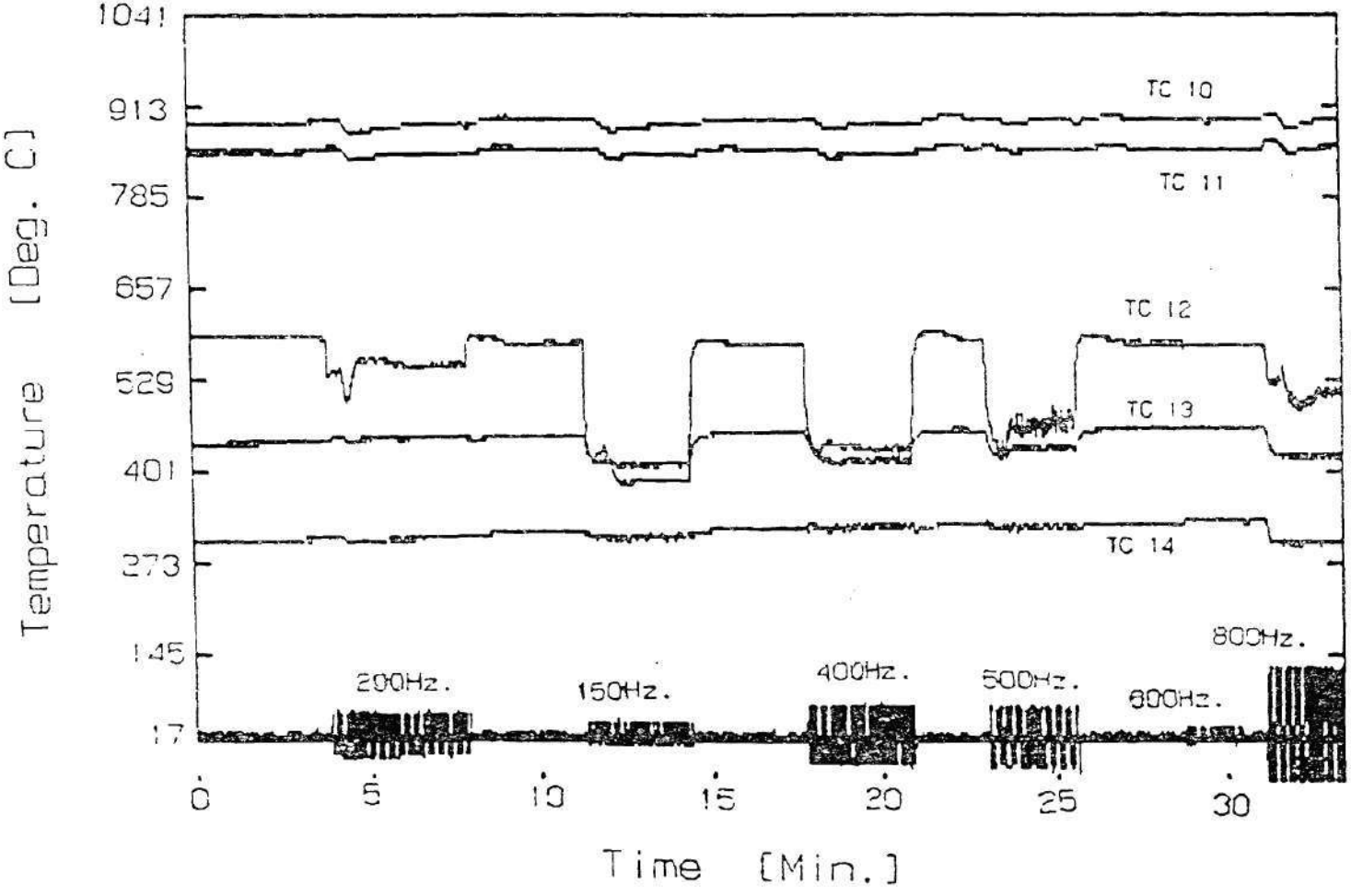

Figure 10: Temperature Histories Downstream of the Catalyst in Test No. 17

lations were observed in all cases when the flow rate was less than about 600 *lit/sec* and decreased with increasing mixture flow rate. This was expected since as this flow rate and the high temperature generated by the reaction (i.e., approximately 1100 °C), the flow velocity is about 13.5 *m/sec* and the Reynolds number for a hollow pipe is approximately 17500. This Reynolds number corresponds to the end of the laminar flow and the beginning of the transition zone where the turbulent flow is not fully developed. Turbulent circulatory flow patterns should appear at about this Reynolds number at the inlets to the catalyst segments as well as between the different catalyst segments and downstream of the catalytic combustion section. Since the catalyst segments are relatively short (i.e., 2.5 *cm* some rotational flow should exist in the catalyst channels, until fully damped. Mixing caused by turbulence might have the same effect on the catalytic combustion as the mixing caused by acoustic waves.

The variations in temperature upon onset of acoustic oscillations are probably the outcome of rotational flows excited by the acoustic pulsations. Such rotational flow patterns should improve mixing and enhance heat transfer by convection, causing both the radial and the axial temperature distributions to change. Chendke and Fogler [20] suggested that the mixing effect induced by acoustic pulsations in gas phase media is caused mainly by acoustic streaming. Circulatory flows excited by acoustic streaming have directionality which depends upon the location on the acoustic standing wave pattern, as shown schematically in Fig. 11. This can explain the frequency dependence of the changes in temperature which were observed in the tests. Circulatory flow patterns which enhance mixing and improve the heat transfer between the center of the tube and the walls can explain the different changes in temperature at different axial locations. A short distance upstream of the combustion zone, the inflowing gases were relatively cold, while the metal tube was very hot due to the heat conducted along the tube from the region where the surface reaction was taking place. The mixing due to acoustic

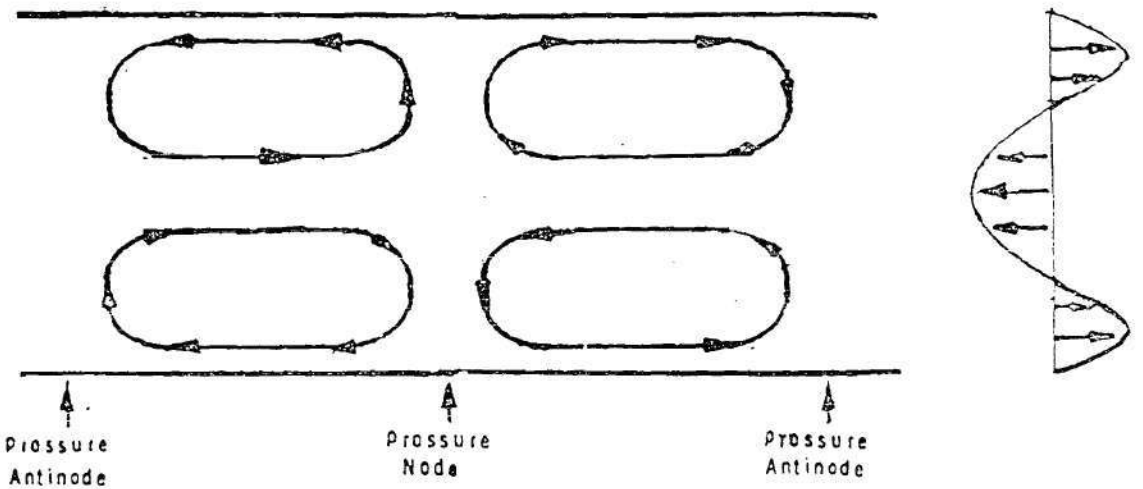

Figure 11: A Schematic of the Flow Pattern Produced by Acoustic Streaming Between Two Plates

waves caused the temperature of the gas in the center of the tube, where the thermocouples were located, to increase in this region. Downstream of the combustion zone both the tube and the gas were hot and the radial temperature gradients in the gas were relatively small. Radial mixing in this region is not expected to cause large temperature changes, which explains why the effect of the acoustic pulsations on thermocouples TC 8, TC 10, and TC 11 shown in Figs. 9 and 10 was very small. Further downstream, the tube cooled down more rapidly than the gas inside it, and improvement in the mixing caused the temperature to decrease, as measured by thermocouples TC 12 and TC 13 shown in Fig. 10.

Chemical analyses of the combustion products were performed in some of the methane combustion tests. Hydrocarbons and CO were detected in the products during stable catalytic combustion only when fuel rich mixtures were used, and no oxygen was available for further combustion. In an attempt to get incomplete combustion, the entire range of flow rates was investigated with four, then two and finally a single catalyst segment. When the flow rate of reactants was increased the reaction was less stable, and lower amplitudes of acoustic pulsations caused extinction of the reactions. In all cases where during combustion of lean methane/air mixtures hydrocarbons were detected, it was an indication that the combustion stopped, and it was followed by a rapid decrease in the temperatures throughout the combustor. The response time of the chemical analyzers, and specifically of the hydrocarbon analyzer, is at least an order of magnitude larger than that of the thermocouples measuring the temperature. Thus, it was impossible to know if incomplete combustion occurred shortly (several seconds) before the reactions stopped and triggered the extinction of the reaction by cooling the catalyst down; or if the reaction was first extingushed by the acoustic pulsations causing the decrease in temperatures.

The temperature changes along the combustor which were observed upon onset and stoppage of acoustic pulsations in the entire range of investigated frequencies

(i.e., 150 to 2000Hz) leads to the conjecture that acoustic pulsations cause better mixing of gas particles in the flow. Since improvement in the mixing was expected to enhance the diffusion processes, these results suggested that improvement of the combustion efficiency could be expected if stable incomplete catalytic combustion is obtained.

Catalytic Combustion of Propane

The results obtained with methane suggested that improvement of mixing due to excitation of acoustic pulsations should be studied at low flow rates rather than at high flow rates where turbulence can cause similar effects. Since the objective was to get stable, but incomplete catalytic combustion, a decision was made to use only a single catalyst segment with relatively low flow rates.

The first attempts to run the combustor with propane revealed that the "ignition" of its catalytic combustion can be done by heating the catalyst with the electrically preheated combustion air. The "light off" temperature depended on the flow rate and the fuel/air ratio, and was in the 300 to 450 °C range. It also proved possible to ignite the catalytic combustion by preheating the catalyst segment by a gas phase flame, as was done with methane. When the gas flame ignition technique was used the input air could be heated to any desired temperature, or not heated at all, enabling better control of the maximum temperature attained in the catalytic section.

Catalytic combustion tests of propane were conducted with flow rates ranging between 70 and 500 *Std. lit./min* and at fuel concentrations below 2.5% propane by volume. At the lowest flow rate (i.e., 70 *Std. lit./min* the axial flow velocity in the catalytic combustion section was 1.2 *m/sec* and the Reynolds numbers were 600 when calculated for the tube, and 12 when calculated for the catalyst channel. At the maximum flow rate of 500 *Std. lit/min* the flow velocity was 11.15 *m/sec*

and the Reynolds numbers for the tube and the channels were 10,000 and 225, respectively. It was found that, as with methane, increasing either the flow rate or the fuel concentration resulted in a higher steady-state temperature at the exit from the catalyst. This reflects a higher catalyst surface temperature. Catalytic reactions were stable in a wide range of flow rates and concentrations. Using concentrations lower than 4,000 *ppm* resulted in very low combustion efficiencies (i.e., 25 to 35%). The temperatures measured during non-pulsating operation at the exit from the catalyst with propane concentrations in the 3,500 - 4,000 *ppm* range were between 250 and 300 °C. Onset of acoustic pulsations at various frequencies and amplitudes caused cooling of the catalyst (as indicated by the temperatures measured at its exit), and extinction of the catalytic reaction. Propane concentrations below 3,500 *ppm* did not support catalytic combustion even at non-pulsating conditions, and caused quick extinction of the reaction. Only traces of hydrocarbons were detected when propane concentrations of about 10,000 *ppm* were used. The combustion reaction proceeded to completion when the propane concentrations were in excess of 12,000 *ppm*. Extinction of catalytic reactions at propane concentrations and flow rates above 4,000 *ppm* and 100 *lit/min*, respectively (i.e., for $\bar{v} \geq 1.4\, m/sec$ and $\mathcal{R}e \geq 800$), were not detected. This was probably due to the lower activation energy and the easier ignition of propane compared to methane. Onset of gas phase flames upon the excitation of acoustic pulsations has occurred only at concentrations above 15,000 *ppm*.

Incomplete reactions were achieved when the temperatures measured downstream of the catalyst were relatively low (i.e., less than 1,000 °C). Increasing the flow rate resulted in higher combustion efficiencies although the residence time of reactants in the catalytic section decreased. "Best" results (i.e., stable, but incomplete catalytic combustion) were achieved when using inlet mixture temperatures of up to approximately 250 °C, flow rates between 100 and 160 *Std. lit./sec.*, and propane concentrations of 4,000 to 9,000 *ppm*. The ranges of flow velocities

and Reynolds numbers for the tube and the catalyst channels calculated for these operation conditions were 1.4 to 8 m/sec, 800 to 7,000, and 17 to 160, respectively. Combustion efficiencies measured while operating within these ranges were between 40 and 85%.

As with methane, test results were not quantitatively repeatable. Temperature and pressures variations of up to ± 75 °C and $\pm 3dB$, respectively, were measured in the experimental setup during "identical" operating conditions.

The Effect of Temperature on Steady-State Propane Combustion Efficiency

In order to investigate the effect of acoustic oscillations on the performance of the developed catalytic combustor, the system was investigated both under steady-state (i.e., non-pulsating) and pulsating conditions. The data obtained during steady-state operation with incomplete catalytic combustion shows the changes in performance of the combustor caused by changing the mixture's flow rate and propane concentration. Measurements of temperatures just downstream of the catalyst, and calculated combustion efficiencies for non-pulsating operation of the catalytic combustor are presented in Tables 1 and 2. Table 1 lists combustion efficiency data for propane/air mixtures at a constant air flow rate of 156.1 lit/min and five different propane concentrations in the 4,000 to 9,000 ppm range. The mean flow velocity calculated from the data for the catalytic combustion section was in the 1.9 to 2.5 m/sec range. Table 2 presents temperature and combustion efficiency data for four different flow rates between 100 and 160 lit/min at concentrations of about 8900 ppm. The data in both tables was measured at different times for each flow rate and concentration and shows the large variations of both temperature and combustion efficiency measured at "identical" conditions. The combustion efficiency data in Tables 1 and 2 was plotted in Figs. 12 and 13 as

Table 1: Temperatures and Combustion Efficiencies Measured During Non-Pulsating Catalytic Propane Combustion – Constant Flow Rate

Propane Concentration	Temperature °C	Combustion Efficiency
	480	44.6%
4023	620	65.3%
ppm	520	49.0%
	550	52.2%
	505	45.7%
	660	62.5%
4817	575	52.0%
ppm	523	50.1%
	605	52.3%
	620	57.5%
	600	55.6%
5996	582	51.9%
ppm	712	68.2%
	696	60.3%
	620	58.2%

Continuation of Table 1.

Propane Concentration	Temperature °C	Combustion Efficiency
	700	54.3
6870	878	70.1
ppm	745	58.5
	785	67.8
	867	69.3
8860	950	83.4
ppm	993	85.0
	907	80.7
	893	75.3

Air flow rate – 156.1 *lit/min*, total mixture
flow rates between 156.7 and 157.5 *lit/min*
mean flow velocities between 1.9 and 2.5 *m/sec*.

Table 2: Temperatures and Combustion Efficiencies Measured During Non-Pulsating Catalytic Propane Combustion – Constant Fuel Concentration

Air Flow Rate	Propane Concentration	Temperature °C	Combustion Efficiency
		867	69.3%
156.1	8860	907	80.7%
lit/min	*ppm*	950	83.4%
$\bar{v} = 3\,m/sec$		993	85.0%
		893	75.3%
		821	80.4%
137.8	8973	904	82.1%
lit/min	*ppm*	793	65.3%
$\bar{v} = 2.5\,m/sec$		864	77.9%
		804	76.0%
121.4	8776	863	79.3%
lit/min	*ppm*	745	59.2%
$\bar{v} = 1.6\,m/sec$		704	62.8%
108.6		623	62.1%
lit/min	8921	713	63.2%
$\bar{v} = 3\,m/sec$	*ppm*	679	55.6%

function of propane concentration and air flow rate, respectively. In spite of the large variations in the data, it can be clearly seen that an increase in either the fuel concentration or the flow rate caused higher combustion efficiencies. The temperature data in Tables 1 and 2 is plotted in Figs. 14 and 15 as function of propane concentration and air flow rate, respectively, and show that the temperature measured at the exit from the catalyst increased with the increase of either the fuel concentration or the mixture's flow rate.

The temperature measured at the exit from the catalyst is a measure of the heat balance between the heat generated by the reaction and the losses to the wall and is an indication of the temperature of the catalyst surfaces. This suggests that the combustion efficiency obtained in the catalytic section could depend upon the catalyst surface temperature. Figure 16, which shows the combustion efficiency as function of the temperature measured at the exit from the catalyst using the data from both tables, supports this suggestion. It shows that the combustion efficiency increased as the temperature measured at the exit from the catalyst increased.

The Effect of Acoustic Pulsations on the Axial Temperature Distribution in Propane Combustion Tests

Observations of the effect of acoustic pulsations on catalytic combustion of propane were in many aspects similar to those observed with methane. The magnitude of acoustic pulsations excited in the combustor by driving the system at a certain power input varied with frequency, and was not quantitatively repetitive. This indicates that acoustic energy absorption by the system is frequency and temperature dependent. Since only a single catalytic segment was used, a shift in the location of the reaction was not detected. The effect of pulsations on the temperature distributions along the combustor was very similar to the effect on temperature which was detected when operating the catalytic combustor with

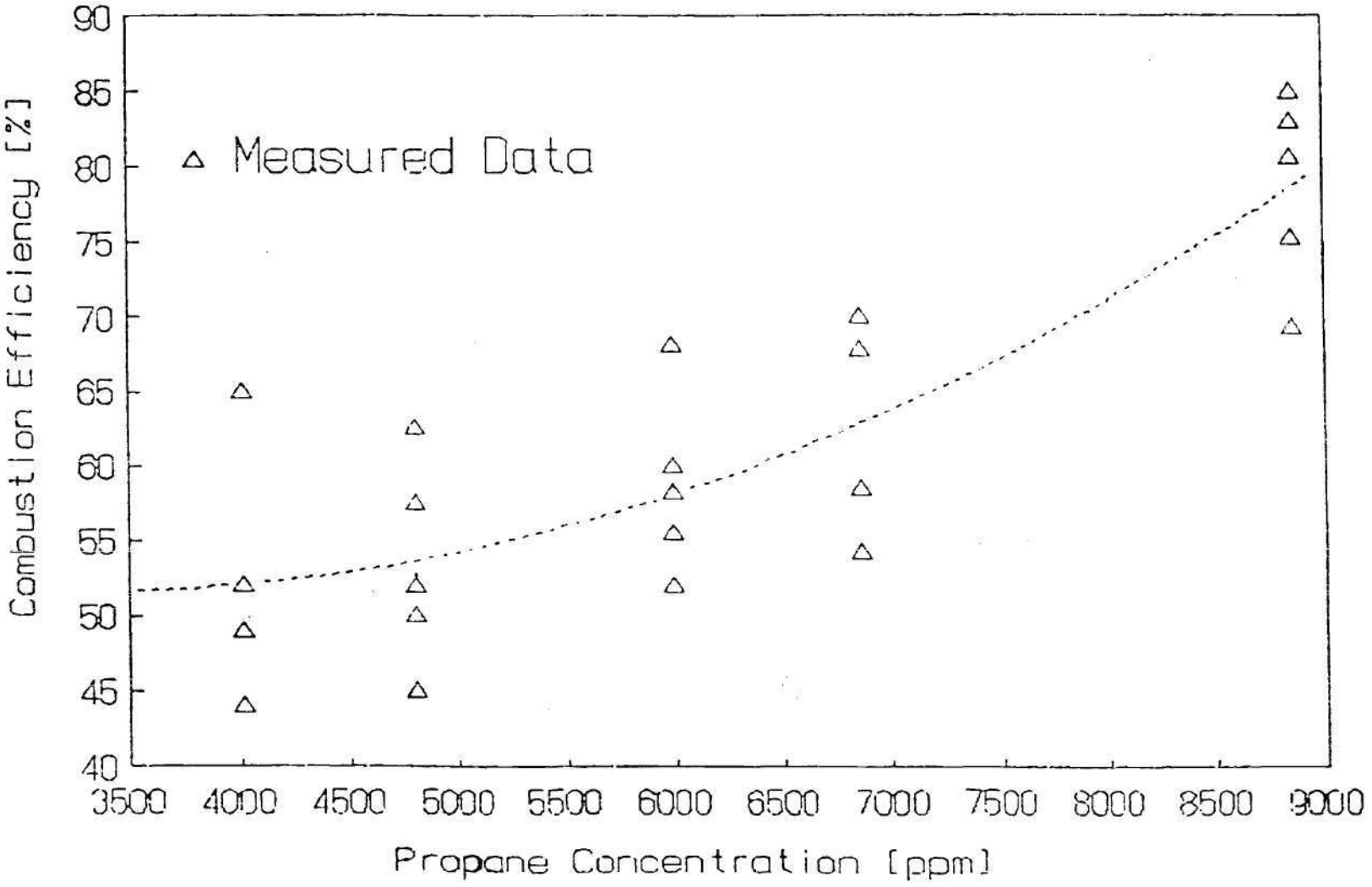

Figure 12: Dependence of Combustion Efficiency on Propane Concentration at an Air Fow Rate of 156.1 *lit/min*.

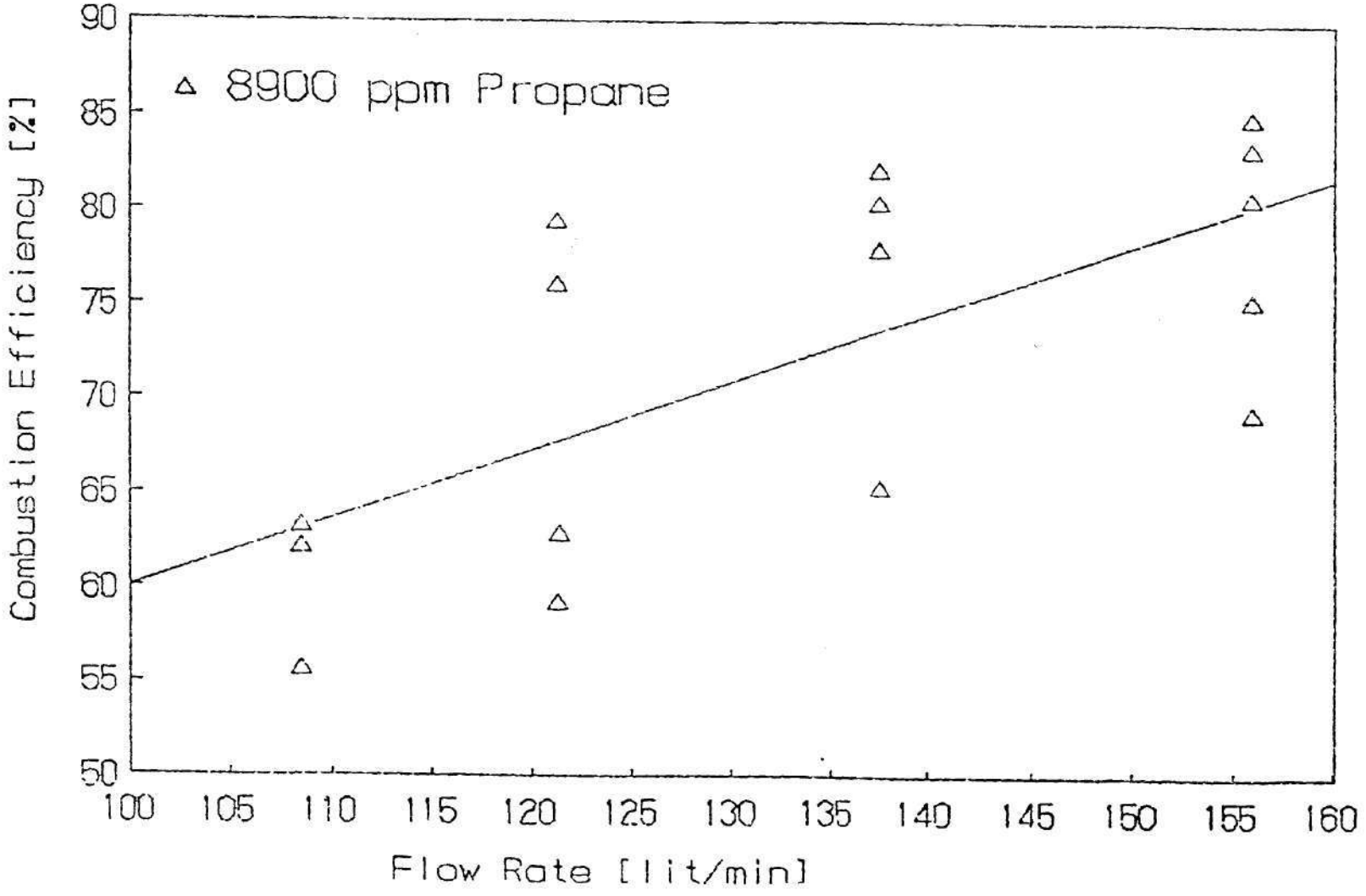

Figure 13: Dependence of Combustion Efficiency on Flow Rate of Propane/Air mixture at Propane Concentrations of 8900 *ppm*.

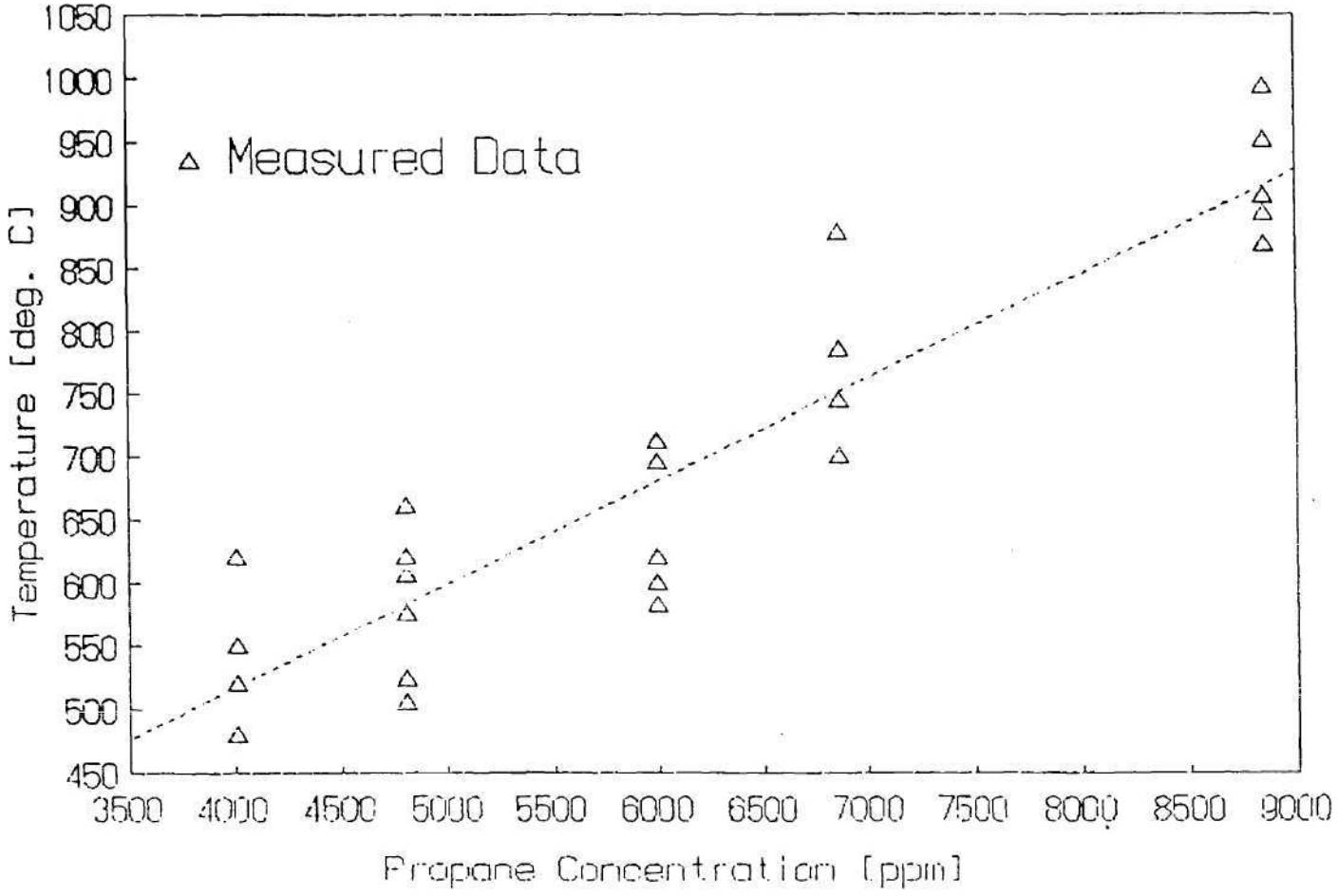

Figure 14: Dependence of Catalyst Temperature on Propane Concentration at an Air Fow Rate of 156.1 *lit/min*.

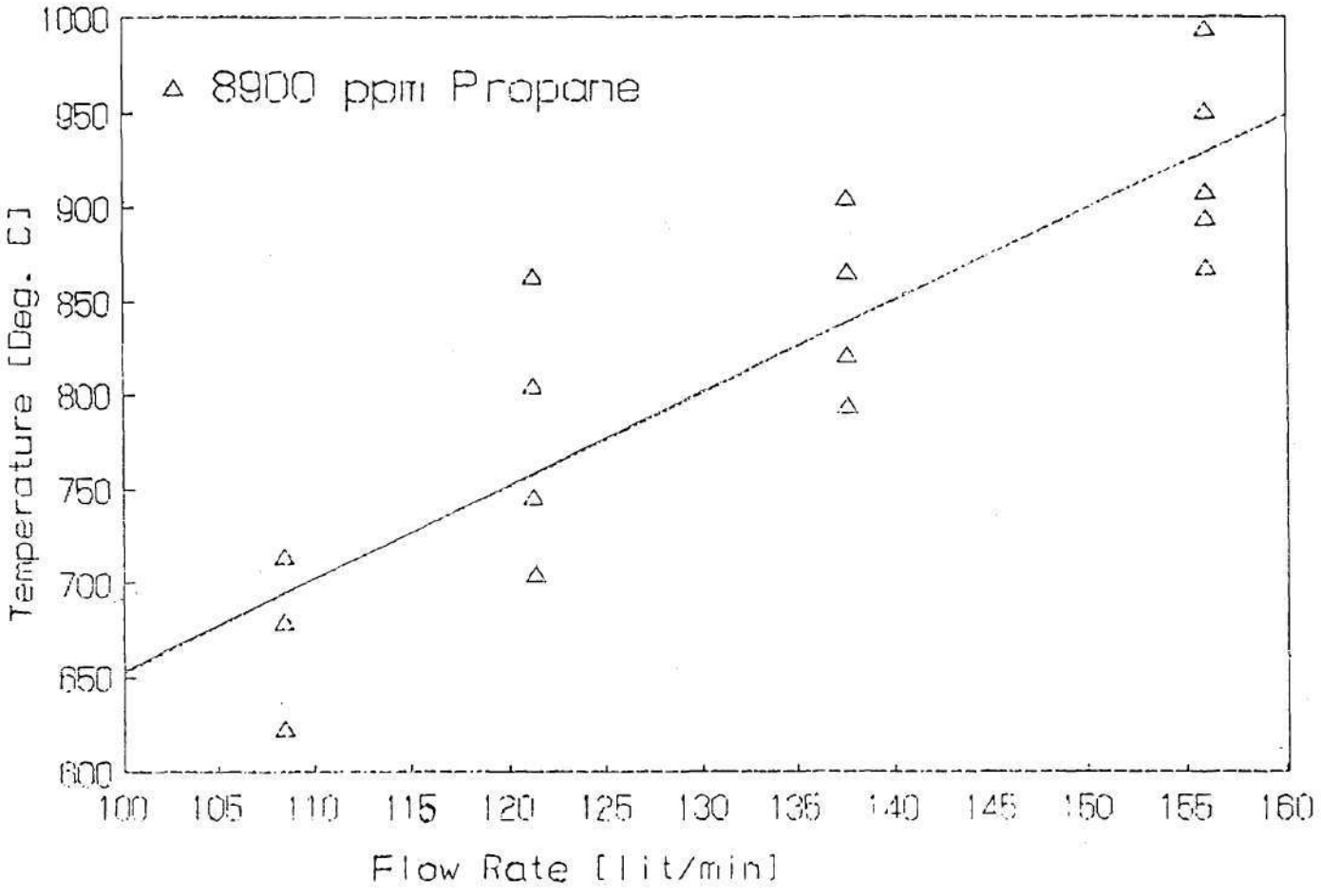

Figure 15: Dependence of Catalyst Temperature on Flow Rate of Propane/Air mixture at Propane Concentrations of 8900 *ppm*.

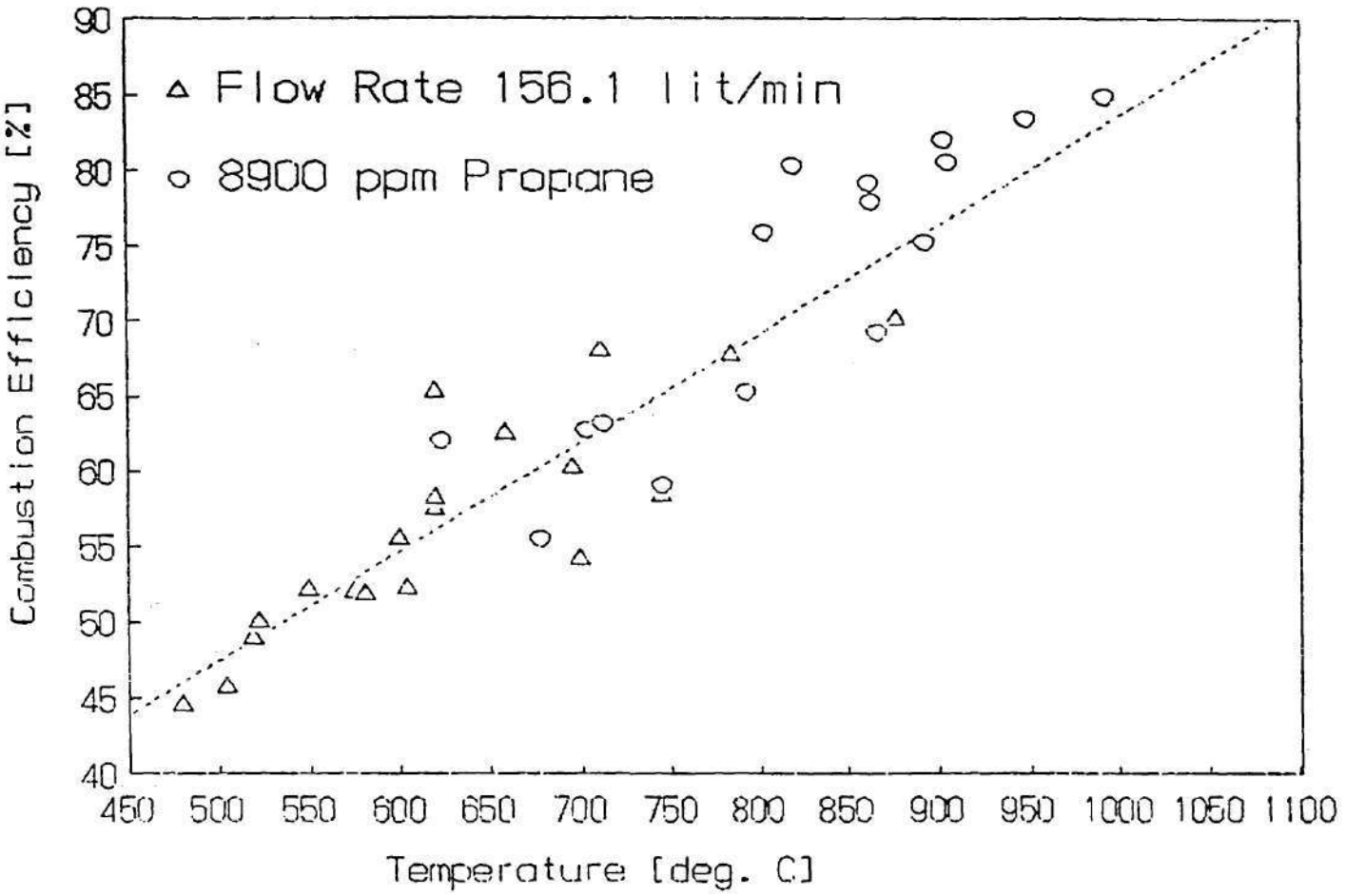

Figure 16: Dependence of Combustion Efficiency on Catalyst Temperature

methane. There were no temperature changes at the mixing section. Onset of oscillations caused some temperature increase (about 10 °C) just upstream of the catalyst. When acoustic waves had no (or slight) effect on the combustion efficiency, very slight temperature increases were detected just downstream of the catalyst, and the temperature changes reached a maximum of 10 to 30 °C about 20 *cm* downstream of the catalyst. The temperature changes decreased further downstream until no significant change could be detected about 60 to 80 *cm* from the catalyst. Further downstream, the effect was opposite, that is, a very large temperature drop occurred when acoustic pulsations were turned on. This temperature drop reached a maximum of 60 to 90 °C about 150 to 250 *cm* from the end of the combustor. From this point towards the end of the experimental setup, the temperature drop decreased and near the exit of the combustor no significant temperature changes were detected.

When an improvement in the combustion efficiency was detected, the temperature increase downstream of the catalyst was larger, between 30 to 100 °C depending upon the increase in the combustion efficiency. This higher temperature increase reflects the additional heat generated by the reaction. The slight increase in temperature upstream of the catalyst, and the large temperature drop in the section 50 to 300 *cm* from the end of the combustor were not affected by the change in the combustion efficiency. Figure 17 presents the temperature gradients along the combustor when a propane concentration of about 9,000 *ppm* and a flow rate of 150 *lit./sec.* were used at pulsating and non-pulsating conditions. The temperatures measured downstream of the catalyst were relatively high (close to 950 °C) for propane, but still lower than the average temperatures measured when the combustor was operated with methane. The temperature scale in Fig. 17 is not sensitive enough to show the small increase in temperature upstream of the catalyst, but the temperature increase downstream of the catalyst caused by an increase of 12% in the combustion efficiency (from 85 to 97%), and the large tem-

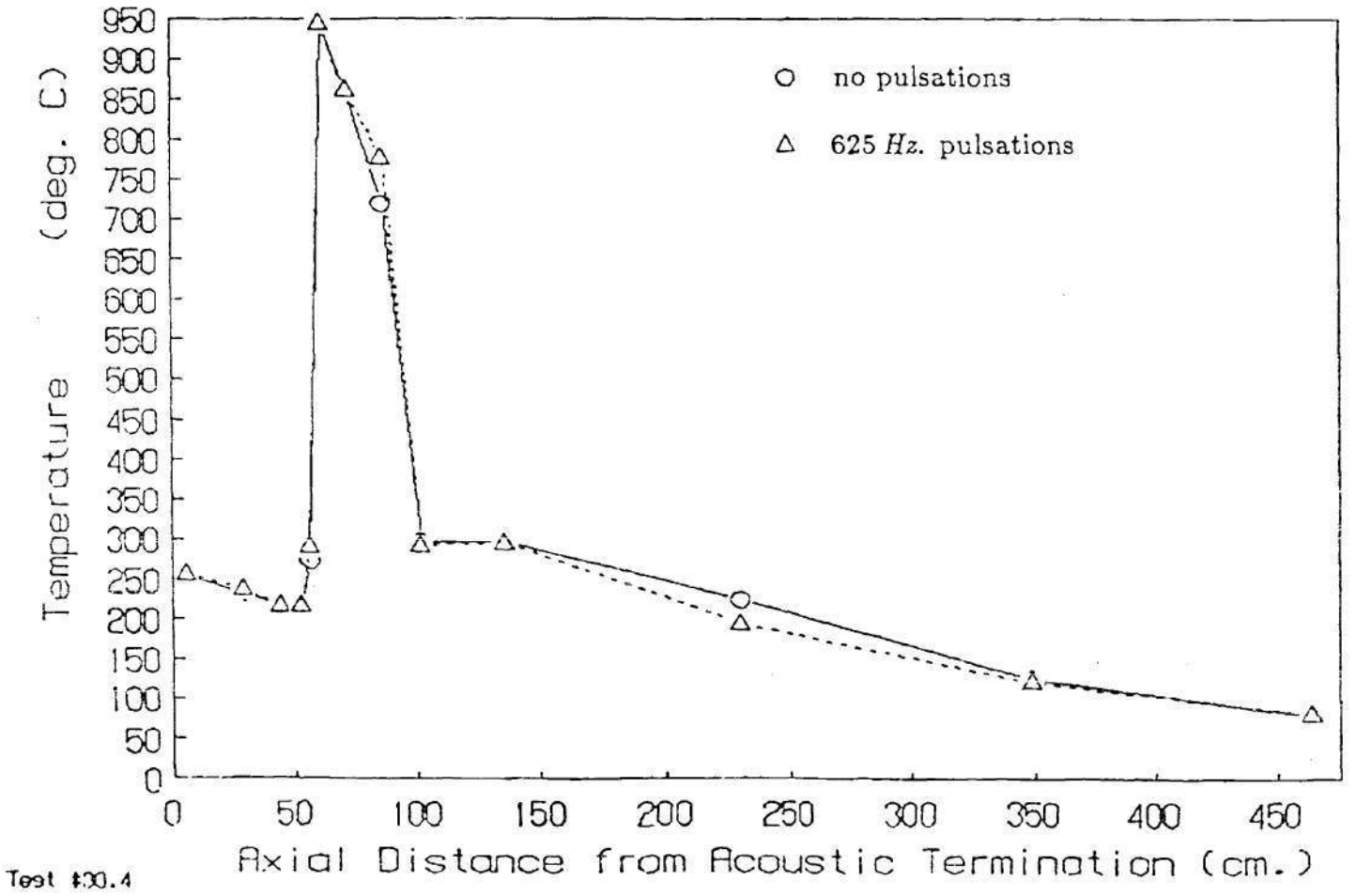

Figure 17: Temperature Distribution Along the Experimental Setup During Combustion of 9,000 *ppm*, 150 *lit/min* Propane Mixture

perature drop caused by onset of acoustic waves at the center of the combustor, are clearly seen. Figure 18 presents similar data for a propane concentration of 6,000 *ppm*. The effects are, generally, very similar to those shown for the concentration of 9,000 *ppm*, with temperature changes in the vicinity of the catalyst (both upstream and downstream of it) somewhat higher. This can be explained by noting the difference between the two tests. When a propane concentration of 9,000 *ppm* was used the combustion efficiency during non-pulsating operation was about 85% and improved upon the excitation of acoustic waves by 12%. With 6,000 *ppm*, the efficiency during non-pulsating operation was only 65% and the onset of acoustic waves increased the efficiency by about 22%. Table 3 presents the temperatures measured along the combustor under non-pulsating conditions and three different amplitudes of 717 *Hz* oscillations. Figure 19 shows the temperature data and the calculated temperature distribution along the combustor during the non-pulsating operation, and Fig. 20 shows the changes caused by the oscillations and the improvement in the combustor's operation upon increasing acoustic power. The data for non-pulsating operation is the average temperature measured during the stoppage of the acoustic drivers between the periods of acoustic excitation at different amplitudes. The data is for an air flow rate of 156.1 *lit/min*, a propane concentration of 5996 *ppm*, acoustic oscillations at 717 *Hz*, mean flow velocity in the catalytic combustion section of 2.15 *m/sec*, and with the catalyst at a distance of 135.3 *cm* from the acoustic termination (the axial reference point, which is the porous plate shown in Fig. 1). This temperature distribution along the combustor and the effects of the acoustic wave amplitude on the temperature distribution are typical for acoustic pulsations which caused increases in the combustion efficiency.

Responses of three thermocouples downstream of the catalyst to onset and stoppage of acoustic oscillations in Test No. 30 are shown in Fig. 21. Thermocouple No. 11 was about 80 *cm* downstream of the catalyst and its temperature increased when the drivers were turned on, and vice versa. Thermocouples Nos. 12 and 13

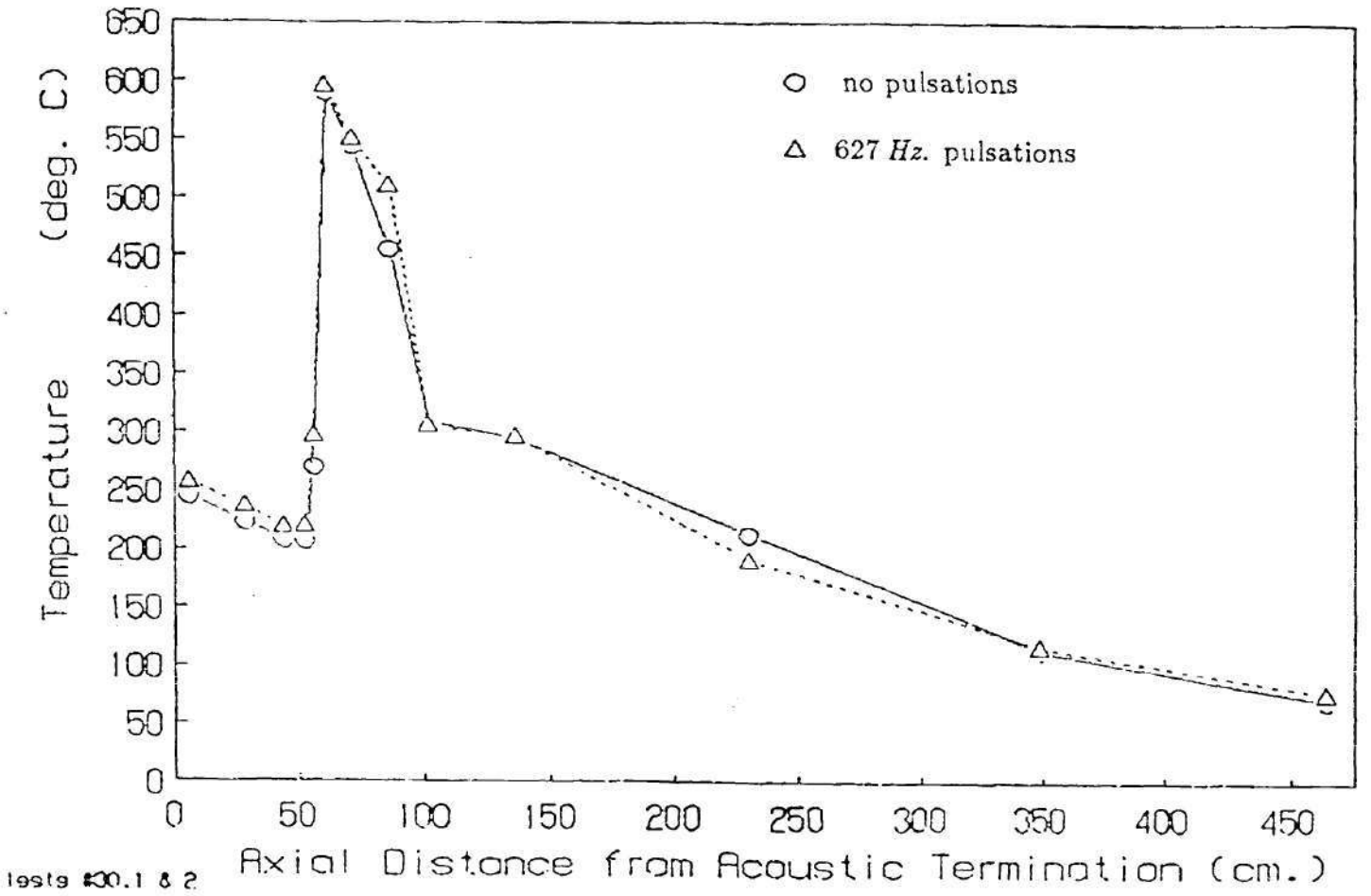

Figure 18: Temperature Distribution Along the Experimental Setup During Combustion of 6,000 *ppm*, 150 *lit/min* Propane Mixture

Table 3: Temperatures Measured Along the Combustor in Tests with Different Acoustic Amplltudes.

Axial Location	Acoustics off	Amplitude of Acoustic Wave		
		139.6 *dB*	148.8 *dB*	161.7 *dB*
x = 7.0 cm	171.8 °C	171.8 °C	171.8 °C	171.8 °C
x = 28.5 cm	141.5 °C	140.8 °C	140.8 °C	141.5 °C
x = 37.6 cm	118.1 °C	118.1 °C	118.8 °C	118.8 °C
x = 78.0 cm	91.9 °C	92.6 °C	92.6 °C	93.3 °C
x = 112.5 cm	100.3 °C	102.3 °C	103.7 °C	104.3 °C
x = 120.9 cm	103.7 °C	105.1 °C	107.7 °C	109.9 °C
x = 128.8 cm	132.3 °C	134.3 °C	137.7 °C	141.1 °C
x = 132.8 cm	145.0 °C	147.7 °C	151.7 °C	155.1 °C
x = 137.8 cm	626.0 °C	646.0 °C	658.1 °C	667.6 °C
x = 152.9 cm	441.8 °C	469.7 °C	482.4 °C	496.2 °C
x = 219.3 cm	161.3 °C	127.3 °C	108.3 °C	94.5 °C
x = 348.9 cm	110.3 °C	100.0 °C	95.9 °C	93.4 °C
x = 463.5 cm	84.0 °C	84.0 °C	84.0 °C	84.0 °C
η_c	55.2 %	72.3 %	86.3 %	93.7 %

Air flow rate 156.1 *lit/min*, 5996 *ppm* propane,

frequency of acoustic pulsations = 717 *Hz*.

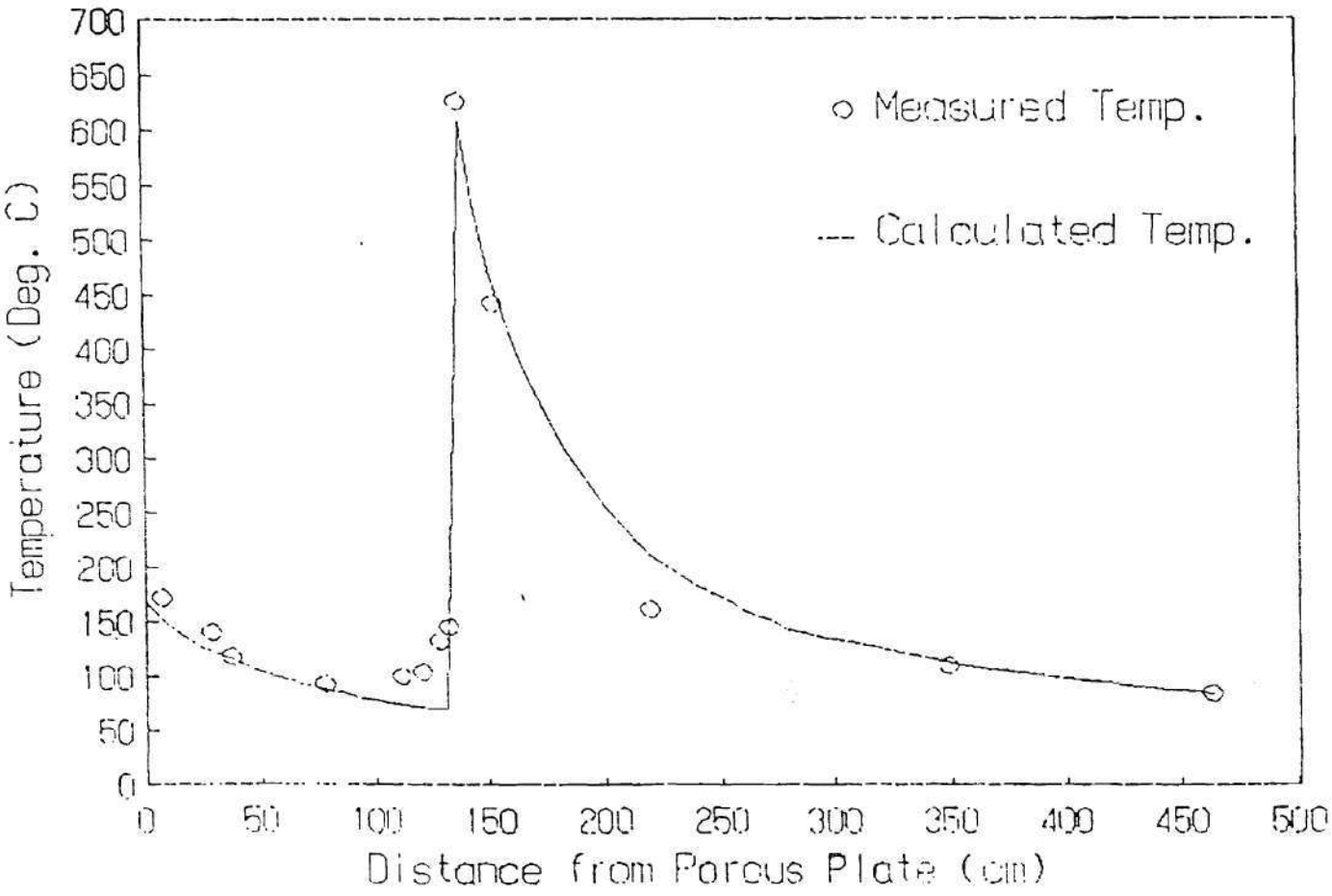

Figure 19: Temperature Distribution Along the Experimental Setup During Non-Pulsating Operation

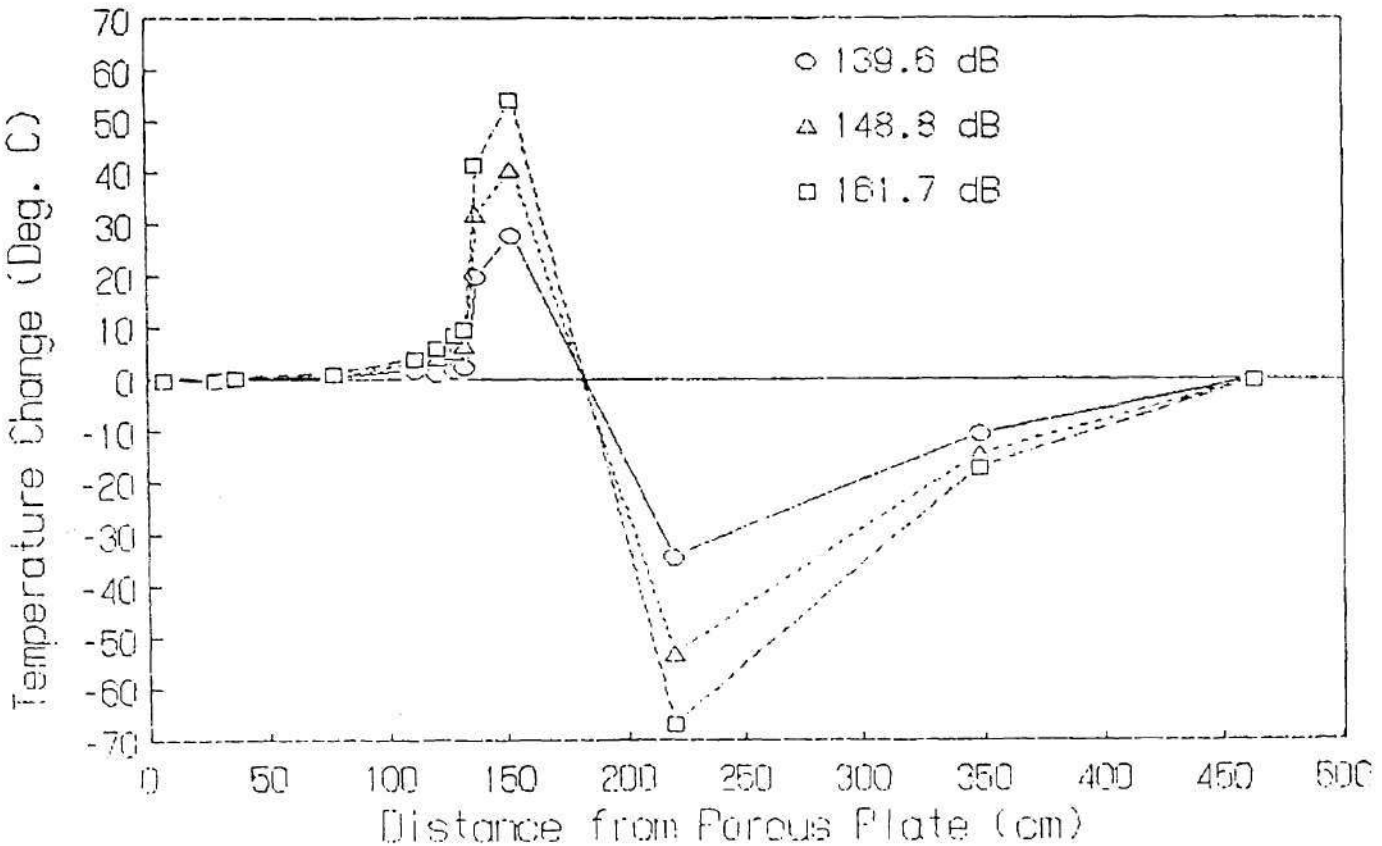

Figure 20: Temperature Changes Caused by 717 *Hz* Pulsations at Three Different Amplitudes

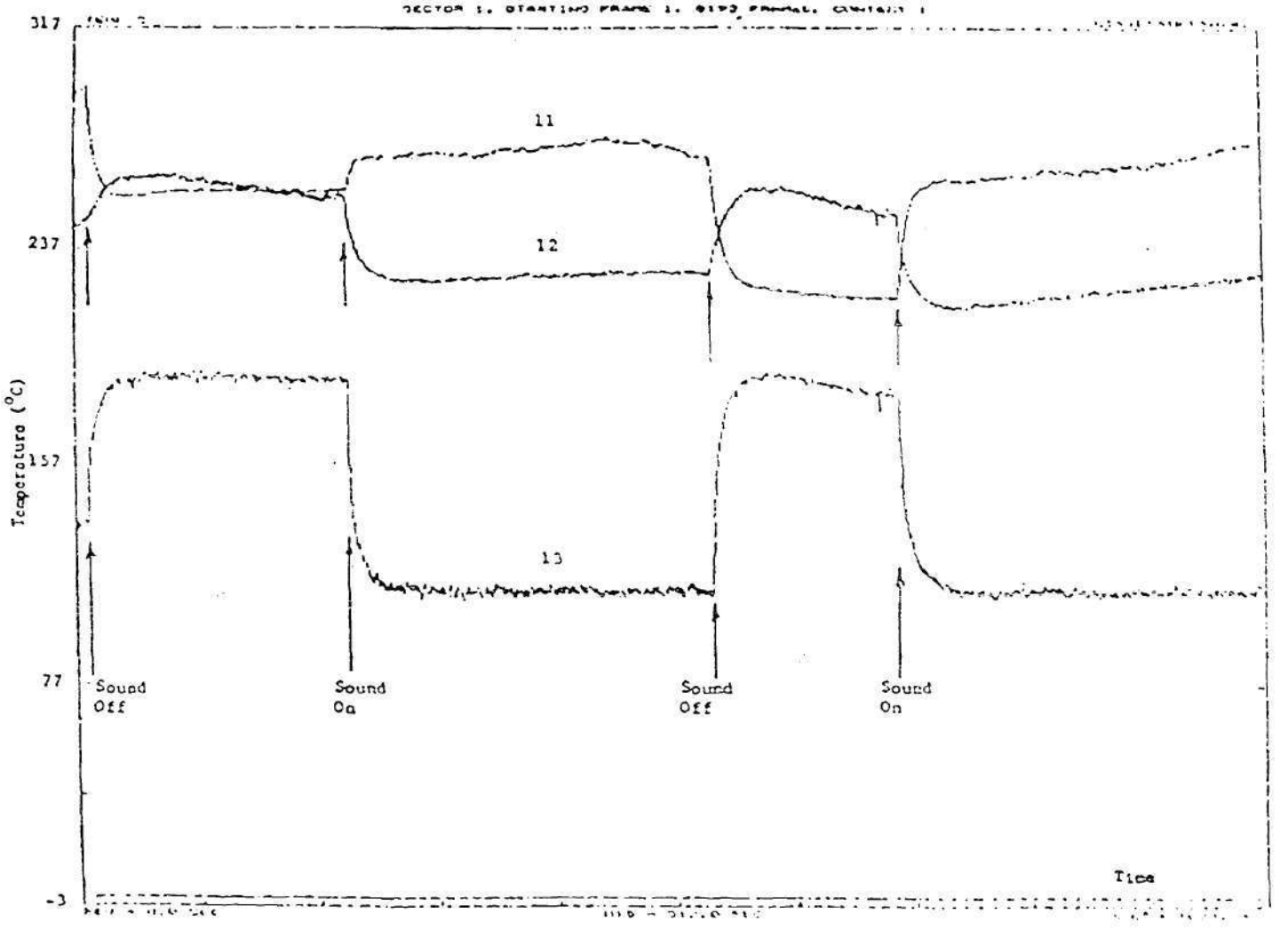

Figure 21: Themperature Histories Indicating "Reversed" Temperature Gradient in Test No. 30

were 120 and 240 *cm* further downstream, respectively, and showed the opposite effect. Similar effects were noted with methane and have been explained. The phenomenon seen in Fig. 21 is that when the acoustic oscillations were stopped the temperature measured by thermocouple No. 12 was in several instances larger than the temperature measured upstream of it by thermocouple No. 11. Figure 22 shows the axial locations of thermocouples Nos. 11 and 12, and the temperatures measured by them before, during, and after the onset of acoustic pulsations, and shows clearly the "reversed" gradient measured after the stoppage of pulsations. It should be noted that the small difference in the temperatures measured by thermocouples Nos. 11 and 12 prior to the onset of acoustic pulsations is due to the similar "reversed" effect caused by the stoppage of the previous acoustic pulsations. Similar effect of "reversed" axial temperature gradient is shown in Fig. 23 for different test conditions. Thermocouple No. 4 was located 84 *cm* downstream of the catalyst, and thermocouple No. 11 is the next thermocouple 130 *cm* further downstream. Onset of acoustic pulsations increased the temperature readings of thermocouple 4 and decreased the readings of thermocouple 12, as explained before. When the pulsations were stopped, the opposite changes occurred with the temperature measured by thermocouple 4 being lower than those measured by thermocouple 12 upstream of it. Such "reversed" temperature gradients downstream of the catalyst which existed during several minutes were observed several times when acoustic pulsations were stopped during catalytic combustion of propane. Although thermoacoustics (see Rott [32] and Swift [33]) can explain "reversed" axial temperature gradients during acoustic pulsations, no explanation was found for such temperature gradients caused by the stoppage of pulsations.

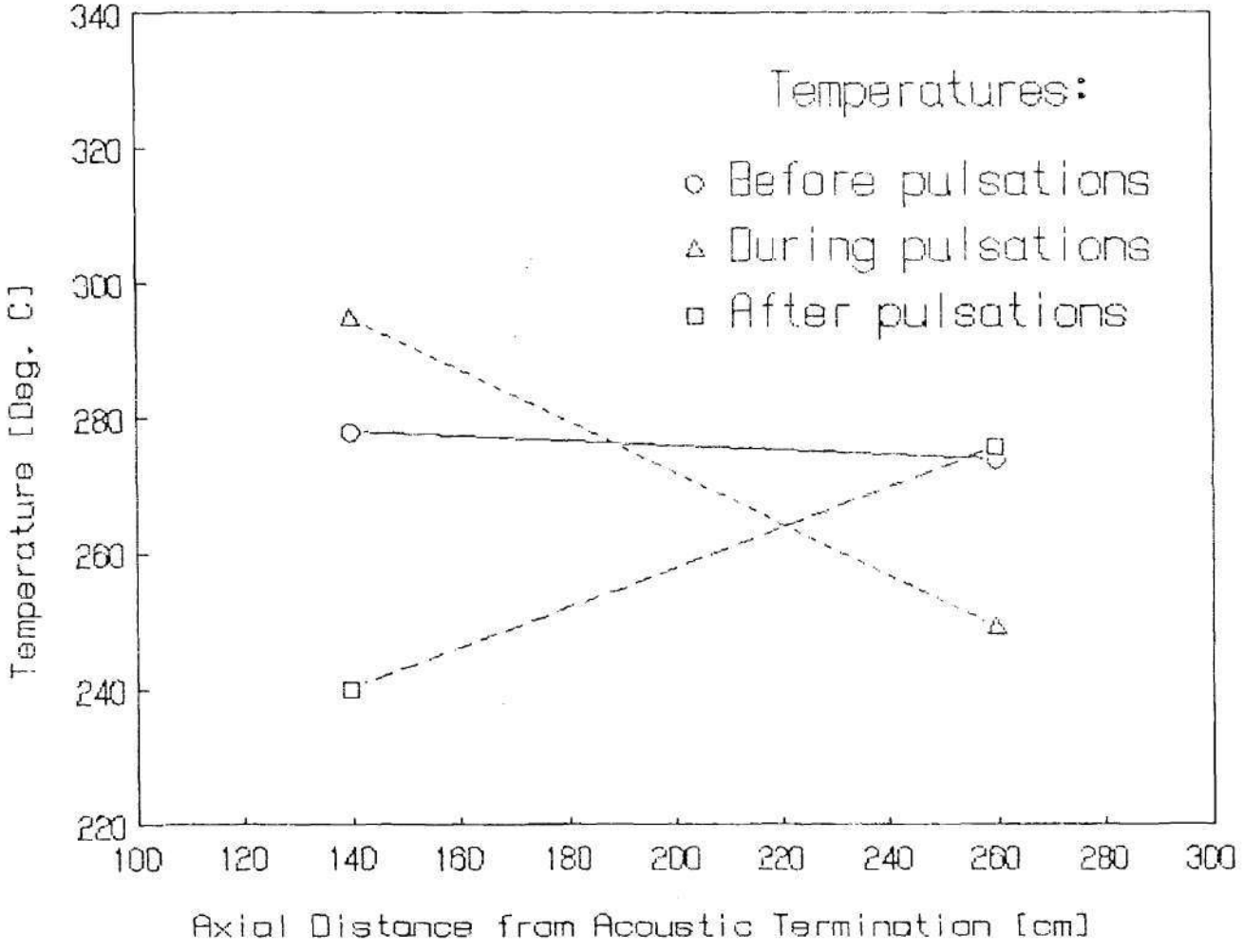

Figure 22: Temperature Measurements of Thermocouples Nos. 11 and 12 Before During and After Onset of Acoustic Pulsations

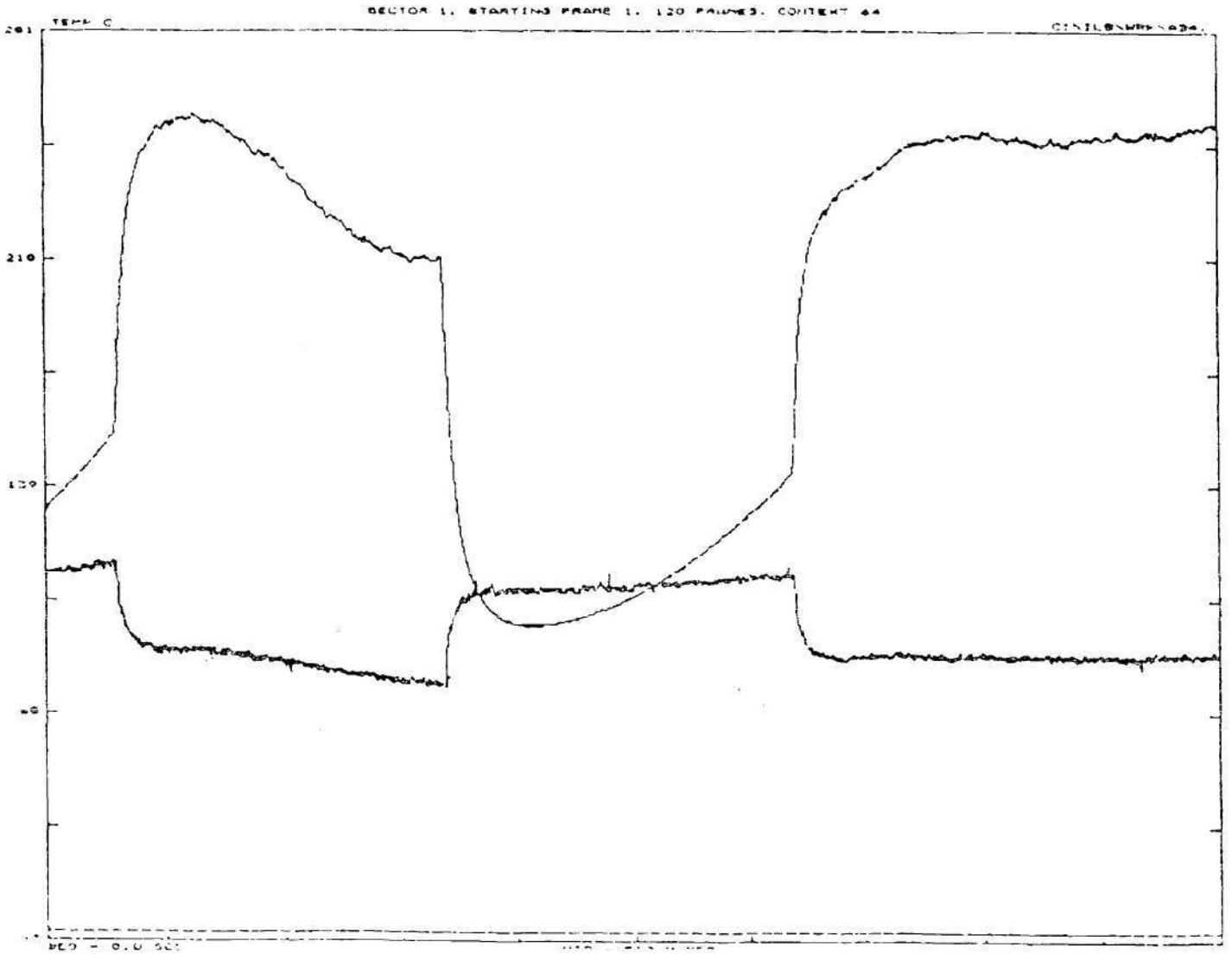

Figure 23: Temperature Histories Indicating "Reversed" Temperature Gradient in Test No. 33

since it was possible to attain stable and incomplete catalytic combustion of propane under non-pulsating operating conditions, it became possible to investigate whether acoustic pulsations can improve the combustion efficiency of the catalytic combustor. Frequencies in the 200 - 2,000Hz range were investigated. The excited wave amplitudes depended on the frequency of the waves and the location of the catalyst. When operating the acoustic drivers at frequencies up to 1,000 Hz and an electrical power input of 100 *watt*, the average *sound pressure levels* in the experimental setup were about 140$\pm$5 dB. Amplitudes of up to 162 dB were measured at several narrow "resonant" frequency ranges. At frequencies above 1,000 Hz, the amplitude of the acoustic pulsations decreased with increased frequency, and "resonant" peaks were not detected. Amplitudes of 130 dB or less were measured at frequencies higher than 1600 Hz The "resonant" frequencies shifted when the axial temperature distribution changed, but the shifts in "resonsnt" frequency ranges and the amplitudes measured were negligible when the axial temperature distribution was approximately constant.

For some operating conditions, large changes in hydrocarbon, O_2 and CO_2 concentrations were detected when pulsations at frequencies in the 300 - 1,000Hz range were excited, and the resulting amplitudes of pulsations exceeded 135 dB. The hydrocarbon and oxygen concentrations decreased in these cases, while the carbon dioxide concentration increased. This indicated that the exitation of acoustic pulsations increased the amount of fuel consumed by the catalytic reaction. The increase in the temperature just downstream of the catalyst, which was observed during these periods (as described in the previous section), also indicated improvement in the combustion efficiency. At different operating conditions, onset of acoustic pulsations produced no or negligible changes in the hydrocarbon, O_2 and CO_2 concentrations. Furthermore, under these conditions practically no temperature changes were observed immediately downstream of the catalyst.

The first improvements in the combustion efficiency were detected during initial tests with propane when acoustic pulsations in the 600 - 680 *Hz* frequency range were excited. In this frequency range, acoustic amplitudes of 137 to 154 *dB* were excited when running the system with a propane concentration of 6,000 *ppm.* and driving the acoustic sound generation system with an electrical input of 100 *watt.* The effects of pulsations in the 600 - 680 *Hz* frequency range upon the combustion efficiency are presented in Figs. 24 to 27. Figure 24 describes the time variations of the amplitude of oscillations, and Figs. 25, 26, and 27, the time variations of the hydrocarbon, CO_2, and oxygen concentrations, respectively. The data presented in all four figures was measured during the same 17 minutes time interval. The initial data were measured when a 627 *Hz* oscillation was stopped. This change to non-pulsating operation decreased the combustion efficiency as reflected by the increase of hydrocaron and oxygen concentrations and the decrease in CO_2 concentration. Upon the excitation of a 650 *Hz*, 150.6 *dB* acoustic pulsation the combustion efficiency increased from 55 to 78%. When the pulsations were stopped, the combustion efficiency decreased to 46%. Similar results were obtained in 15 tests conducted in the 600 - 680 *Hz* frequency range with the acoustic drivers operating at maximum power. Although the combustion efficiency during the non-pulsating operation periods varied from 46 to 62 percent, the onset of acoustic pulsations increased the efficiency by 20 to 40%, yielding efficiencies of 75 to 94%. It was clear from these measurements that the onset of acoustic pulsations improved considerably the combustion efficiency. When the electrical input to the acoustic drivers was decreased, causing lower *Sound Pressure Levels* in the combustor, the increases in combustion efficiencies were smaller. No improvement in combustion efficiencies was detected when the acoustic amplitude was reduced below 135 *dB*. This proved that the effect of acoustic pulsations is amplitude dependent.

During the initial tests the catalyst was located about 60 *cm* downstream of the porous plate which acted as acoustic termination. The acoustic pressure and

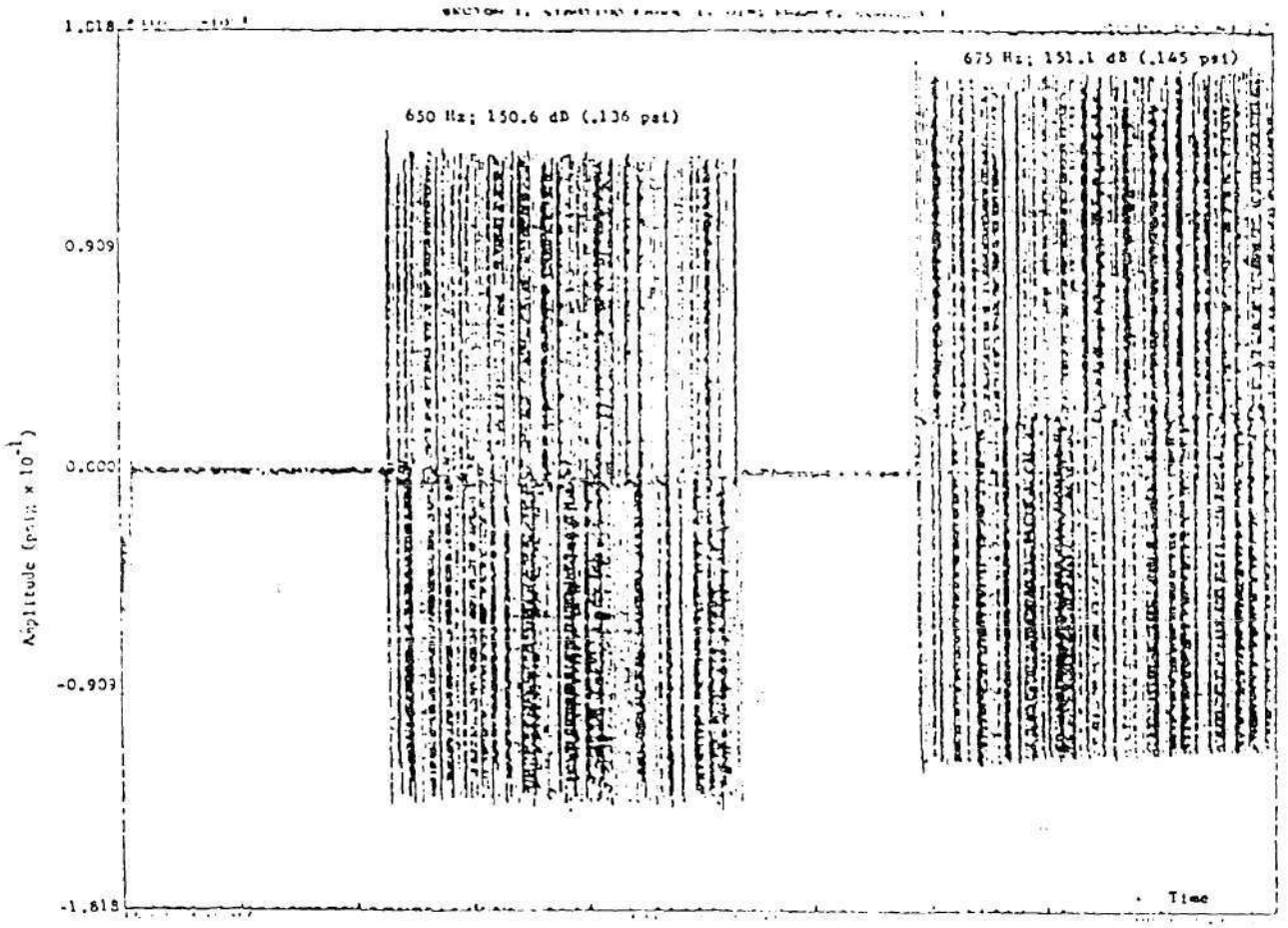

Figure 24: The Variation of Acoustic Pressure with Time in Test No. 30

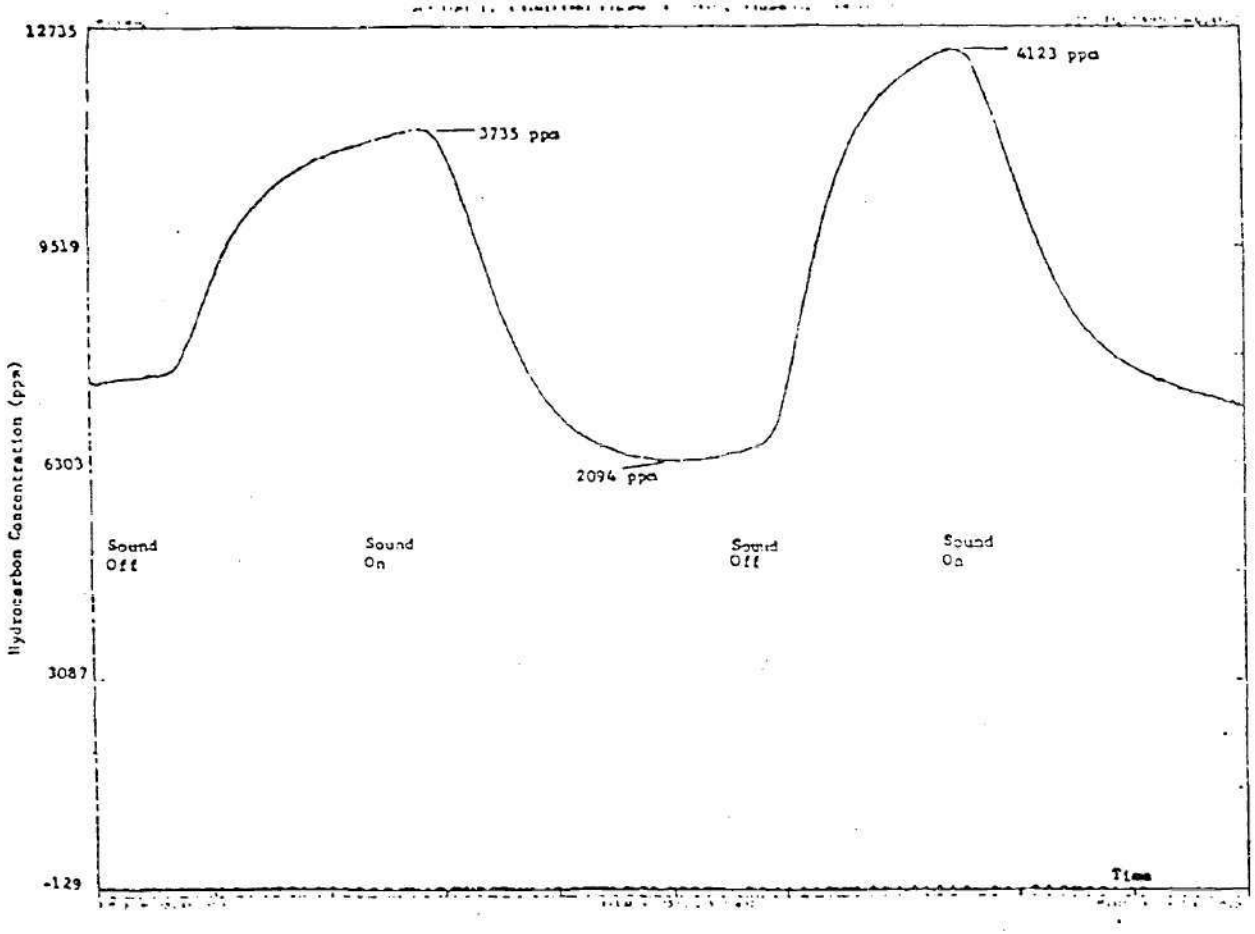

Figure 25: The Variation of Hydrocarbon Concentration with Time in Test No. 30

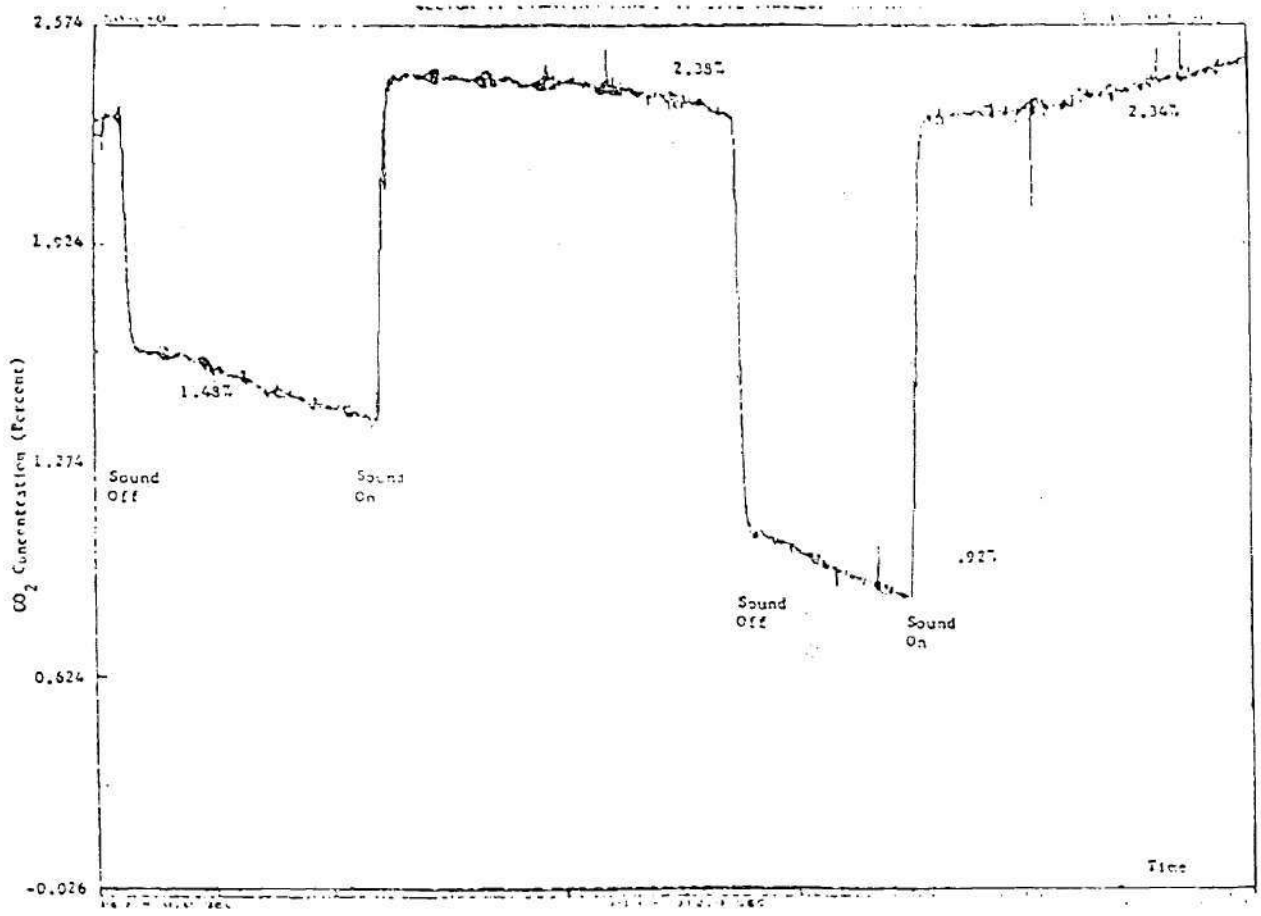

Figure 26: The Variation of CO_2 Concentration with Time in Test No. 30

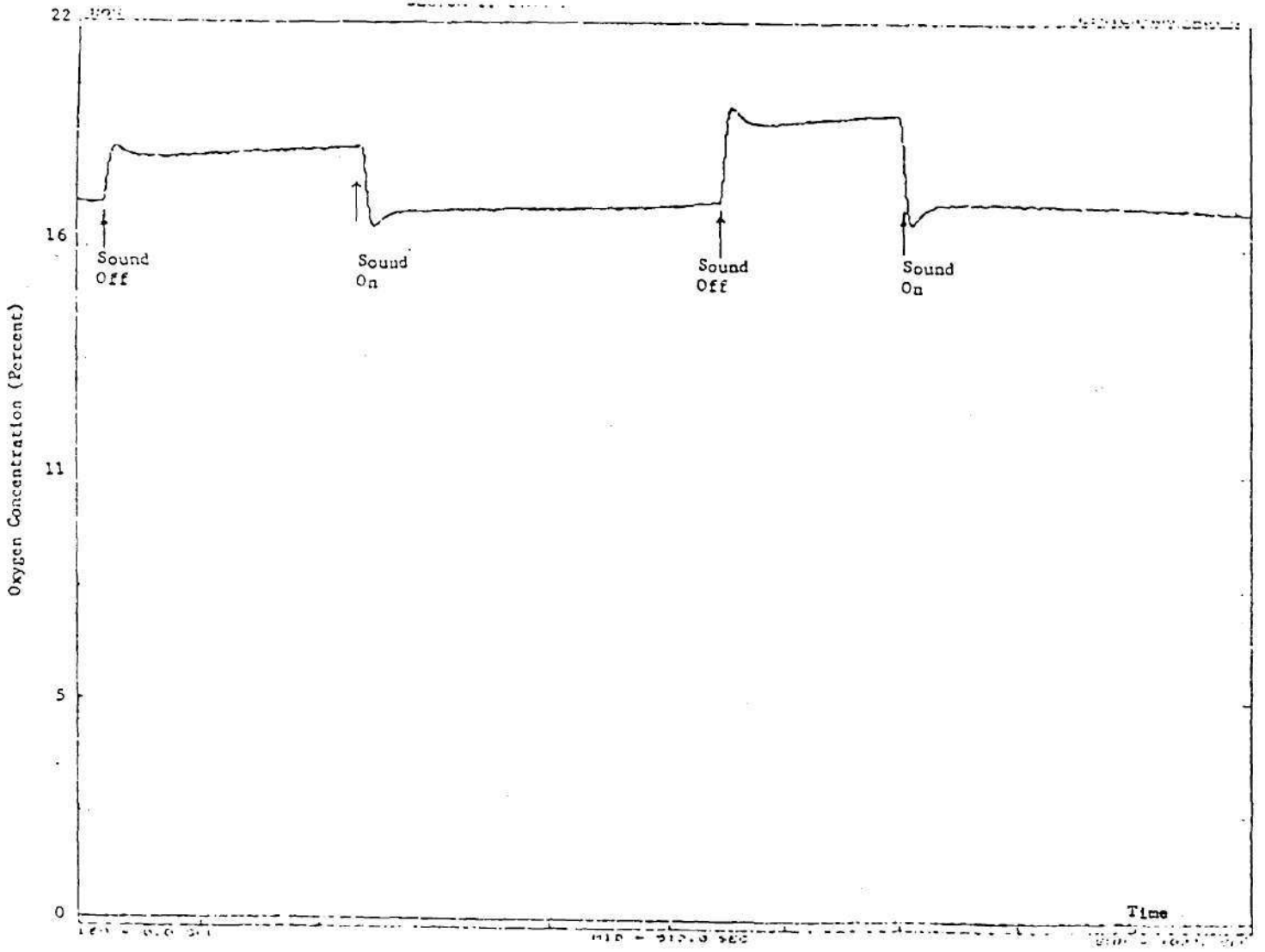

Figure 27: The Variation of Oxygen Concentration with Time in Test No. 30

velocity amplitude distributions inside the experimental setup were calculated for the excited frequencies. These calculations indicated that whenever combustion efficiencies improved upon the onset of pulsations, the catalyst was located between an upstream pressure node and a downstream velocity node. Figures 28 and 29 show the calculated acoustic wave patterns for 627 and 649 Hz, respectively, where the catalyst was located at such a position (i.e., located after the second pressure node at $x = 60\,cm$). When operating the combustor with methane, the same relative location of the catalytic section on the standing wave pattern caused shifts in the location of the combustion and onset or extinction of gas phase combustion. These changes were probably caused by extensive local circulatory flows induced by the onset of pulsations, which changed the temperature distribution in the catalytic section. Such circulatory flow patterns can effect both the temperature and the propane concentration distributions in the catalytic combustion section and cause the changes in combustion efficiency.

During the initial tests with propane, during which the catalyst segment was located about 60 cm downstream of the porous plate, only one "resonant" frequency range (i.e., the 600 - 680 Hz range) existed. Outside the frequency range the maximum detected *sound pressure levels* obtained with the acoustic drivers operating at maximum power were less than 140 dB. In order to understand the effect of the frequency of pulsations and to find whether the location of the catalyst with respect to the acoustic standing wave is an important factor, a broader frequency range at which high amplitude acoustic oscillations can be stabilized was needed. Two changes in the operation of the combustor could produce higher amplitude acoustic pulsations in the experimental setup; acquisition of more powerful acoustic drivers, or changing the acoustic characteristic of the experimental setup by changing the location of the catalyst and/or changing the experimental setup length. In order to change the acoustic characteristics, the catalytic section was moved towards the downstream end of the combustor and placed

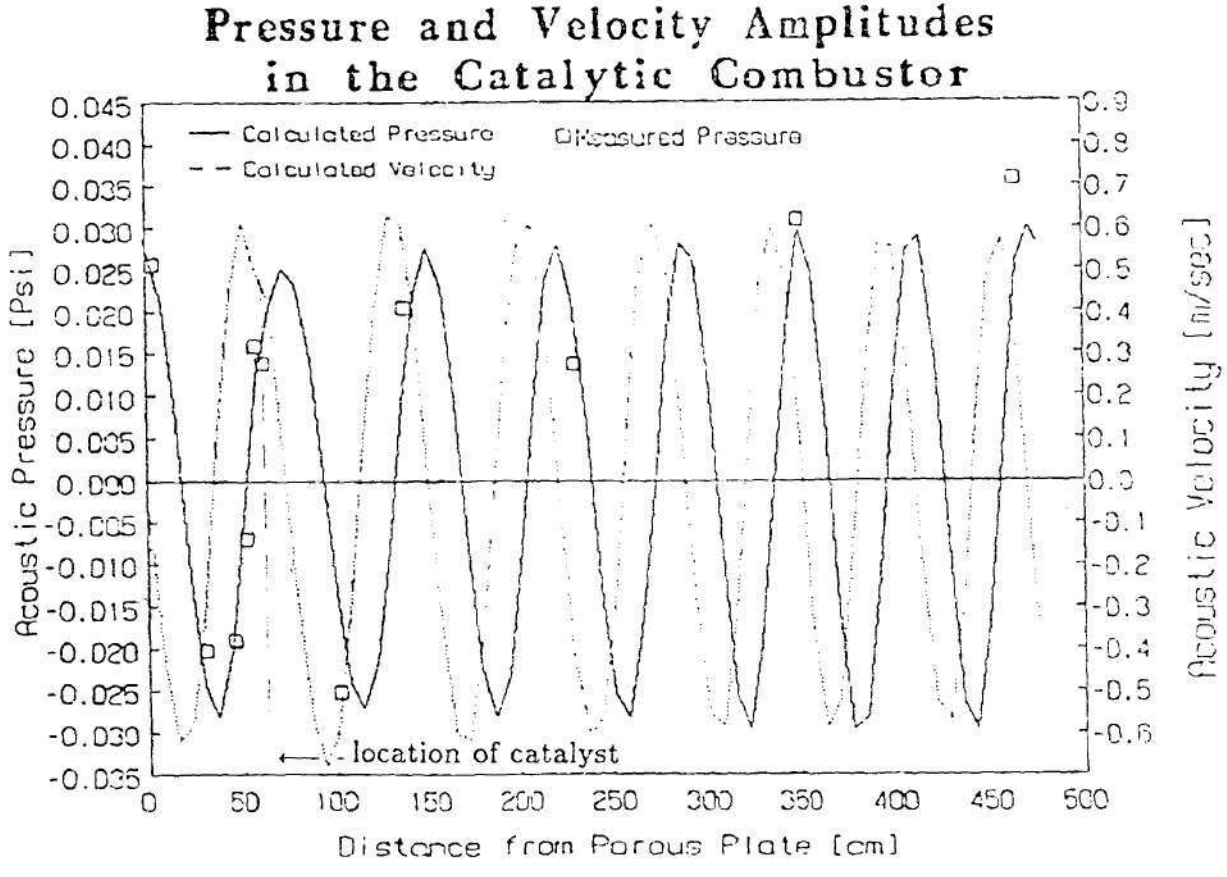

Figure 28: The Acoustic Wave Pattern for Oscillations of 627 *Hz*.

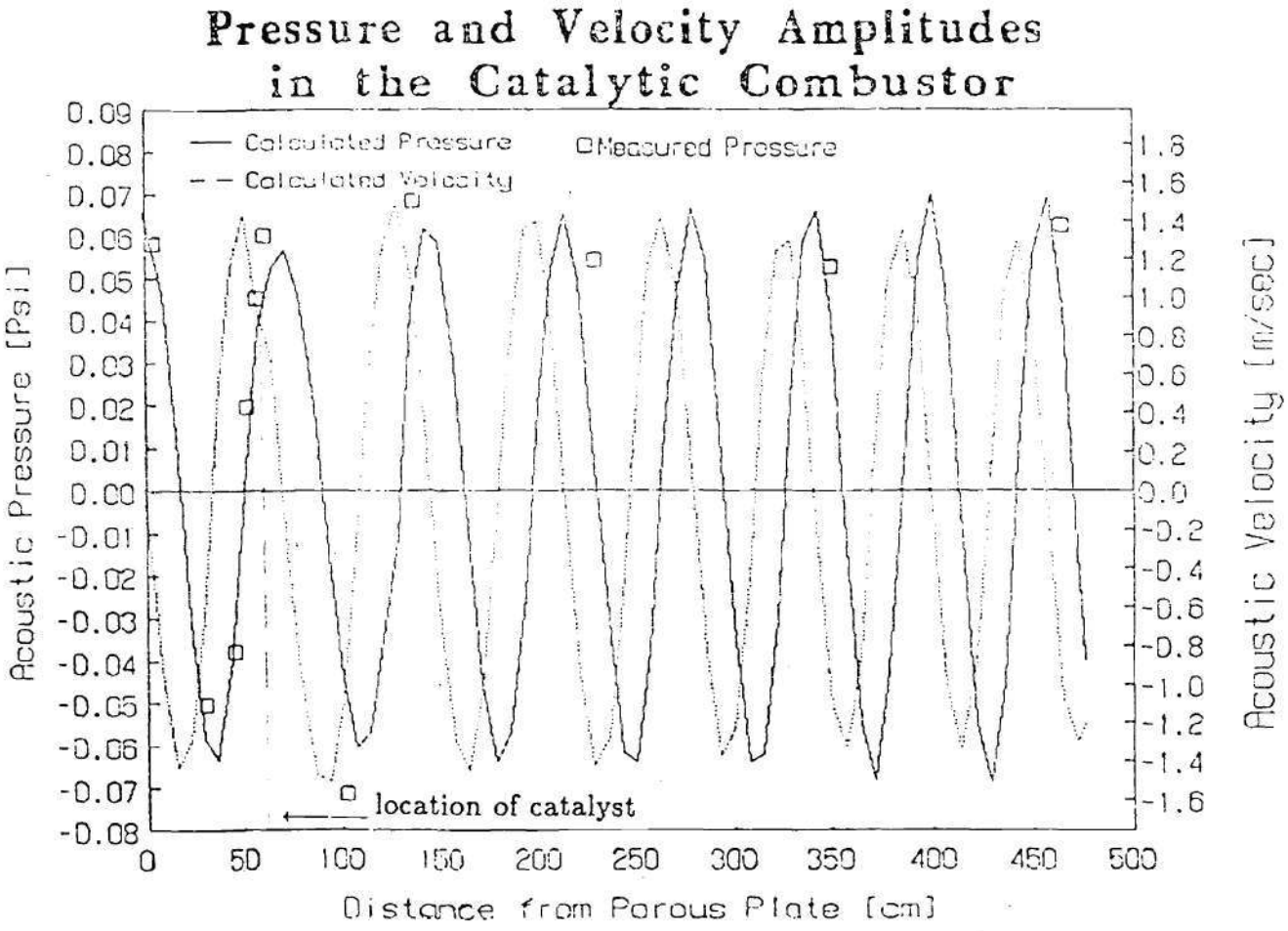

Figure 29: The Acoustic Wave Pattern for Oscillations of 649 *Hz*.

approximately 135 *cm* from the "acoustic hard wall termination". With the modified configuration, 6 to 8 new "resonant" frequencies were detected (depending on operating conditions), compared to the single "resonant" frequency (the 600 – 680 *Hz* range) with the original configuration. When operating near these frequencies, amplitudes between 140 and 162 *dB* could be excited. The existence of these "resonant" frequency ranges provided an opportunity for a more systematic investigation of the parameters which affect the combustion efficiency. In more than 15 tests, onset of pulsations at amplitudes in excess of 150 *dB* produced no or at most 2 to 5% increase in the combustion efficiency. Since the efficiencies measured during non-pulsating operations used to vary by about 5% without noticable change in the operating conditions, such changes were considered to be negligible. In all of these tests (which were conducted at different frequencies, flow rates and fuel concentrations) the calculations of acoustic pressures and velocities indicated that the location of the catalyst was between an upstream velocity node and a downstream pressure node; that is, in an "out of phase" location. When considerable improvements in combustion efficiency were detected upon onset of acoustic pulsations, calculations showed that the catalyst was in an "in-phase" location (i.e., between an upstream pressure node and a downstream velocity node). These results proved that the location of the catalyst on the standing wave pattern is a critical factor which determins whether the onset of pulsations would improve the performance of the catalytic combustor.

In order to determine the dependence of the combustion efficiency upon the amplitude of pulsations, the performance of the combustor was investigated at several "resonant" frequencies and flow rates with the catalyst at an "in phase" location. The results of these tests, in which the power input into the acoustic drivers was increased gradually, are summarized in Tables 4 to 7. Up to a power input of about 60 *watts* the measured concentrations of hydrocarbons, oxygen and carbon dioxide remained unchanged at the values reached during the non-pulsating

Table 4: Combustion Efficiency as Function of Acoustic Pressure Amplitude for 156.1 *lit/min* Air, 5996 *ppm* Propane and 717 *Hz* Pulsations.

Electric Power to Drivers	Amplitude at "Hard Wall"	η_c before Pulsations	η_c during Pulsations	η_c after Pulsations
0 *w*	112±3 *dB*	51.9% to 60.3%		
60 *w*	134.2 *dB*	51.9%	51.9%	51.9%
70 *w*	139.6 *dB*	51.9%	72.3%	55.6%
80 *w*	145.4 *dB*	55.6%	78.8%	—
80 *w*	144.8 *dB*	—	80.1%	52.4%
85 *w*	148.8 *dB*	52.4%	86.2%	60.3%
90 *w*	153.1 *dB*	60.3%	89.1%	58.2%
95 *w*	158.0 *dB*	56.4%	91.4%	54.1%
100 *w*	161.7 *dB*	54.1%	93.7%	58.3%

Table 5: Combustion Efficiency as Function of Acoustic Pressure Amplitude for 156.1 *lit/min* Air, 5996 *ppm* Propane and 663 *Hz* Pulsations.

Electric Power to Drivers	Amplitude at "Hard Wall"	η_c before Pulsations	η_c during Pulsations	η_c after Pulsations
0 *w*	112±3 *dB*	50.8% to 59.4%		
60 *w*	128.8 *dB*	52.1%	52.1%	52.1%
70 *w*	133.4 *dB*	52.1%	52.1%	52.1%
75 *w*	137.9 *dB*	52.1%	63.4%	50.8%
80 *w*	141.1 *dB*	50.8%	70.9%	—
80 *w*	140.9 *dB*	—	71.0%	54.2%
85 *w*	144.6 *dB*	54.2%	79.6%	56.7%
90 *w*	148.7 *dB*	56.7%	84.3%	59.4%
95 *w*	151.3 *dB*	51.3%	86.7%	56.1%
100 *w*	156.2 *dB*	56.1%	89.9%	52.0%

Table 6: Combustion Efficiency as Function of Acoustic Pressure Amplitude for 156.1 *lit/min* Air, 4817 *ppm* Propane and 665 *Hz* Pulsations.

Electric Power to Drivers	Amplitude at "Hard Wall"	η_c before Pulsations	η_c during Pulsations	η_c after Pulsations
0 *w*	115±3 *dB*	45.7% to 57.5%		
60 *w*	132.4 *dB*	45.7%	45.7%	45.7%
65 *w*	135.7 *dB*	45.7%	50.1%	50.1%
70 *w*	139.1 *dB*	50.1%	62.9%	48.3%
75 *w*	142.0 *dB*	48.3%	68.4%	52.3%
80 *w*	145.3 *dB*	54.1%	76.6%	52.0%
85 *w*	149.1 *dB*	52.0%	82.5%	49.8%
90 *w*	152.5 *dB*	49.8%	88.1%	52.6%
95 *w*	156.6 *dB*	52.9%	89.7%	57.5%
100 *w*	159.4 *dB*	57.5%	92.4%	54.9%
100 *w*	160.2 *dB*	54.9%	91.9%	49.3%

Table 7: Combustion Efficiency as Function of Acoustic Pressure Amplitude for 121.4 *lit/min* Air, 8776 *ppm* Propane and 453 *Hz* Pulsations.

Electric Power to Drivers	Amplitude at "Hard Wall"	η_c before Pulsations	η_c during Pulsations	η_c after Pulsations
0 *w*	109±4 *dB*	62.8% to 79.3%		
60 *w*	126.4 *dB*	64.3%	64.3%	64.3%
65 *w*	129.9 *dB*	64.3%	69.8%	62.8%
70 *w*	133.1 *dB*	62.8%	76.5%	68.1%
75 *w*	136.7 *dB*	64.9%	83.7%	69.2%
80 *w*	140.0 *dB*	69.2%	93.4%	72.7%
85 *w*	145.1 *dB*	72.7%	97.6%	76.0%
90 *w*	148.0 *dB*	75.2%	98.0%	79.3%
95 *w*	151.8 *dB*	79.3%	98.4%	69.9%
100 *w*	153.2 *dB*	69.9%	97.9%	65.4%
100 *w*	160.2 *dB*	54.9%	91.9%	49.3%

operation. A further increase in the electric power input to the drivers caused improvement of the combustion efficiency. Table 4 shows the data for 5996 *ppm* propane and air flow rate of 156.1 *lit/min* for acoustic pulsations of 717 *Hz.*; Table 5 for the same concentration and flow rate, but for a 663 *Hz* pulsation; Table 6 for an air flow rate of 156.1 *lit/min*, propane concentration of 4817 *ppm* and a pulsation frequency of 665 *Hz*; and Table 7 for an air flow rate of 121.4 *lit/min*, propane concentration of 8776 *ppm* and a 453 *Hz* pulsation. The flow velocities through the catalyst channels were between 1.9 and 2.5 *m/sec*. Zero electric power input means that the acoustic drivers were turned off. The combustion efficiency data in Tables 4 to 7 show that the values measured when the pulsations were turned off varied by up to $\pm 8\%$. Figures 30 to 33 present the data in Tables 4 to 7, respectively. The combustion efficiency is plotted vs. the amplitude of pulsations in *dB*. These figures show that for pressure amplitudes below 130 *dB* the pulsations exerted no effect on the combustion efficiency. However for amplitudes higher than 130 *dB* the combustion efficiency increased as the amplitude of oscillations increased. Figures 34 through 37 show the improvement in combustion efficiency for the conditions described in Tables 4 through 7, respectively, by plotting the ratio of combustion efficiency measured during operating the combustor under pulsating conditions to the combustion efficiency measured during non-pulsating operation both before and after onset of the oscillations. These figures show, as do Figures 30 through 33, that for pulsations larger than the threshold of about 130 *dB*, the improvement in combustion efficiency increased with the increase in the amplitude of the acoustic oscillations.

Proposed Mechanisms

The observed improvements in the performance of the pulsating catalytic combustor when the catalyst was located between an upstream pressure node and a

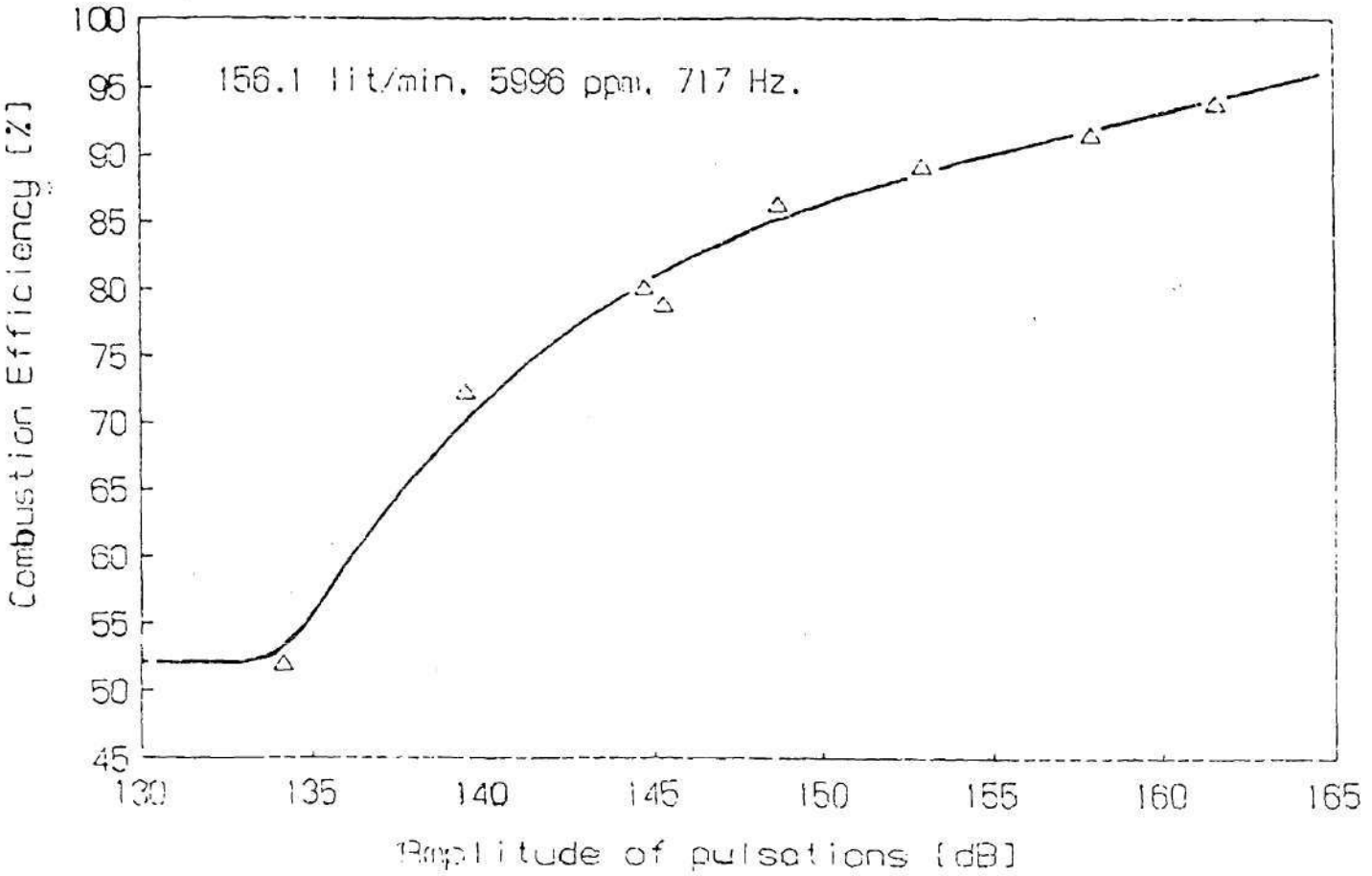

Figure 30: Combustion Efficiency as Function of the Pressure Amplitude for 717 *Hz* Oscillations

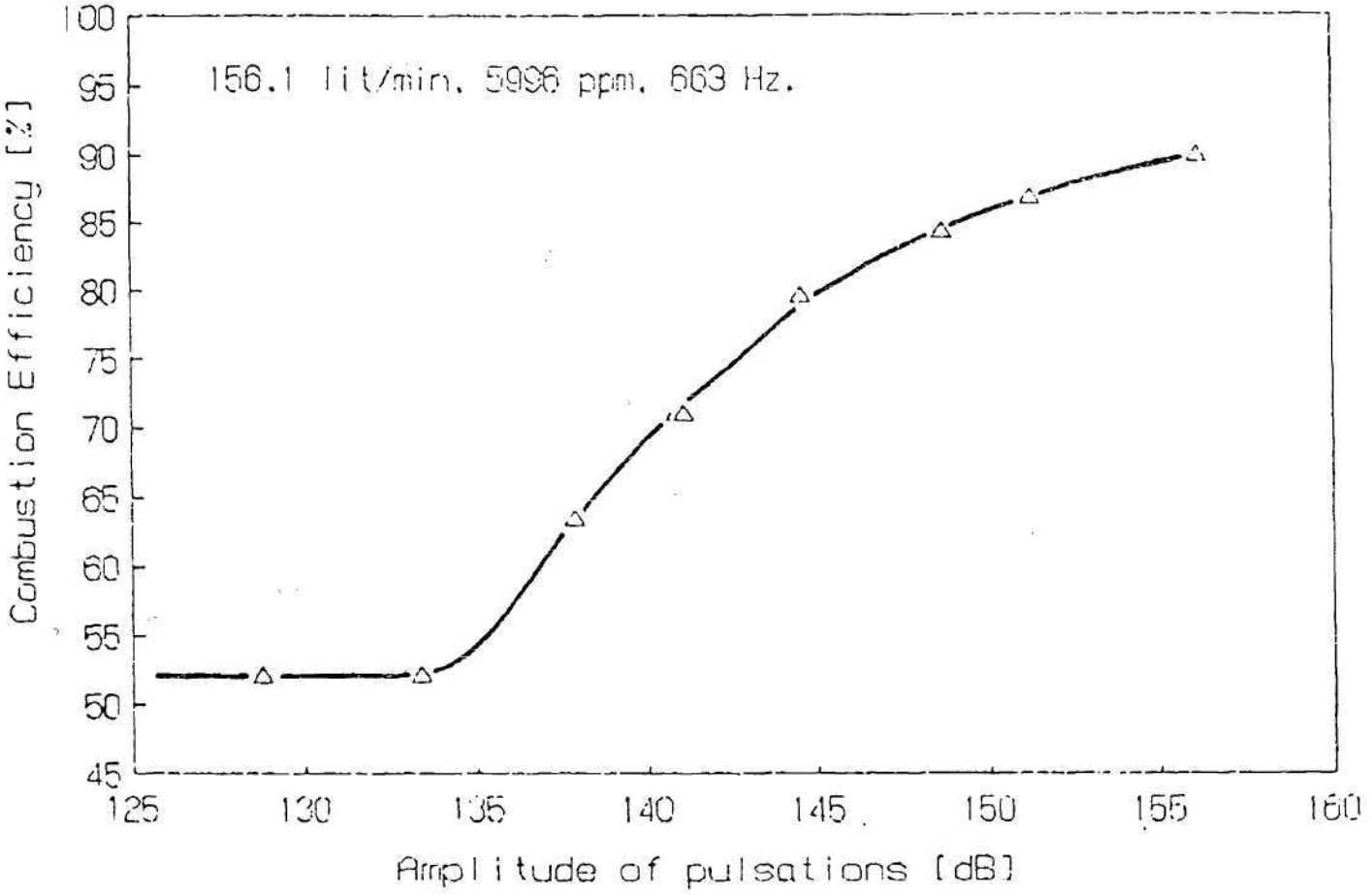

Figure 31: Combustion Efficiency as Function of the Pressure Amplitude for 663 *Hz* Oscillations

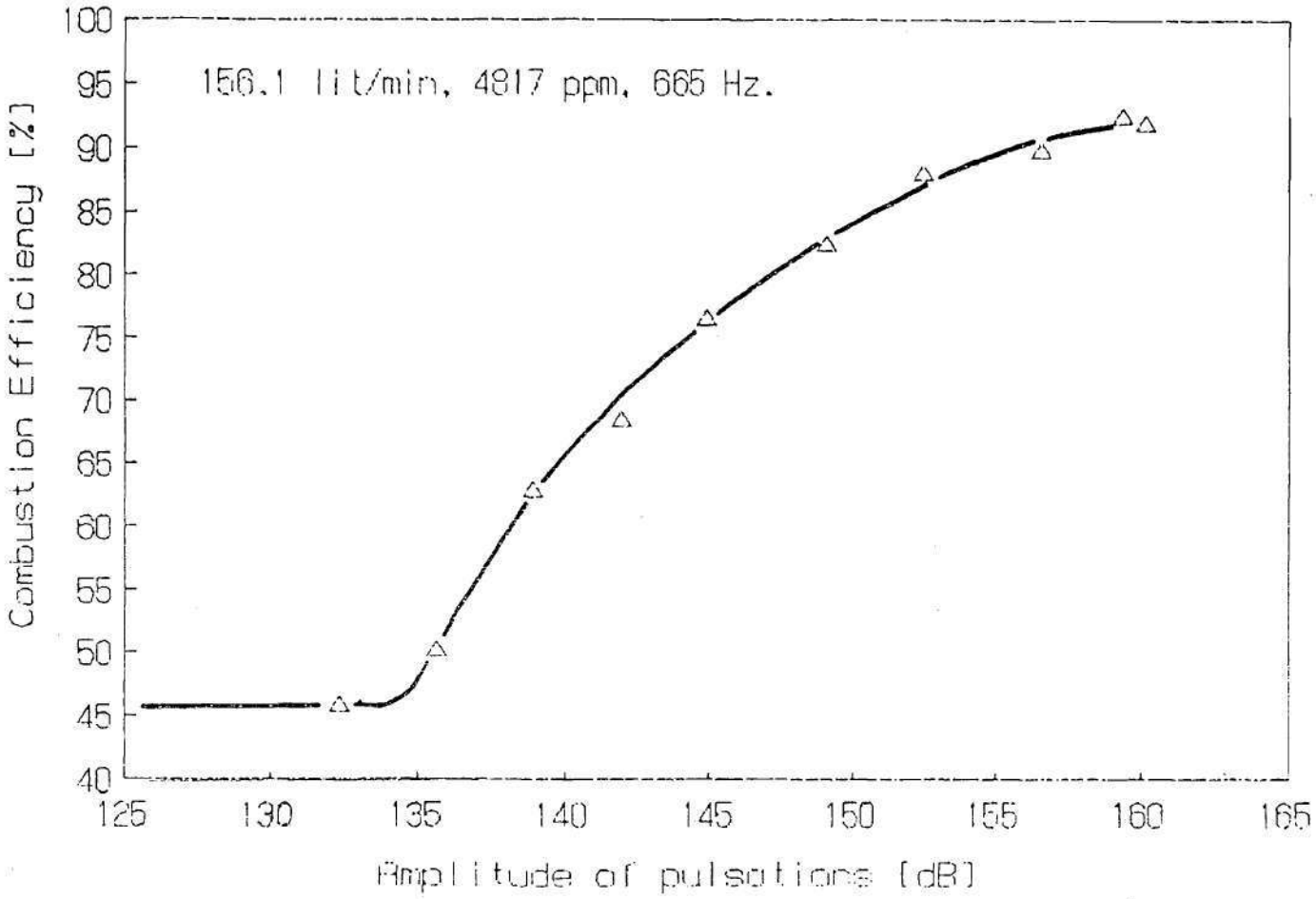

Figure 32: Combustion Efficiency as Function of the Pressure Amplitude for 665 *Hz* Oscillations

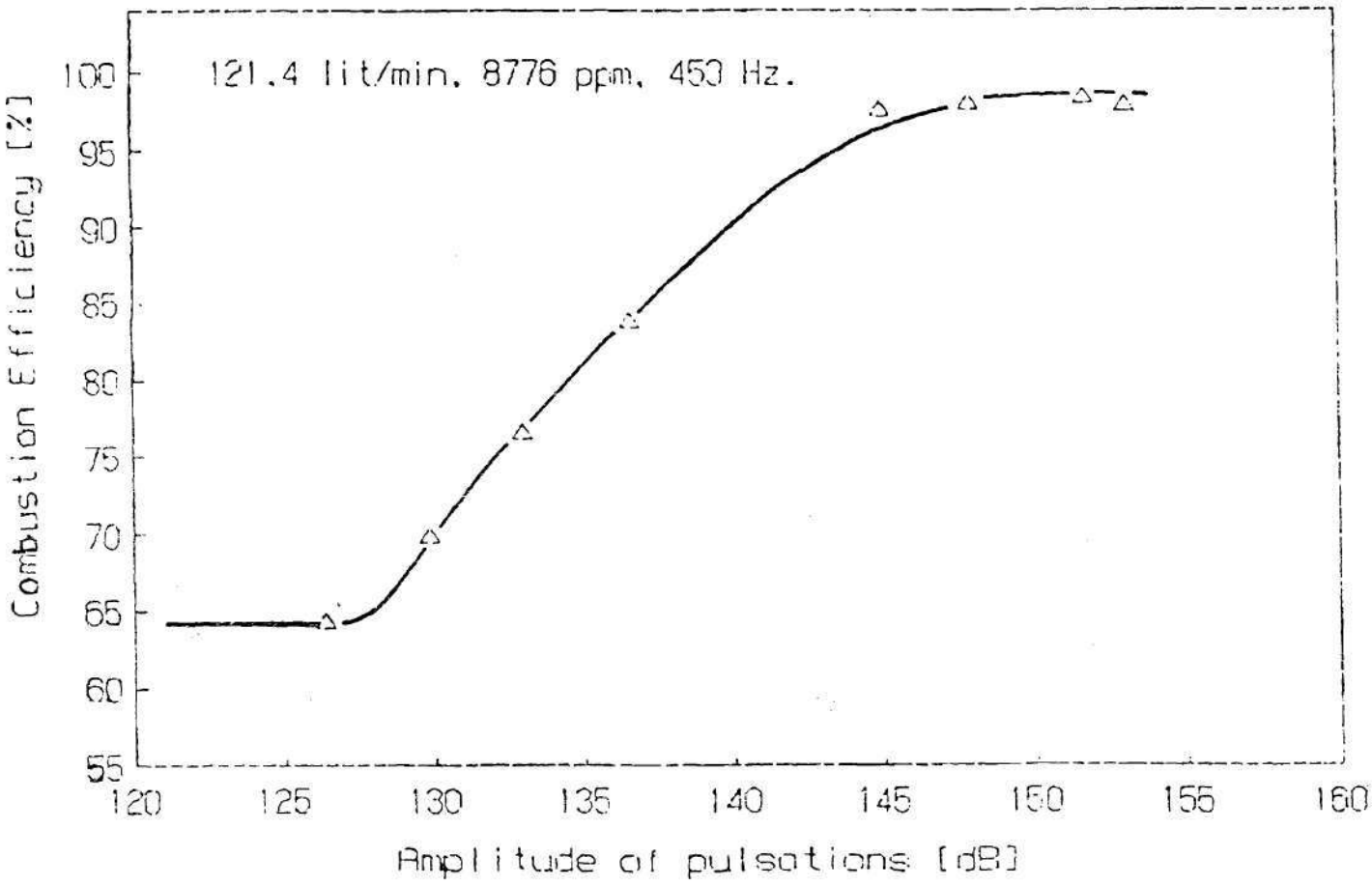

Figure 33: Combustion Efficiency as Function of the Pressure Amplitude for 453 *Hz* Oscillations

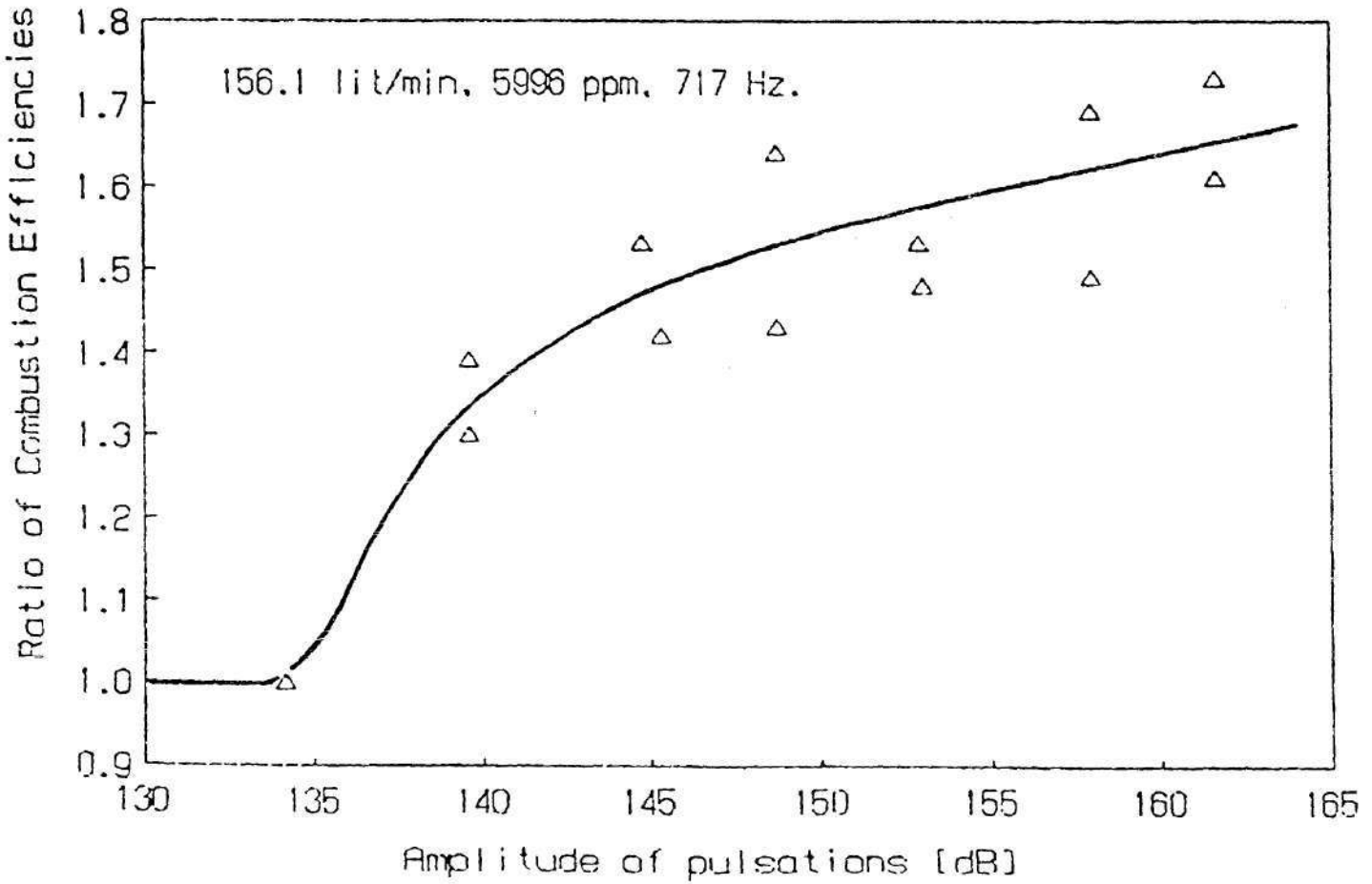

Figure 34: Ratio of Combustion Efficiencies vs. the Pressure Amplitude of 717 *Hz* Oscillations

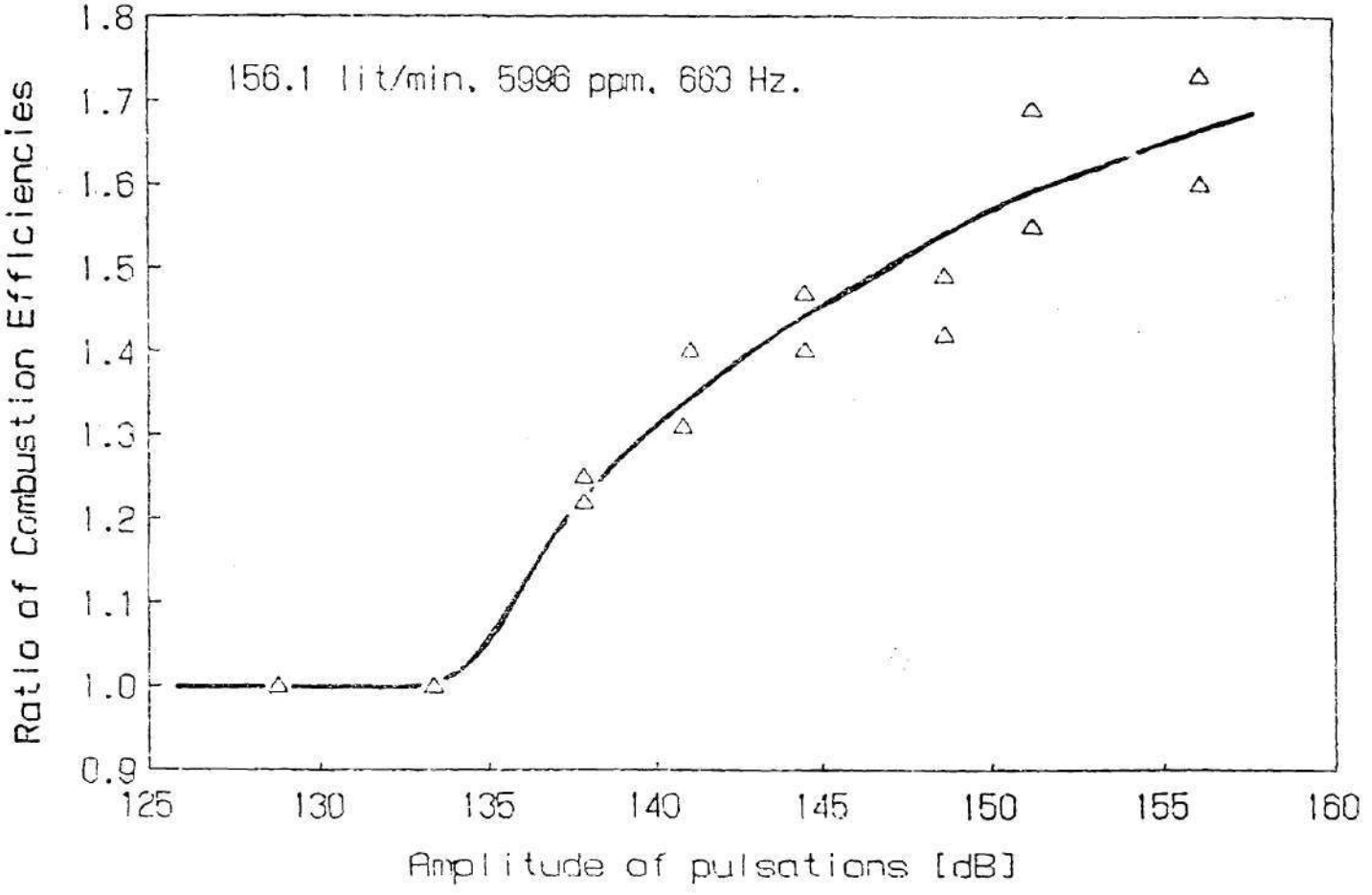

Figure 35: Ratio of Combustion Efficiencies vs. the Pressure Amplitude of 663 *Hz* Oscillations

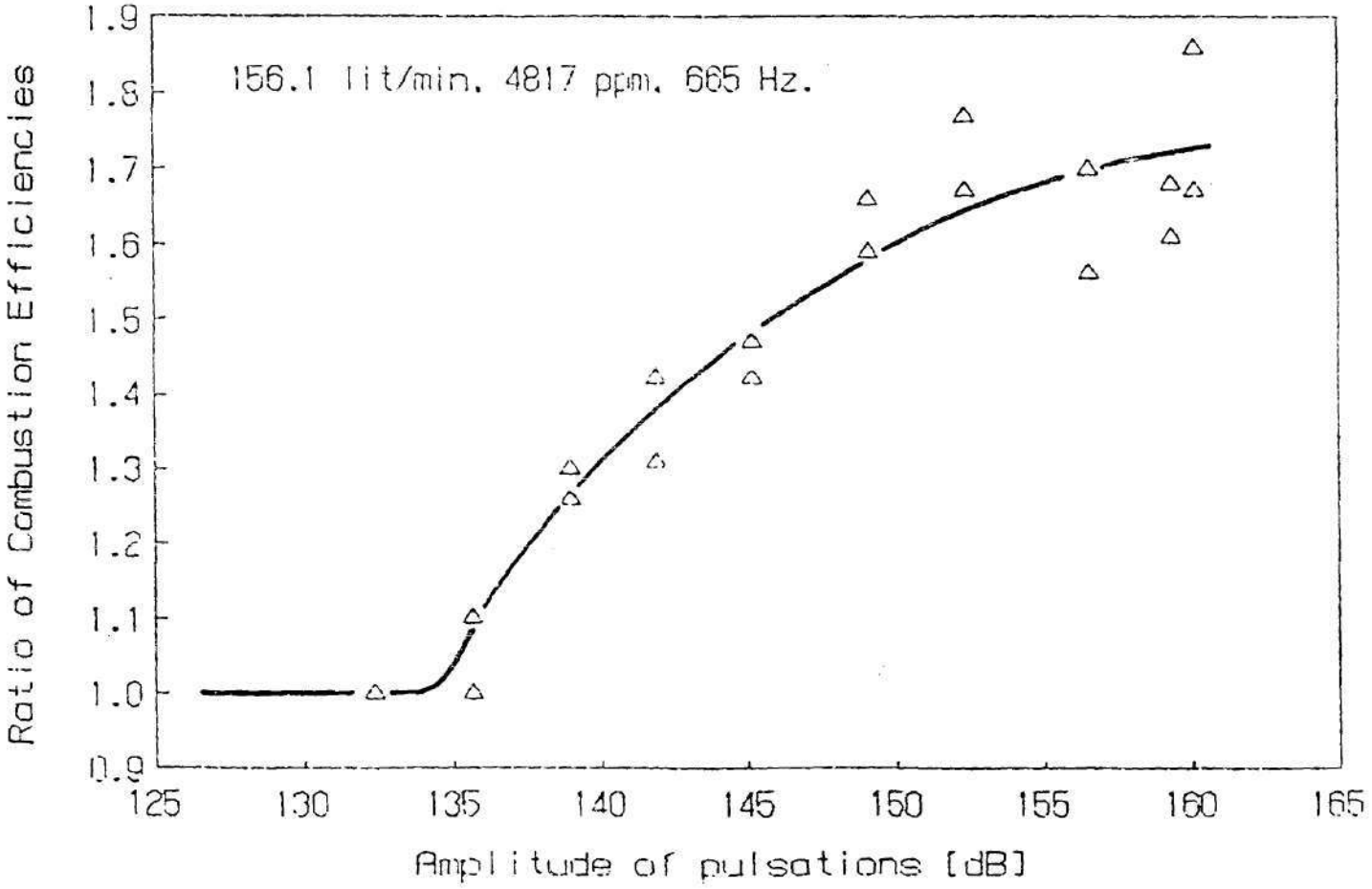

Figure 36: Ratio of Combustion Efficiencies vs. the Pressure Amplitude of 665 *Hz* Oscillations

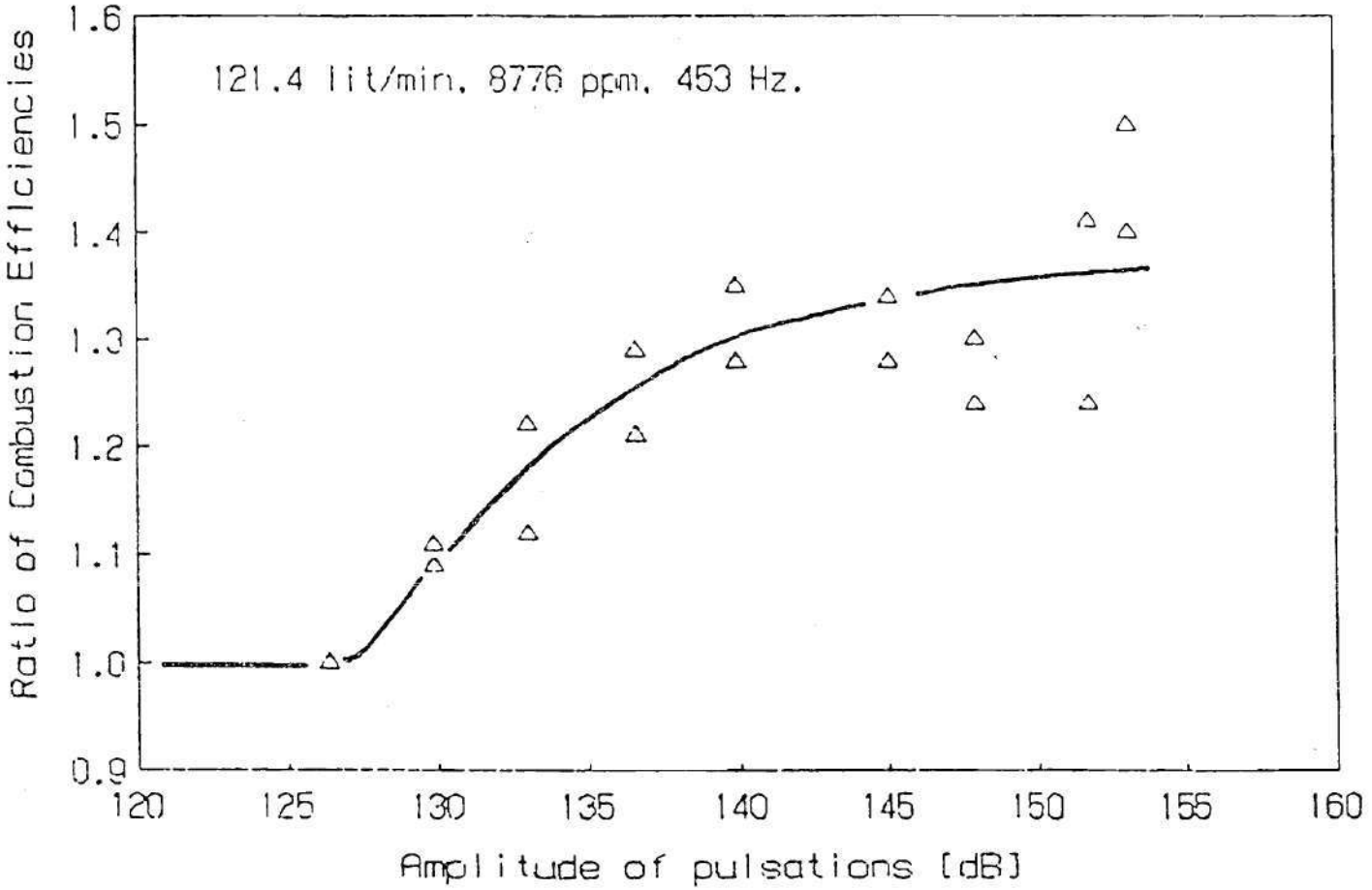

Figure 37: Ratio of Combustion Efficiencies vs. the Pressure Amplitude of 453 *Hz* Oscillations

downstream velocity node can be explained by acoustic streaming. Lord Rayleigh [34] was the first to derive approximate equations for the second order gas particle motions in a viscous medium between two parallel plates due to acoustic pulsations. Both Lord Rayleigh and Eckart [35], who introduced a more rigorous approach, found that time independent circulatory flows are induced due to the damping effect of friction in the viscous boundary layer. These circulatory flow patterns, termed acoustic streaming, are flowing from the pressure nodes in the direction of the velocity nodes in the viscous boundary layer near the plate, and in the opposite direction, near the plane of symmetry in the center between the plates. A schematic of these second order, time independent flows is shown in Fig. 11.

The monolith catalyst used in this study consisted of rectangular channels having a cross section area of about $1.5\,mm^2$. The flow within each channel is laminar and viscous throughout the channel due to its very low Reynolds number (based on catalyst channels properties Reynolds numbers were alway less than 200). The axial flow velocity near the catalyst surfaces is very small and most of the flow is taking place at the centers of the channels, where the velocity is much higher. When the catalyst is located at an "in phase" condition, the acoustic streaming superimposed on the steady state flow increases the axial velocity near the catalyst surfaces and slows the flow at the center. The higher axial flow velocity in the downstream direction near the walls causes higher reactant concentrations at the surface due to axial mass convection. The lower flow velocity at the centers of the channels causes a longer residence time for the reactants flowing through the centers of the channels in the catalytic section. This allows more time for radial diffusion of reactants from the center to the catalytic surfaces. This decreases the amount of fuel passing the catalytic section without undergoing reaction. Similarly, the acoustic streaming improves the removal of products from the catalytic surfaces. The higher overall diffusion rates of both the reactants and the products

to and from the catalyst surfaces, respectively, enhances the catalytic reaction if, as has been assumed, the diffusion processes are limiting the overall reaction rate. Although the location of the nodes which deside the acoustic streaming flow pattern is frequency dependent, the acoustic streaming velocities are frequency independent. The acoustic streaming velocities are determined by the amplitudes of the pulsations. This can explain the dependence of the measured improvements of the combustion efficiencies upon pulsations' amplitudes and the insensitivity of the combustion efficiency to the frequency of the acoustic pulsations.

When the catalyst is at an "out of phase" location, the flow directions due to acoustic streaming are reversed relative to the axial coordinate. In this case, the flow near the catalyst surfaces is slowed, while at the same time the velocity in the centers of the channels increases. This change in flow velocities shortens the residence time of the reactants at the centers of the channels and it can cause reversed flow (i.e., flow in the upstream direction) in the boundary layer near the catalytic surfaces. Such a flow pattern does not allow more fuel molecules to reach the catalytic surfaces and is not expected to improve the performance of the combustor, as has been observed in this study.

The circulatory flows caused by acoustic streaming move hotter gas particles from the center of the tube downstream of the catalytic section to the boundary layer near the wall and increase the heat losses causing the measured decrease in temperature at the downstream part of the combustor. Since the radial temperature gradient is much larger than the axial gradient, direction of the circulatory flow has only minor importance on the enhancement of the heat transfer through the wall of the combustor. This explains why such temperature changes occurred whenever pulsations were excited. Upon the stoppage of the acoustic oscillations, the circulatory flows stopped and a streamlined flow pattern in the axial direction was reestablished. This decreased the heat losses and restored the axial temperature distribution to the situation prior to onset of pulsations.

Chapter VI

SUMMARY OF RESULTS AND CONCLUSIONS

The experiments conducted in this study showed that catalytic combustors can be operated under pulsating conditions and that their performance can be improved by acoustic oscillations.

Stable, incomplete catalytic combustion of propane was attained under certain operating conditions when the catalyst surfaces were kept at a relatively low temperatures (i.e., below 1000 °C). The operating conditions producing such low temperatures but still supporting stable catalytic combustion were flow rates between 100 and 160 *lit/min* and propane concentrations in the range of 4000 to 9000 *ppm*. Although the results were not quantitatively repeatable, the repeatable trends permitted the determination of the effects of different variables on both pulsating and non-pulsating operation of the experimental catalytic combustor.

When operating under non-pulsating conditions both combustion efficiencies and temperatures at the exit from the catalyst increased when the total mixture flow rate and/or propane concentration increased. Combustion efficiency increased as the temperature measured downstream of the catalyst segment increased. The dependence of combustion efficiency on catalyst temperature is the reason why incomplete propane combustion was attained only at relatively low propane concentrations and low reactants flow rates. Although high combustion efficiencies can be achieved by increasing the temperature in the catalytic section, such operating conditions are not always desired or possible. Combustion of very lean fuel/air mixtures, the need to keep NO_x concentrations as low as possible and the need

to avoid damage to the catalyst due to exposure to elevated temperatures calls for operation of catalytic combustors at low temperatures, which could result in incomplete combustion. Enhancement of such incomplete catalytic reactions by introduction of acoustic pulsations can make implementation of this technology more feasable.

Acoustic oscillations caused changes in the temperature distributions along the combustor. Upon onset of acoustic pulsations, temperatures increased near the catalyst section, while further downstream they decreased considerably. The temperature decreases at the downstream part of the combustor were detected both when the combustion was enhanced by the pulsations and when no improvement in combustion efficiency was evident. This suggests that heat transfer coefficients are larger when the system pulsates as compared to non-pulsating operation. Increase in the heat transfer coefficient makes utilization of the heat produced in the combustor more economical.

The effect of acoustic pulsations at different frequencies on the combustion efficiency of the experimental setup was studied. No improvement was found when the acoustic intensities were lower than 135 dB and when the catalyst was in an "out of phase" location. Pulsations with amplitudes in excess of 140 dB were obtained only for frequencies between 300 and 1000 Hz. When the catalyst was located between an upstream pressure node and a downstream velocity node, pulsations of more than 140 dB caused considerable increase in combustion efficiency. The increase in efficiency was between 15 and 50 percent and depended upon the steady-state efficiency and the amplitude of the acoustic waves. For amplitudes in excess of the threshold of approximately 135 dB and with catalyst at the proper "in phase" location, increase in the sound pressure level increased the combustion efficiency. The improvement in the performance of the catalytic combustor due to acoustic oscillations suggests that pulsating catalytic combustors operated at low temperatures will be more efficient if the catalyst is located properly relative to

the acoustic standing wave pattern (i.e., where the acoustic pressure and particle displacement are "in phase").

Acoustic streaming is the mechanism suggested to cause the changes in the catalytic combustor upon onset of oscillations. It explains why combustion efficiencies are improved when the catalyst is at an "in phase" location, and why the acoustic amplitude has a large influence on the combustor's performance while the frequency of pulsations is of much lesser importance. The design of the current system did not make it possible to measure the flow velocity near the acoustic surfaces to verify the mechanism. In order to perform such velocity measurements, a combustor consisting of two parallel catalytic plates and optical windows is suggested. Such a design will provide capabilities for both Schlieren imaging and laser Doppler velocimetry. This two diagnostic methods can provide information about flow directions and velocities near the catalyst surfaces, and help understand what processes are occurring in the catalyst channels. Optical windows will also provide the capability to measure temperatures and changes in combustion rates using radiation diagnostic methods.

The poor properties of the catalyst used in this study prevented investigation of the effect of acoustic pulsations on combustion efficiency of methane/air mixtures. A more active catalyst could support stable catalytic combustion of methane at low temperatures (catalyst surface temperatures of less than 800 °C). If methane combustion at low temperatures proves possible, incomplete catalytic reaction could be obtained, and the effect of acoustics on catalytic combustion of methane can be investigated. It is believed that such investigation can show that acoustic pulsations can improve the performance of catalytic combustors burning methane. Since commercial methane (or natural gas) is a more common fuel than propane, and since methane is more difficult to ignite and burn, implementation of pulsating catalytic combustor for methane combustion could be more feasable if such improvements are possible.

Appendix A

CALCULATION OF THE COMBUSTION EFFICIENCY

Combustion efficiency is defined as the fraction of heat generated by the combustion reaction relative to the heat that would be produced if the reaction proceeded to completion. Since in catalytic combustion of lean gaseous hydrocarbon/air mixtures the concentration of CO is negligible, the assumption was made that all hydrocarbon molecules undergoing reaction are oxidized to CO_2 and water according to a single global reaction. Thus, combustion efficiency is given by the fraction of hydrocarbon molecules consumed by the reaction. Since in our study all experiments with methane combustion proceeded to completion, combustion efficiencies were calculated only for propane.

Propane combustion in the catalytic combustor proceeds according to the following chemical equation:

$$C_3H_8 + 5\,O_2 \longrightarrow 3\,CO_2 + 4\,H_2O$$

If the mole (or volume) fraction of propane entering the combustor is X_p and we assume the air to consist of 21% oxygen and 79% nitrogen, the oxygen and nitrogen mole fractions are $.21(1 - X_p)$ and $.79(1 - X_p)$, respectively. The fraction of propane undergoing reaction equals to the combustion efficiency – η_c, and out of each mole of mixture entering the combustion zone we get $3\eta_c X_p$ moles of CO_2 and $4\eta_c X_p$ moles of water vapor. The number of moles of unburned propane and oxygen is given by $X_p(1-\eta_c)$ and $.21(1-X_p)-5\eta_c X_p$, respectively, and the number of nitrogen moles stays unchanged. We do not take into account

the formation of NO_x from nitrogen and oxygen in air, which was found in the products in negligible concentrations.

The combustion products in the sampling line leading to the chemical analyzers pass through a dryer which eliminates the water vapor. Thus, the total number of moles produced from one mole of reactants (i.e., propane and air) reaching the analyzers is $1 - 3\eta_c X_p$. The mole fraction of propane oxygen and carbon dioxide passing through the analyzers are given by Equations (A-1), (A-2) and (A-3), respectively:

$$Y_p = \frac{X_p(1-\eta_c)}{1-3\eta_c X_p} \qquad (A-1)$$

$$Y_{O_2} = \frac{.21(1-X_p) - 5X_p\eta_c}{1-3\eta_c X_p} \qquad (A-2)$$

$$Y_{CO_2} = \frac{3\eta_c X_p}{1-3\eta_c X_p} \qquad (A-3)$$

The mole fraction of propane in the reactants (X_p) is calculated from the air and fuel rotameters measurements, and the mole fractions in the products sampling line are measured by the analyzers. Thus, the combustion efficiency can be calculated from the concentrations measured by either of the analyzers.

- From propane concentration measurements:

$$\eta_c = \frac{1 - \frac{Y_p}{X_p}}{1-3Y_p} \qquad (A-4)$$

- From oxygen concentration measurements:

$$\eta_c = \frac{.21(1-X_p) - Y_{O_2}}{X_p(5-3Y_{O_2})} \qquad (A-5)$$

- From carbon dioxide concentration measurements:

$$\eta_c = \frac{Y_{CO_2}}{3X_p(1+3Y_{CO_2})} \qquad (A-6)$$

Practically, combustion efficiency was usually calculated using only Equations (A-5) and (A-6) since the time needed for the hydrocarbon analyzer to reach a constant reading was in excess of 10 minutes. The agreement between the calculations using the oxygen and CO_2 concentrations was good and the efficiency results were never more than two percent apart from one another. The average of the two calculated efficiencies was always used. When the combustion efficiency was calculated using the the concentration measured by the propane analyzer after running the combustor at constant conditions for more than 15 minutes, it was found to be within 5% from the average combustion efficiency calculated using the O_2 and CO_2 concentrations.

BIBLIOGRAPHY

[1] Kesselring, J. P., *Catalytic Combustion*, in F. Weinberg – Editor, *Advanced Combustion Methods* Academic Press, Inc. (London), pp. 237–275, 1986.

[2] Pfefferle, W. C., *The Catalytic Combustor: An Approach to Cleaner Combustion*, Journal of Energy, Vol. 2, No. 3, pp. 142–146, May–June 1978.

[3] Snow, G. C., Krill, W. V. and Kendall, R. M., *Mechanisms and Kinetics in Catalytic Combustion*, AIChE Manuscript No. 5989, Presented at the AIChE Annual Meeting, New Orleans, LA, Nov. 8–12, 1981.

[4] Prasad, R., Kennedy, L. A. and Ruckenstein E., *Catalytic Combustion*, Catal. Review — Science & Eng., Vol. 26, No. 1, pp. 1-58, 1984.

[5] Spencer, D., *Advanced Power Systems Division, R & D Status Report*, EPRI Journal, Vol. 10, No. 2, pp.39–41, March 1985.

[6] Kezerle, J. A., *Results of Catalytic Combustion Workshop* — Summary of 1984 GRI Catalysis Workshop.

[7] Anderson, D. E., Tacina, R. R. and Mroz, T.S., *Catalytic Combustion for the Automotive Gas Turbine Engine*, NASA Report TM X-73589, 1985.

[8] Arkhangel'skii, M. E. and Statnikov, Yu. G., *Acceleration Mechanism of Heterogeneous Processes in a Standing-Wave Sound Field*, Soviet Physics – Acoustics, Vol. 14, No. 4, pp. 432–435, April–June, 1969.

[9] Borisov, Yu. Ya., and Gynkina, N. M., *On Acoustic Drying in a Standing Sound Wave*, Soviet Physics — Acoustics, Vol. 8, No. 1, pp. 95–96, July – Sept., 1962.

[10] Borisov, Yu. Ya., Dolgopolov, N. N. and Simonyan, S. G., *Comparison of Acoustical, Contact, and Infrared Drying Methods*, Soviet Physics — Acoustics, Vol. 11, No. 3, Jan.– March 1966.

[11] Burdukov, P. and Nakoryakov, V. E., *Mass Transfer in an Acoustic Field*, Zhurnal Prikladoni Mekhaniki i Tekhnicheskoi Fiziki, No. 2, pp. 62–66, 1965.

[12] Carvalho, J. A. et al., *Controlling Mechanisms and Performance of Coal Burning Rijke Type Pulsating Combustors*, Twentieth Symposium (International) on Combustion, 1984.

[13] Carvalho, J. A. et al., *Combustion Characteristics of Unpulverized Coal under Pulsating and Non-Pulsating Conditions Combustors*, Fuel, Vol. 66, pp. 4–8, January 1987.

[14] Hodgins, J. W., Hoffman, T. W. and Pei, D. C., *The Effect of Sonic Energy on Mass Transfer in Solid-Gas Contacting Operations*, Canad. J. of Chem. Eng., pp. 18–24, June 1957.

[15] Zinn,B. T., Miller, N., Carvalho, J. A. and Daniel, B. R., *Pulsating Combustion of Coal in a Rijke Type Combustor*, Proc. of the Nineteenth Symposium (International) on Combustion, pp. 1197–1203, 1982.

[16] Drummond, C. K., *Mass Transfer from Naphtalene Sphere Under Oscillatory Flow*, M.S. Thesis, M. E., Syracuse University, April 1981.

[17] Kamenkovich, V. V. and Mednikov, E. P., *Mechanism of the Acoustic Drying of Cappilary-porous Materials*, Soviet Physics — Acoustics, Vol. 13, No. 3, pp. 382–384, Jan – March 1968

[18] Low, D. I. R., and Hodgins, J. W., *The Effect of Acoustic Turbulence on Mass Transfer at a Column Wall*, Canad. J. of Chem. Eng., pp. 241–245, December 1963.

[19] Taweel, A. M. and Landau J., *Mass Transfer between Solid Spheres and Oscillating Fluids — A Critical Review*, The Canadian Journal of Chemical Engineering, Vol. 54, pp. 532–539, December 1976.

[20] Chendke, P. K. and Fogler, H. S., *Second-Order Sonochemical Phenomena — Extentions of Previous Work and Applications in Industrial Processing*, The Chem. Eng. Journal, Vol. 8, pp. 165–178, 1974.

[21] Cormack, D. E. and Beattie, G. I., *Viscous Flow Effects in the Periodic Cycling of Gas-Phase Catalytic Reactions*, Chem. Eng. Science, Vol. 34, pp. 1001–1005, 1979.

[22] Gutkowicz-Krusin D., *Interfacial Sound Modes and Heterogeneous Catalysis*, J. Chem. Phys., Vol. 79, No. 12 pp. 6331–6337, 1983.

[23] Hamer, J. W. and Cormack, D. E., *Influence of Oscillating External Pressure on Gas-Phase Reactions in Porous Catalysts*, Chem. Eng. Science, Vol. 33, pp. 935–944, 1978.

[24] Lintner, W., *Ph. D. Dissertation*, Newark College of Engineering, Newark, New Jersey, 1973.

[25] Lintner, W. and Hanesian, *The Effect of Ultrasonic Vibrations on Heterogeneous Catalysis*, Ultrasonics, pp. 21–26, Jan. 1977.

[26] Kesselring, J. P., Private communication.

[27] National Bureau of Standards, *Thermocouple Reference Tables, NBS Monograph #125*, National Bureau of Standards, Washington, DC, 1979.

[28] Cheng, Xian-Chen, *Sampling System and Data Aquisition System — Operation Manual,* Georgia Institute of Technology, School of Aerospace Eng., July 1987.

[29] Kapur, A., Cummings, A. and Mungur, P., *Sound Propagation in a Combustion Can with Axial Temperature and Density Gradients*, Journal of Sound and Vibrations, Vol. 25, No. 1, pp. 129–138, 1972.

[30] Cummings, A., *Ducts with Axial Temperature Gradients: An Approximate Solution for Sound Transmission and Generation*, Journal of Sound and Vibrations, Vol. 51, No. 1, pp. 55–67, 1977.

[31] Trimm, D. L.,*Catalytic Combustion (Review)*, Applied Catalysis, Vol. 7, pp. 249–282, 1983.

[32] Rott, N., *Thermoacoustics*, Advances in Applied Mechanics, Vol. 20, p. 135, 1980.

[33] Swift, G. W.,*Thermoacoustic Engines*, A Review for the Condensed Matter and Thermal Physics Group, Los Alamos National Laboratory, Los Alamos, NM 87545.

[34] Lord Rayleigh, *On the Circulation of Air Observed in Kundt's Tubes, and on some Allied Acoustical Problems*, Philosophical Transactions of the Royal Society of London, Vol. 175, pp. 1–21, 1883.

[35] Eckart, C., *Vortices and Streams Caused by Sound Waves*, Physical Review (second series), Vol. 75, pp. 68–76, January 1945.

VITA

Mr. Reuven Gal - Ed was born in Zagreb, Yugoslavia on October 12,1945 and emigrated to Israel in 1948. He received a B. S. degree *cum laude* from the Department of Chemical Engineering at the Technion – Israel Institute of Technology in 1967. Mr. Gal - Ed joined the Propulsion Department of Rafael – the Armament Development Authority in Haifa, Israel in 1967. He worked in research, development and design in the fields of solid rocket propulsion and pyrotechnics. He held the posts of research engineer, group leader and acting section head, and was in charge of development, design and small scale production of rocket motors and pyrotechnically actuated systems. Mr. Gal - Ed lead development projects involving composite propellant systems, smoke generators and obscurants, and infra red radiation sources (decoys). During the academic year 1979 – '80 Mr. Gal - Ed was a visiting research engineer at the School of Chemical Engineering, Cornell University and conducted research in water desalination. Mr. Gal - Ed came to Georgia Institute of Technology in September 1984 and was awarded an M. S. in Aerospace Engineering in December 1986.